12-2007

Arsenic phytoremediation: Engineering of an arsenic-specific phytosensor and molecular insights of arsenate metabolism through investigations of *Arabidopsis thaliana, Pteris cretica,* and *Pteris vittata*

Jason Miles Abercrombie
University of Tennessee - Knoxville

To the Graduate Council:

I am submitting herewith a dissertation written by Jason Miles Abercrombie entitled "Arsenic phytoremediation: Engineering of an arsenic-specific phytosensor and molecular insights of arsenate metabolism through investigations of *Arabidopsis thaliana, Pteris cretica,* and *Pteris vittata*." I have examined the final electronic copy of this dissertation for form and content and recommend that it be accepted in partial fulfillment of the requirements for the degree of Doctor of Philosophy, with a major in Plants, Soils, and Insects.

C. Neal Stewart, Jr., Major Professor

We have read this dissertation and recommend its acceptance:

Albrecht von Arnim, Janice Zale, Michael E. Essington

Accepted for the Council:

Carolyn R. Hodges

Vice Provost and Dean of the Graduate School

(Original signatures are on file with official student records.)

To the Graduate Council:

I am submitting herewith a dissertation written by Jason Miles Abercrombie entitled "Arsenic phytoremediation: Engineering of an arsenic-specific phytosensor and molecular insights of arsenate metabolism through investigations of *Arabidopsis thaliana*, *Pteris cretica*, and *Pteris vittata*." I have examined the final electronic copy of this dissertation for form and content and recommend that it be accepted in partial fulfillment of the requirements for the degree of Doctor of Philosophy, Plants, Soils, and Insects.

C. Neal Stewart, Jr. Major Professor

We have read this dissertation
and recommend its acceptance:

Albrecht von Arnim

Janice Zale

Michael E. Essington

Accepted for the Council:

Carolyn R. Hodges
Vice Provost and Dean of the
Graduate School

(Original signatures are on file with official student records.)

Arsenic phytoremediation: Engineering of an arsenic-specific phytosensor and molecular insights of arsenate metabolism through investigations of *Arabidopsis thaliana*, *Pteris cretica*, and *Pteris vittata*

A dissertation presented for the Doctor of Philosophy degree

The University of Tennessee, Knoxville

Jason Miles Abercrombie

December 2007

Dedication

This dissertation is dedicated to my parents, Donnie and Ruth, and my fiancé Laura, for their love and support.

Acknowledgements

I am grateful to Dr. Neal Stewart for providing me with financial support, the freedom to conduct a range of research projects, and for always being approachable for guidance whenever I had questions. I appreciate the guidance and support of my committee members Dr. Albrecht von Arnim, Dr. Janice Zale, and Dr. Michael Essington. I am grateful to all the members of the Stewart Lab for their assistance and good humor. I would also like to acknowledge the National Science Foundation and the National Institutes of Health for funding of the arsenic phytosensor project, as well as our collaborators EdenSpace Systems, Inc. for their support, especially Mark Elless, David Lee, and Bruce Ferguson. I appreciate the help of Renee Hoyos at the Tennessee Clean Water Network and Barry Sulkin at Public Employees for Environmental Responsibility in the early stages of my work at the Smoky Mountain Smelter site. Many thanks are due to Burl Maupin and the Tennessee Division of Remediation, Knoxville Field Office for efforts in providing information on and permission to conduct research at the SMS site.

Abstract

This dissertation is a compilation of four studies that were conducted in the laboratory of Dr. C. Neal Stewart, Jr. at the University of Tennessee, Knoxville. The first study describes an investigation into arsenate metabolism in *Arabidopsis thaliana* using microarray technology. The second study summarizes progress made to date towards the development of an As-specific phytosensor, or a plant genetically engineered to detect the presence of As in the environment. The third study describes efforts towards genetic transformation of *Pteris cretica* and *Pteris vittata*, both As-hyperaccumulating ferns that have been recently demonstrated as effective in the removal of As from contaminated areas. This paper demonstrates the development of a modified tissue culture protocol that was effective in callus generation from both *Pteris vittata* and *Pteris cretica* gametophytes as well as regeneration of plantlets from that callus. Attempts towards genetic transformation were made via biolistic bombardment and *Agrobacterium*-mediated transient expression using leaf infiltration. Optimization of the *Pteris* tissue culture protocol will facilitate continued efforts towards the genetic transformation of this unique plant, thereby enabling means of more effectively exploring the underlying mechanisms of As hyperaccumulation. The final study reports a field-scale investigation of plant metal uptake at a local contaminated site in Knoxville, TN. The Smokey Mountain Smelters Site is an abandoned secondary aluminum smelter where waste product from the smelting process (slag) was illegally dumped in large piles over much of the property. Interestingly, wild vegetation was found growing on the slag piles without any obvious symptoms of toxicity. Therefore, a study was conducted to quantify the

metal uptake of these plants, characterize the metal profile of the slag material, and investigate the capacity of *Pteris cretica* in extracting arsenic from slag on-site. As a result, these studies have provided new insights into arsenate metabolism in plants, and generated many testable hypotheses to enhance our understanding of plant genetic responses to metal stress. The following introduction serves to provide a background on phytoremediation, arsenic, and plant responses to the toxic metalloid.

Table of contents

List of Tables

List of Figures

Introduction

Phytoremediation, or the use of plants to clean up contaminated sites, has provided an opportunity to employ transgenic plants as tools for environmental benefit. Because plants are solar powered and aesthetically pleasing, they present a cost-efficient, non-invasive alternative to expensive and destructive remediation methods (i.e. excavation). Each contaminated site presents a unique set of challenges due to the variation in pollutant type, soil characteristics, hydrologic factors, climate and other environmental factors specific to that location. Plants have evolved a broad range of novel remediation traits from uptake, accumulation, and sequestration or volatilization of toxic metals to degradation of organic contaminants. Therefore, WEcan not only exploit the existing natural variation for these traits among plant genera, but also introduce novel traits into a customized plant designed to fit a particular niche. Recent advances in our understanding of gene function have facilitated improved phytoremediation strategies using transgenic plants.

The field of phytoremediation research is generally divided into categories that reflect specific mechanisms by which plants facilitate either degradation or detoxification of contaminants. These are phytoextraction, phytostabilization, rhizodegradation / rhizostimulation, phytodegradation, and phytovolatilization (Figure 1). Phytoextraction refers to the process whereby contaminants are taken up by plant roots and stored in the above-ground biomass for subsequent removal. Phytostabilization is the process of detoxification and/or immobilization of contaminants in the plant tissue via sequestration of these toxic substances (i.e. cell wall or tonoplast), thereby preventing disruption of

critical metabolic processes. During phytodegradation, organic contaminants are either metabolized in the plant to a less toxic compound or in some cases, completely mineralized. Rhizodegradation involves contaminant degradation by the associated microbes in the rhizosphere, which is often enhanced by the plant root exudates (rhizostimulation). Phytovolatilization is a process by which the contaminant is taken up by the plant and then released into the atmosphere via leaf stomata (Salt *et al*., 1998; Burken *et al*., 2000). As we continue to explore and understand the genetic mechanisms associated with these processes, innovative approaches for more effective and efficient phytoremediation strategies via plant genetic engineering are enabled.

The model system *Arabidopsis thaliana* has provided an invaluable platform for basic plant research due to its small size, short generation time, large number of offspring, and small nuclear genome size (AGI 2000), however phytoremediation projects require plants that display desirable traits for field-scale application. For example, an ideal plant for phytoremediation would be a fast-growing perennial species that tolerates a wide range of toxic elements, produces high biomass, and has the capacity for hyperaccumulation in the above-ground tissues for subsequent harvest and disposal (Yang 2005). Therefore, a common strategy has become studying gene function in Arabidopsis to discover candidates for engineering high-biomass species (e.g. *Brassica juncea*) for use in the field. Understanding the molecular mechanisms involved in metal hyperaccumulation has become a primary objective to enable transgenic plants with optimal capacity for metal extraction. Hyperaccumulation is typically defined as the capacity of a plant to accumulate metals at levels that are toxic to most organisms and will be discussed in greater detail in the following text. Over 400 metal

hyperaccumulators have been reported and show great promise for revealing the genetic and physiological basis for this phenomenon.

Understanding the problem of arsenic

Arsenic (As) is a toxic metalloid found ubiquitously in the environment (Moore *et al*., 1977) that has been classified as a human carcinogen (IARC, 1987). Naturally high levels of arsenic in drinking water have caused major human health problems in the United States, China, Argentina, Taiwan, and most notably in Bangladesh and India where millions of people have been harmed (Chakraborti *et al*., 2003; Mukhopadhyay *et al*., 2002; Nriagu, 2001). Arsenic is the 20th most abundant element in the earth's crust, and natural processes such as volcanic activities and weathering of As-bound minerals result in elevated levels in soils and groundwater (Nriagu, 1994). In terrestrial environments, redox conditions typically result in the inorganic forms of arsenate [As(V); $H_2AsO_4^-$] or arsenite [As (III); H_3AsO_3], however environmental conditions ultimately dictate As speciation, thereby influencing its mobility, bioavailability, and toxicity (Mukhopadhyay *et al*., 2002). Arsenate predominates under aerobic conditions, whereas arsenite may be the dominant form in anoxic environments such as flooded soils (Rosen, 1999). Arsenite, exhibiting more metal-like behavior, easily permeates biological membranes and forms strong metal-thiol bonds with cysteines, thus inhibiting critical metabolic enzymes such as pyruvate dehydrogenase (Rosen, 1999).

The toxicity of arsenic has been exploited for applications in agriculture (pesticides, herbicides, sheep and cattle dips, etc.), treatments of infectious diseases, and

common wood preservatives such as chromated copper arsenate (CCA), most of which have contributed to elevated As levels in soils and groundwater globally (Fitz and Wenzel, 2002). Major anthropogenic sources also include industrial smelting and fossil fuel combustion which have led to thousands of tons of As emission into the atmosphere (Nriagu and Pacyna, 1988). As-rich ores released during mining operations result in the accumulation of As via redox conditions found in acidic mine waste (Mukhopadhyay *et al*., 2002). Additionally, the U.S. Environmental Protection Agency (EPA) has declared arsenic to be one of the five most toxic substances found at Superfund (the most polluted in the country) sites (Johnson and Derosa, 1995). In the wake of the aforementioned evidence, the U.S. National Research Council (NRC, 1999) and the EPA (Pontius *et al*., 1994) have prompted the reduction of arsenic levels in U.S. drinking water to a safety threshold of 10 $\mu g\ L^{-1}$.

Plant responses to arsenic

A thorough understanding of arsenic toxicity in plants is a prerequisite to developing transgenic plants for remediation applications. Plants typically encounter arsenic in the anionic forms of As (V) and As (III), both of which have different cytotoxic effects (Quahebeur and Rengel, 2003). As (III) reacts with the sulfhydryl groups of enzymes and proteins, thereby inhibiting cellular function and resulting in death (Ullrich-Eberius *et al*., 1989). Alternatively, As (V) is a phosphate analog, so it competes with phosphate for uptake in the roots, as well as in the cytoplasm where it may disrupt metabolism by replacing phosphate in ATP to form unstable ADP-As (Ullrich-

Eberius *et al*., 1989). It is well known that As(V) is readily taken up in the plasma membrane of root cells via phosphate transporters (Asher and Reay, 1979; Clark *et al*., 2000; Meharg and Macnair, 1992; Otte and Ernst, 1994), but little is known about the mechanisms of translocation from root to shoot (Quahebeur and Rengel, 2003).

Plants that have evolved mechanisms of tolerance to high levels of As or other metals (i.e., Cd, Cu, Ni, Pb, etc.) generally avoid cellular incorporation of these metals by means of detoxification and/or sequestration for storage in the vacuole or cell wall (Salt *et al*., 1998; Baker *et al*., 2000). A common response in plants that are challenged with toxic concentrations of metals is the production of phytochelatins (PCs) (Cobbett *et al*., 2000). PCs are low molecular weight thiolate peptides of the general structure $(\gamma\text{-Glu-Cys})_n\text{-Gly}$ (n = 2-11) that are synthesized from glutathione by the constitutively present phytochelatin synthase (PCS) (Grill *et al*., 1989). Both As (V) and As (III) efficiently induce the production of PCs in plants (Schmoger *et al*., 2000), however it is believed since As (V) has no affinity for the sulfhydryl groups in PCs, As (V) is reduced in the cytoplasm, resulting in As (III)-PC complexes (Quahebeur and Rengel, 2003). Pickerling *et al*. (2000) reported that glutathione and PCs form As (III)-tris-thiolate complexes in Indian mustard (*Brassica juncea*) upon exposure to As (V). These authors also demonstrated that addition of a chemical chelator (dimercaptosuccinate) to the hydroponic solution increased translocation of arsenic to the shoot, and suggested the chelator as a potentially useful soil amendment to facilitate As phytoremediation. Li *et al*. (2004) showed that overexpression of PCS in *Arabidopsis* lead to enhanced As tolerance and hypersensitivity to Cd. Plants overexpressing this transgene exhibited high tolerance to arsenic and accumulated 20-100 times more biomass on 250 and 300 μM

arsenate compared with nontransgenic plants. Despite these results, the plants did not accumulate more aboveground arsenic, therefore the authors suggested that complementary genetic amendments may be required to enhance hyperaccumulation.

Lee *et al*. (2003) isolated an *Arabidopsis thaliana* mutant (*ars1*) with increased tolerance to arsenate and increased phosphate uptake, but showed As-tolerance was neither attributed to phytochelatins nor glutathione. Exploring the genetic mechanisms responsible for this uncharacterized phenotype may bring to light how this particular mutant tolerates higher levels of arsenate without production of PCs, thus providing novel genes for engineering arsenic tolerance (Lee *et al*., 2003). Natural hyperaccumulators of arsenic have recently been discovered in the fern genus *Pteris* (Ma *et al*., 2001; Zhao *et al*., 2002). Chinese brake fern (*Pteris vittata*), the most studied As hyperaccumulator, can accumulate over 1% of its dry mass shoots (Wang *et al*., 2002). Cai *et al*. (2003) confirmed that low molecular weight thiols were formed in *Pteris vittata* upon exposure to As and other metals (Cd, Cu, Cr, Zn, Pb, Hg, and Se), but found an unidentified thiol was specifically induced in response to arsenic.

Considering the current gaps in our knowledge of the molecular mechanisms involved in As tolerance and accumulation, studies of *Arabidopsis thaliana,* and the As-hyperaccumulators *Pteris vittata* and *Pteris cretica* have been the focus of this dissertation research. The research presented here demonstrates both the utility and the shortcomings of global scale transcriptional profiling in Arabidopsis in the context of arsenate stress. Additionally, the other studies in this dissertation highlight the potential of developing a transgenic plant that for detection of As in the environment, the utility of wild vegetation and Pteris cretica in phytoremediation of a local contaminated site, and

novel approaches toward developing an efficient genetic transformation sytem for the hyperaccumulating ferns *Pteris cretica* and *Pteris vittata*. The lessons learned throughout this process have helped to construct a solid foundation for my development as a scientist.

Transcriptional profiling of *Arabidopsis thaliana* grown under arsenate stress reveals antioxidant activity and repression of the phosphate starvation response[1]

[1] This manuscript has been submitted to BMC Plant Biology and is under review.

Authors:

Jason M. Abercrombie[1], Matthew D. Halfhill[2], Priya Ranjan[1], Murali R. Rao[1], Arnold Saxton[3], Joshua Yuan[1], and C. Neal Stewart, Jr. [1]

[1] Department of Plant Sciences, University of Tennessee, 2431 Joe Johnson Blvd., Knoxville, TN 37996-4561, USA

[2] Biology Department, St. Ambrose University, 518 West Locust St., Davenport, IA 52803, USA

[3] Department of Animal Science, University of Tennessee, 2505 River Dr., Knoxville, TN 37996-4561, USA[1]

Abstract

Whole genome oligonucleotide microarrays were employed to investigate the transcriptional responses of *Arabidopsis thaliana* plants to arsenate [As (V)] stress. Non-parametric rank product statistics were used to detect differentially expressed genes. Antioxidant-related genes (i.e. coding for superoxide dismutases and peroxidases) play prominent role in response to arsenate. The microarray experiment revealed induction of chloroplast Cu/Zn superoxide dismutase (SOD) (at2g28190), Cu/Zn SOD (at1g08830), as well as an SOD copper chaperone (at1g12520). On the other hand, Fe SODs were strongly repressed in response to As (V) stress. These observations were confirmed with RT-PCR and SOD activity assays. Additionally, microarray data suggest that As (V) represses transcription of genes induced by phosphate starvation. Our results also suggest that As (V) stress affects the transcription of a wide range of genes including peroxidases, glutathione *S*-transferases, transporters, and genes involved in cell wall growth, thus providing new putative targets for future research.

Introduction

Arsenic (As) is a toxic metalloid found ubiquitously in the environment (Moore *et al*., 1977) and is classified as a human carcinogen (IARC, 1987). Currently, the US Environmental Protection Agency declares arsenic as the highest priority hazardous substance found at contaminated sites in the United States (http://www.atsdr.cdc.gov/cercla/05list.html). Naturally high levels of arsenic in drinking water have caused major human health problems in the United States, China, Argentina, Taiwan, and most notably in Bangladesh and India where tens of millions of people have been affected (Chakraborti *et al*., 2003; Mukhopadhyay *et al*., 2002). Arsenic is highly toxic at low concentrations, therefore drinking water safety standards were lowered from 50 to 10 µg/ L in the U.S. (National Research Council, 1999).

Plants typically encounter arsenic in the anionic forms of arsenate [As (V)] and arsenite [As (III)], both of which have different cytotoxic effects (Quaghebeur and Rengel, 2003). As (III) reacts with the sulfhydryl groups of enzymes and proteins, thereby inhibiting cellular function and resulting in death (Ullrich-Eberius *et al*., 1989). Alternatively, As (V) is an analog of the macronutrient phosphate, so it competes with phosphate for uptake in the roots, as well as in the cytoplasm where it may disrupt metabolism by replacing phosphate in ATP to form unstable ADP-As (Meharg and McNair, 1992). Once taken up by the roots, arsenate is reduced to a more highly toxic species, arsenite, which is subsequently detoxified via soluble thiols such as glutathione and/or phytochelatins (PCs) and transported for vacuolar sequestration (Pickering *et al*., 2000). PCs are low molecular weight thiolate peptides of the general structure (γ-Glu-

Cys)$_n$-Gly (n = 2-11) and are synthesized from glutathione by the constitutively present phytochelatin synthase (Grill *et al*., 1989). Both arsenate and arsenite efficiently induce the production of PCs in plants (Schmoger *et al*., 2000), however it is believed since arsenate has no affinity for the sulfhydryl groups in PCs, As (V) is reduced in the cytoplasm, resulting in As(III)-PC complexes (Quahebeur and Rengel, 2003). Pickerling *et al*. (2000) reported that glutathione and PCs form As(III)-tris-thiolate complexes in *Brassica juncea* upon exposure to As(V). Therefore, PC synthesis causes a depletion of cellular glutathione, resulting in a decreased capacity to quench reactive oxygen species (ROS) (Hartley-Whitaker *et al*., 2001).

Phytoremediation has emerged as a promising, cost-efficient technology for removing toxic metals from contaminated soils and groundwater. The potential for phytoremediation to be an effective means of removing arsenic from contaminated sites has been demonstrated in hyperaccumulators of the *Pteris* genus (Kertulis-Tartar *et al*., 2006; Tu *et al*. 2002; Wei and Chen, 2006) and may be enhanced by a better understanding of plant transcriptional responses to arsenic. Many plant studies have demonstrated the direct involvement of thiol-containing molecules (glutathione, phytochelatins, etc.) in arsenic detoxification, however more robust approaches (i.e. microarrays) should help to clarify how arsenic affects plant physiological processes on a global scale. The goals of this study were to test the hypothesis that many genes would be differentially expressed in response to arsenate stress and to identify genes previously unidentified as significant players in As (V) detoxification using Arabidopsis as a model. In this paper, we investigate the transcriptional responses to As (V) in *Arabidopsis thaliana* using oligonucleotide microarrays. The results demonstrate that As (V) stress

strongly induces Cu/Zn superoxide dismutase (SOD) activity, but represses the production of Fe SODs. This data also suggests the involvement of other antioxidant genes, various transcription factors, tonoplast proteins, and proteins associated with cell wall growth. Of particular interest is the observation that As (V) stress represses a wide range of genes induced by phosphate starvation. The physiological implications of these findings are discussed and we suggest new and exciting avenues for research of arsenic metabolism in plants.

Results

Gene ontology for genes affected by As (V)

Forty-six genes were induced by As (V) treatment. The largest functional categories affected included unknown function, hydrolase, and antioxidant activity. Other functional categories affected by As (V) included genes with transferase, kinase, lyase, transporter, and binding activity (Fig. 1.4; Table 1.1). Alternatively, 113 genes were repressed by As (V), with unknown function, hydrolase, and binding activity representing the largest categories. Genes with transporter, kinase, transferase, and transcriptional regulator activity were also repressed by As (V). (Fig. 1.4; Table 1.2). Differentially expressed As (V)-induced and –repressed genes are listed below (Table 1.1 and Table 1.2, respectively). Most interestingly, it was discovered that As (V) stress repressed transcription of many genes involved the phosphate starvation response (Table 1.4), and also repressed several transcriptional factors.

Superoxide dismutases

SODs represented the highest ranked of both significantly induced as well as repressed genes in response to As (V) stress (Tables 1.1 and 2.1), therefore these genes presented logical primary targets for the validation of our microarray data. Results demonstrated 4.57-fold induction of a chloroplast Cu/Zn SOD (at2g28190), 2.38-fold induction of a Cu/Zn SOD (at1g08830), as well as a 3.16-fold induction of an SOD copper chaperone (at1g12520). Alternatively, Fe SOD (at4g25100) transcripts were downregulated in response to arsenic stress (-5.17-fold change). These findings were confirmed with RT-PCR (Table 3).

Based upon the observations of transcript-level changes in SOD gene expression, we predicted that As (V)-mediated induction of Cu/Zn SOD activity and repression of FeSOD activity would be reflected by nondenaturing PAGE enzyme activity assays (Beauchamp and Fridovich, 1971). This method enables the distinction between the three SOD isoenzymes found in Arabidopsis (CuZnSOD, FeSOD, and MnSOD) by using inhibitors of specific SODs. Gels were preincubated with KCN, which inhibits CuZn SOD, as well as H_2O_2, which inhibits both CuZn SOD and Fe SOD. MnSOD is resistant to both inhibitors (Fig. 1.2). Plants were harvested from control plates containing no arsenate and treated plates containing 100 μM arsenate at seven-, ten-, and thirteen days post-germination. Irrespective of harvest date, CuZnSOD activity was strongly induced by arsenate treatment, whereas FeSOD activity was repressed, and MnSOD showed no change in activity, therefore providing sufficient evidence to confirm our microarray results.

As (V)-treated plants demonstrated lower concentrations of superoxide in leaves as revealed by nitroblue tetrazolium (NBT) staining (Fig. 1.3), suggesting that superoxide is being consumed by elevated levels of SODs following 10 days of As (V) stress. Lower levels of superoxide anions in As (V)-stressed plants cannot be attributed to a change in expression of univalent oxidases (i.e. xanthine oxidase, NAD(P)H oxidase, aldehyde oxidase) which generate superoxide, as differential expression of this gene was not detected by our microarray analysis.

Other antioxidant genes

Other genes with antioxidant activity were induced at lower levels. A peroxiredoxin Q (at3g26060) was induced 1.53-fold. Peroxiredoxin Q is a soluble thioredoxin-dependent reductase located in the thylakoid lumen that reduces hydroperoxides . Unlike peroxidases, which contain a heme group in their active site, peroxiredoxins utilize redox-active thiol groups for their catalytic activity (Petersson *et al*., 2006). The functional role of this protein has not been clearly defined, however studies of peroxiredoxin Q suggest both its involvement in antioxidant defense and possibly redox-regulated signaling (Horling *et al*., 2003; Petersson *et al*., 2006).
Four peroxidases were induced by As (V) treatment (Table 1.1). The following peroxidases exhibited increased levels of transcription (in order of descending transcript abundance): at5g64100 (2.50-fold) > at1g02540 (2.05-fold) > at1g05250 (1.90-fold) > at5g17820 (1.68-fold). Glutathione S-transferases, which are known to respond to oxidative stress, were also affected by As (V) stress.

Transcription factors

The microarray experiment indicated that eight different genes encoding proteins with known transcription factor activity all displayed lower expression levels in As (V)-stressed plants (Table 1.2). One of these transcription factors (at1g12610) encodes a member of the DREB subfamily A-1 of the *ERF/AP2* transcription factor family (*DDF1*). One other AP2-domain-containing transcription factor (at4g34410) that encodes a member of the ERF (ethylene response factor) subfamily B-3 of the *ERF/AP2* transcription factor family was also repressed in response to As (V). Two zinc finger (C2H2 type) genes (at3g46090, at3g46080) encoded a ZAT7 and a protein similar to ZAT7, respectively. Also exhibiting lower expression in As (V)-treated plants were three members of the WRKY family of transcription factors (at2g38470, at4g23810, at1g80840), *WRKY33*, *WRKY53*, and *WRKY40*, respectively as well as one gene encoding NAC domain containing protein 81.

As (V) represses genes involved in phosphate starvation response

The transcriptional trends that we report from this study suggest that As (V) stress results in repression of the Pi starvation response. This phenomenon suggests that high concentrations of As (V) are "perceived" by the plant as high Pi, thereby repressing genes upregulated in response to Pi deprivation. In Table 1.4 we present those genes from our microarray experiment that were affected by As (V) and have also been shown to be induced upon Pi starvation in Arabidopsis by Mission *et al*. (2005) and Morcuende *et al*., (2007). Surprisingly, only 6 genes that were induced upon As (V) stress are known to be

induced by Pi starvation, whereas 22 As (V)-repressed genes have been shown to be induced by Pi starvation (Table 1.4). However, 3 genes that were repressed by As (V) were also reported to be repressed by Pi starvation by Mission *et al*. (2005).

Table 1.4 elucidates some interesting genes for further investigation, particularly in the cases where genes were induced by As (V) as well as shown by Mission *et al*., (2005) as induced by Pi starvation. These included genes encoding a CuZnSOD, a P-type cyclin (*CYCP4;2*; at5g61650), myrosinase-associated proteins (at1g54010; at1g54000), a glycine-rich protein (at2g05510), and a C2-domain-containing protein (at4g15740). Of particular interest, a P-type cyclin (at5g61650) that was induced by As (V) shares significant homology to the *PHO80* gene from yeast.

Sulfate assimilation

The role that thiol groups play in arsenic detoxification has been well characterized, therefore we expected to see induction of genes involved in sulfate assimilation and metabolism in response to arsenic stress. Ferredoxin (at1g10960), a key redox protein found in the chloroplast was As (V)-induced. Expression levels for another gene involved in the sulfate reduction pathway, 5'-adenylylsulfate reductase (*APR3*) (at4g21190) were also elevated in response to As (V) stress. This enzyme catalyzes the reduction of 5'-adenylylsulfate to sulfite using glutathione as an electron donor. Although not involved in sulfate assimilation, the cysteine-rich metal-binding protein, metallothionein (MT) 1A (at1g07600) was also induced. Zimeri *et al*. (2005) showed that *Arabidopsis* knockout mutants for class 1 MTs accumulated significantly less

aboveground As, Cd, and Zn, suggesting that class 1 MTs may play a role in metal and metalloid ion translocation.

Genes involved in cell wall assembly, architecture, and growth

A wide range of genes encoding proteins involved in cell wall activities exhibit altered expression levels in response to As (V) (Table 1.1; Table 1.2). Peroxidases, which were indeed affected by As (V) stress, are known to strengthen the cell wall in response to biotic stress via formation of lignin, extension cross-links, and dityrosine bonds (Passardi *et al*. 2005). Several glycine-rich proteins, which are well-defined structural proteins of the plant cell wall (Mousavi and Hotta, 2005), displayed differential expression in response to As (V). Transcription of glycine-rich protein (at2g05510) was among the most strongly induced genes in As (V)-treated plants, whereas four genes encoding glycine-rich genes (Table 1.2) exhibited lower expression compared to control plants. Additionally, As (V) affected transcription of a multitude of xyloglucan endotransglucosylase / hydrolases (XTHs) and glycosyl hydrolase genes (Table 1.1; Table 1.2), with the majority of these exhibiting lower expression in the presence of As (V).

Transporters and proteins of the tonoplast

Our microarray data suggests the involvement of specific genes with transporter activities in response to As (V) stress in Arabidopsis (Table 1.1; Table 1.2). Genes encoding a plasma membrane intrinsic protein 2 (*PIP2;2*) (at2g37170) and a tonoplast

intrinsic protein (TIP) gamma (at2g36830) were both induced by As (V) treatment (Table 1.1). Both of these genes belong to the aquaporin gene family, which in Arabidopsis consists of 35 members (Alexandersson *et al*., 2005). Both TIPs and PIPs are membrane proteins that facilitate passive transport across membrane. Alternatively, a gene encoding a multidrug and toxic compound extrusion (MATE) efflux protein (at1g61890) was repressed by As (V) (Table 1.2). The functions of MATE family proteins are not defined, and only inferred based on their sequence homology to genes that encode bacterial efflux pumps (Diener *et al*., 2001). Although the function of this protein is also unclear, it has recently been reported to have 12 transmembrane domains and shown to be associated with the tonoplast (Shimaoka *et al*., 2004).

Shimaoka *et al*. (2004) has reported the association of 163 proteins from purified tonoplasts of Arabidopsis, and several of their respective genes were differentially expressed in the current study. Of the As (V)-induced genes, both myrosinase-associated proteins (at1g54010; at1g54000), alcohol dehydrogenase (at1g77120), and the meprin and TRAF domain-containing protein (at5g26280) were all found by these authors to be associated with Arabidopsis vacuoles. There were also genes repressed by As (V) represented among the 163 tonoplast proteins; these included a glycosyl hydrolase family 17 protein (at4g31140), a MATE efflux protein (at1g61890), and a band 7 family protein that is involved in N-terminal protein myristoylation.

Discussion

Arsenic and oxidative stress

Superoxide dismutases

Increasing evidence from mammalian studies demonstrates that ROS are generated in response to exposure to inorganic forms of arsenic (Hei *et al*., 1998; Liu *et al*., 2001; Qian *et al*., 2003). The reduction of arsenic is linked with *in vivo* and *in vitro* ROS production in mammalian cells (Hei *et al*., 1998), but little is known about the mechanisms by which arsenic-induced ROS generation occurs in plants. It is believed that the reduction of As (V) to As (III), which is well documented in plants, results in the production of ROS (Meharg and Hartley-Whitaker, 2002; Mylona *et al*, 1998). However, this increase in ROS may also be due to either depletion of glutathione or inhibition of antioxidant enzymes. Plants have evolved both nonenzymatic antioxidants (i.e. glutathione, ascorbate, and carotenoids), as well as antioxidant enzymes (i.e. superoxide dismutases, catalases, and peroxidases) to manage the balance of ROS in the cell .

SODs represent a first line of defense by converting superoxide radicals to H_20_2, whereas catalases and peroxidases remove H_20_2. Three classes of SODs have been identified according to the active site metal cofactor: FeSOD, MnSOD, and Cu/ZnSOD. Mylona *et al*. (2001) showed that both As (V)- and As (III)-induced expression of glutathione-s-transerases (GSTs), catalases, and SODs in *Zea mays*. An increase in SOD activity was correlated with an increase in As (V) treatment in *Holcus lanatus* (Hartley-

Whitaker *et al*., 2001). Srivastava *et al*. (2005) observed higher levels of SOD, catalase, and ascorbate peroxidase in *Pteris vittata*, an arsenic hyperaccumulator, than in arsenic-sensitive fern species *Pteris ensiformis* and *Nephrolepsis exaltata*. These researchers concluded that arsenic-induced increases in antioxidant enzymes levels may represent a secondary defensive mechanism against oxidative stress in *Pteris vitatta* and correspond with its arsenic accumulation and lack of toxicity symptoms. Cao *et al*. (2004) showed that *Pteris vittata* SOD, catalase, and peroxidase levels rose sharply in response to low levels of As (V), but leveled off at As (V) levels that rose above 20 mg kg^{-1}, which was consistent with changes in biomass in the arsenic hyperaccumulator.

Lower levels of superoxide anions in As (V)-stressed plants (Figure 3) cannot be attributed to a change in expression of univalent oxidases (i.e. xanthine oxidase, NAD(P)H oxidase, aldehyde oxidase) which generate superoxide, as differential expression of this gene was not detected by our microarray analysis. However, an alternative hypothesis may be that reduction of extracellular ATP due to *arsenolysis* or As (V) substitution for phosphate in ATP synthesis causes a reduction of superoxide accumulation. Song *et al*. (2006) showed that extracellular ATP and ADP induce the accumulation of superoxide via NADPH oxidases in Arabidopsis. Based on the reports of these researchers, it is likely that our NBT staining results may also be a reflection of As (V)-induced ATP depletion.

Although the strong induction of SODs in response to As (V) stress was not surprising, the dramatically lower levels of FeSODs were unexpected. We suggest the involvement of an NAC domain-containing transcription factor to explain the observed decrease in FeSOD transcription based on our microarray results (Table 1.2). Tran *et al*.

(2004) generated transgenic plants to overexpress three different Arabidopsis NAC transcription factors and identified NAC-dependent genes using microarrays. Not only was at4g25100 (FeSOD) expression found to be NAC-dependent, but transcription of other genes we have observed to be repressed by As (V) stress also appear to be dependent on NAC-domain containing transcription factors.

Peroxidases

Peroxidases are functionally diverse and participate in two major cycles: the hydroxylic cycle where peroxidases regulate H_20_2 levels and release ROS (·OH, HOO·) and the peroxidative cycle where various substrates (e.g. phenolic compounds) are oxidized or polymerized. Their involvement in a broad range of physiological processes allows peroxidase expression in all plant organs from germination to early senescence, however they are predominantly expressed in the roots (Passardi *et al*. 2005).

Despite the involvement of peroxidases in response to arsenic-induced oxidative stress, these enzymes may also play a detoxifying role via their capacity for production of phenolic polymers. Phenolic substrates are often polymerized by peroxidases to strengthen the cell wall in response to biotic stress (formation of lignin, extension cross-links, dityrosine bonds) (Passardi *et al*. 2005), however it is also believed that these phenolic polymers may protect the cell from toxic metals. An interesting example comes from a report by Lavid *et al*. (2001) that demonstrated polyphenols and high constitutive levels of peroxidases in *Nymphaeae* epidermal glands played a major role in cadmium

accumulation and tolerance. It would be appropriate to investigate the potential role of peroxidase-generated phenolic polymers in arsenic-stressed Arabidopsis plants.

It is possible that arsenic detoxification may occur via oxidation of the As (III) to the less toxic As (V) by increased levels of H_2O_2, which is suggested by our data. For example, superoxide dismutases generate H_2O_2 as a result of the dismutation of superoxide radicals, whereas peroxidases may either consume or generate H_2O_2. Aposhian *et al*. (2003) demonstrated *in vitro* evidence that As (III) is oxidized to As (V) by H_2O_2 in the absence of enzyme. We would expect an accumulation of H_2O_2 due to a decrease of glutathione peroxidase-mediated H_2O_2 consumption by considering depletion of the glutathione pool by glutathione and phytochelatin detoxification of As (III). Additionally, catalase mRNA (at1g20620) levels were lower in As (V)-treated plants as indicated by microarrays (Table 1.2.), which would also contribute to increased abundance of H_2O_2. Strong induction of CuZnSOD enzymes also results in elevated levels of H_2O_2, as this metabolite is produced by SOD dismutation of superoxide. Based on our data, We propose H_2O_2 oxidation as a potential arsenic detoxification mechanism in plants, however, further experimentation is required to test this hypothesis.

GSTs

Glutathione *S*-transferases (GSTs) are a functionally diverse group of proteins that catalyze the conjugation of glutathione to a wide range of xenobiotic compounds (Marrs *et al*., 1996). GSTs are induced by various biotic and abiotic stresses (Marrs *et al*. 1996) and seem to play a significant role in antioxidant defense (Frova, 2003). Therefore, it is

likely that As (V)-mediated induction of GST transcription (GST20; Table 1.1) results from oxidative stress. However, it is interesting to note that our data show differential expression between a GST member of the Tau GST class (GST20; Table 1.1) and repression of two members of the phi GST class (GST6 and GST7; Table 1.2). These results corroborate the work of others that have demonstrated differential transcriptional response to salicylic acid treatments between GST19 (tandem duplicate of As (V)-induced GST20) and GST6 and GST7 (Sappl *et al*., 2004). Additionally, these authors present evidence that GST6 and GST7 basal protein levels differ drastically (3-fold vs. 90-fold induction) in response to SA treatment, and suggest possible sub-functionalization (Force *et al*., 1999) of genes that seemingly arise from tandem duplication.

Based on the work of Wagner *et al*. (2002), We are hopeful that GST20 (at1g78370) exhibits some specificity to an arsenic species, thus playing some defined role in arsenic detoxification. These authors performed substrate specificity experiments that suggests tau-class GSTs display only transferase activities and have narrow substrate specificity, whereas phi-class GSTs demonstrate both transferase and peroxidase activities with more promiscuous specificities. Based on these data, we are performing additional experiments to elucidate the putative role of Arabidopsis GST20 in As (V) metabolism.

Transcription factors

Most interestingly, our data corroborates those of Tran *et al*. (2004), suggesting the involvement of a different NAC domain-containing transcription factor (at5g08790) in expression of FeSOD, as well as several other genes known to exhibit NAC-dependent expression. NAC proteins comprises a large gene family (>100 members in Arabidopsis) of plant-specific transcription factors that have roles in wide-ranging processes such as development, defense, and abiotic stress response (Olsen *et al*., 2005). Tran *et al*. (2004) employed microarray analysis of NAC-overexpression Arabidopsis mutants to discover genes exhibiting dependence on NAC transcription factors for transcription. Therefore, we speculate that repression of *NAC81* (at5g08790) in As (V)-stressed Arabidopsis may be responsible for the observed repression of FeSOD (at4g25100), ferritin 1 (FER 1) (at5g01600), *XTH15* (at4g14130), *XTH24* (at4g30270), *erd1* ATP-dependent Clp protease ATP-binding subunit (at5g51070), and a branched-chain amino acid amino transferase 2 (at1g10070), as these genes were reported by Tran *et al*. (2004) as exhibiting NAC-dependent expression. We are currently investigating the putative role of *NAC81* in As (V)-mediated stress responses in Arabidopsis.

The WRKY gene family represents a large group of plant-specific transcription factors. These transcription factors are characterized by their conserved WRKYGQK DNA-binding sequence followed by a Cys_2His_2 or $Cys_2HisCys$ zinc finger binding motif (Ulker and Somssich, 2004) and have been implicated to play regulatory roles in plant defense response, senescence, and trichome development (Eulgem *et al*., 2000). WRKY proteins bind preferentially to the TTGAC(C/T) W-box, which is found in the promoter

region of a wide range of defense-related genes (Dong *et al*., 2003). There are 74 genes in Arabidopsis that encode for WRKY transcription factors and they have been divided into three classification groups based on the number and type of zinc finger motif (Eulgem *et al*., 2000).

Interestingly, one member from each of the three WRKY classification groups was represented as repressed by As (V) in our microarray data (Table 1.2), which may infer some sort of co-regulatory relationship. *WRKY33* (at2g38470), *WRKY53* (at4g23810), and *WRKY40* (at1g80840) all displayed lower expression levels in As (V)-stressed plants and belong to group 1, group 3, and group 2, respectively. Recent work has shown that activation of *WRKY33* and *WRKY53* involved a MAP kinase pathway (Wan *et al*., 2004). Although one study reported that *WRKY33* was localized in the chloroplast (Mahalingam *et al*., 2005), more recent evidence from transient expression assays demonstrates that *WRKY33* is localized to the nucleus (Zheng *et al*., 2006; Lippok *et al*., 2007). *WRKY33* exhibits strong and rapid induction upon pathogen associated molecular patterns (PAMPs), a wide range of pathogens, chitin, and oxidative stress (Lippok *et al*., 2007). Like many other Arabidopsis WRKY genes, *WRKY33* contains three W-box motifs within its promoter, which suggests that this gene is under positive or negative feedback regulation (Lippok *et al*., 2007). Perhaps arsenic-mediated disruption of disulfide bonds within the zinc finger DNA binding domain could explain decreased WRKY transcript abundance.

The involvement of *WRKY40* in response to pathogenic infection has also been well established (Dong *et al*., 2003; Xu *et al*., 2006). Additionally, nuclear localization of *WRKY40* has been demonstrated, which suggests it acts as a transcriptional regulator

(Xu *et al*., 2006). Interestingly, transgenic Arabidopsis plants that constitutively expressed *WRKY40* displayed a phenotype with more serrated leaves than wild type, suggesting a role in growth regulation (Xu *et al*., 2006). Investigating the Arabidopsis *WRKY40* overexpression, as well as knockout mutants generated by Xu *et al*. (2006) may elucidate the significance that this protein plays in As (V) stress response.

It is unclear why WRKY transcription factor expression levels were lower in As (V)-treated plants, however it may be the result of arsenic-mediated disruption of disulfide bonds within the active site of the zinc finger binding motifs. Due to the presence of multiple W-box motifs within the promoters of WRKY genes, it is likely that expression of these genes is under negative or positive feedback control (Lippok *et al*., 2007), therefore disruption of the DNA binding domain would indeed affect transcription. This may also explain the decreased abundance of Cys_2His_2-type zinc finger gene transcripts (at3g46090; at3g46080) in As (V)-stressed plants.

An alternative explanation for the observed suppression of these transcription factors comes from the chemical similarity of As (V) and Pi. Devaiah *et al*. (2007) elucidated the involvement of a WRKY transcription factor in phosphate acquisition. These authors demonstrated that expression of several genes including phosphatases and high-affinity phosphate transporters was decreased when *WRKY75* was suppressed. As a result of *WRKY75* suppression, phosphate uptake was also reduced. In light of our microarray results, perhaps lower levels of WRKY proteins indicate an As (V)-specific perception by the plant. Interestingly, Mission *et al*. (2005) reported that *WRKY53* was induced by phosphate starvation in Arabidopsis leaves, which suggests it may play an important role in As (V)-mediated repression of transcription. It would be interesting to

further investigate the involvement of *WRKY33*, *WRKY40*, and *WRKY53* transcription factors in response to various As (V) and/or phosphate treatments.

As (V) stress represses genes induced by Pi deprivation

Our microarray data show that many genes repressed by As (V) stress have been reported by others (Morcuende *et al*., 2007; Mission *et al*., 2005) to be induced in response to Pi deprivation in *Arabidopsis thaliana*. Our results are also in agreement with the recently proposed ideas of Catarecha *et al*., (2007) who studied an Arabidopsis mutant that displayed enhanced arsenic accumulation. These authors identified a Pi transporter mutant with a decreased rate of As (V) uptake and increased As (V) accumulation. By comparing gene expression of the mutant with wild-type plants, it was shown that in Arabidopsis, As (V) rapidly repressed genes involved in the Pi starvation response and induced the expression of other As (V)-responsive genes. Interestingly, the repression of Pi starvation genes was shown to be specific for As (V), whereas the As (V)-induced genes were also induced by As (III). This led Catarecha *et al*. (2007) to propose a model that suggests arsenic acts via two separate signaling pathways. Due to the chemical similarity of As (V) and Pi, As (V) fools the Pi sensor, thus initiating the repression of the Pi starvation response. Although this study did not show differential expression of the high-affinity Pi transporter, which may be due to differences in experimental approach, Catarecha *et al*. (2007) illustrated the high sensitivity of the Pi transporter to As (V) and suggested that plants have evolved an As (V) sensing system

whereby As (V) and Pi signaling pathways oppose each other to protect the plant from arsenic toxicity.

Although not reported as responsive to Pi deprivation, an interesting gene candidate that caught our attention was the *RSH 2* (rela-spot homolog; at3g14050), which participates in guanosine tetraphosphate metabolism. In bacteria, this protein is known for its role in the "stringent response" to nutrient deprivation, pathogen attack, and other stresses, whereas in plants, its role is unclear (van der Biezen *et al*., 2000; Givens *et al*., 2004). It is of particular interest with respect to As (V) stress in plants because it synthesizes the unique nucleotide guanosine-3',5'-(bis) pyrophosphate (ppGpp), thus leading us to suspect that As (V) affects its suggested role (Givens *et al*., 2004) in regulation of chloroplast gene expression in response to stress signals. The unusual nature of this poorly understood phosphorylated nucleotide may uncover a new, putative gene target for discovering mechanisms of As (V) signaling in plants.

We are particularly interested in uncovering new pathways involved in As (V) signaling in plants. The P-type cyclin (at5g61650) that was induced by As (V) shares significant homology to the *PHO80* gene from yeast. Cyclins bind and activate cyclin-dependent kinases, which play key roles in cell division via phosphorylation of critical substrates, such as the retinoblastoma protein, transcription factors, nuclear laminar proteins, and histones (Morgan, 1997). Interestingly, Torres Acosta *et al*. (2004) demonstrated that expression of this cyclin from Arabidopsis restored the phosphate signaling pathway in a *PHO80*-deficient yeast mutant, suggesting a putative key Pi signaling role.

Recent investigations into the global-scale transcriptional changes to phosphate deprivation in *Arabidopsis* have elucidated a broad range of genes involved in phosphate metabolism (Morcuende *et al*., 2007; Mission *et al*., 2005). Here we report that many of these genes are also affected by As (V) (Table 1.4). It is likely that this observation can be explained by a saturation effect of the phosphate analog, As (V), thereby misleading metabolic and regulatory perception of the toxic metalloid to be a plentiful supply of Pi. Interestingly, the three highest ranking differentially expressed genes found by Morcuende *et al*. (2007) to be strongly induced by Pi starvation (at1g73010 > at5g20790 > at1g17710, respectively), were also repressed by As (V) in our study. Table 1.4 illustrates the overlap of differentially expressed genes found in the current study compared with those found by two separate global investigations of Pi starvation in *Arabidopsis*.

The comparison of As (V)-repressed genes that have also been shown to be induced by Pi deprivation elucidate some promising candidates for future studies. For example, we are particularly interested in genes with unknown function that are strongly induced in both roots and leaves by Pi starvation (i.e. at1g73010; at1g17710; at2g04460; at5g20790; Mission *et al*. 2005, supplemental data; Morcuende *et al*. 2007). These putative gene candidates may provide opportunities for gaining insight into As (V) / Pi dynamics in *Arabidopsis thaliana*.

Arsenate may affect cell wall growth

Due to the role that XTHs play in cell wall loosening, their activity contributes to cell wall growth and cell expansion (Rose *et al*., 2002). Repression of mRNA transcripts for these genes may not reflect protein activity, however the As (V)-stressed plants display a phenotype of reduced growth compared to wild type, therefore, decreased *XTH* expression may be a contributing factor. Decreased expression of other genes involved in cell wall growth that are consistent with the As (V)-stressed phenotype include a polygalacturonase inhibitory protein and an invertase / pectin methylesterase family protein (Table 1.2).

Putative arsenic transport mechanisms

Specific transporters have been discovered for arsenic detoxification in yeast, bacteria, and humans, however the molecular mechanisms of cellular arsenic transport in plants are unclear. In mammalian cells, one defined arsenic detoxification pathway involves the reduction of As (V) and subsequent glutathione conjugation via GSTs to form As (III) triglutathione [$As(GS)_3$] which is then excreted through a multi-drug resistance-associated protein transporter (MRP2/cMOAT) (Kala *et al*., 2000; Leslie *et al*., 2004). Vacuolar accumulation of arsenic in *Saccharomyces cerevisiae* is known to occur via transport of As (III)-GS_3 complexes across an ABC-type transporter (Ghosh *et al*., 1999), however a yeast aquaglyceroporin Fps1p was found to be involved with transport of arsenic trioxide [$As(OH)_3$] (Liu et al. 2006), the protonated form of arsenite that is

more prevalent and more toxic at physiologic pH (Ramirez-Solis et al. 2004). Additional evidence points towards the role of aquaglyceroporins in mediating transport of arsenite and methylated forms of arsenic from the *E. coli* GlpF (Meng et al. 2004; Sanders et al., 1997) to the rat AQP9 (Liu et al. 2002; Liu et al. 2006) , suggesting that arsenite movement is a ubiquitous property of aquaglyceroporins (Liu et al. 2006). Currently, there is no *in vivo* evidence of $As(GS)_3$ or As-PC complex transport in plants, nor have there been any reports of specific transporters involved in vacuolar deposition of arsenic (Tripathi *et al*., 2007). However, our data suggests that two members of the aquaporin family, *PIP2;2* and a tonoplast intrinsic protein gamma (at2g36830) may be involved in As (V) transport. Due to the high sequence conservation of aquaporins from prokaryotes to eukaryotes, we expect that PIP2;2 and Gamma TIP (at2g36830) are likely involved in arsenic transport in plants.

Conclusion

The transcriptional data seem to suggest a central role for H_20_2 in response to arsenate stress, which also plays a predominant role in signal transduction (Vranova *et al*., 2002). The results clearly support the recent study by Catarecha *et al*. (2007) that suggests As (V) and Pi signaling pathways act in opposition to protect plant health. Here we provide a global snapshot of the *Arabidopsis* transcriptome under As (V) stress that strengthens and complements their proposed model. This study opens new, unanticipated avenues of research, particularly in the areas of transcriptional regulation and signaling

pathways involved in As (V) detection, while providing insight into genes with poorly defined or unknown function.

Materials and methods

Plants and growth conditions

Seeds of *Arabidopsis thaliana* ecotype Columbia plants were surface sterilized and plated on agar-solidified Murashige and Skoog culture medium supplemented with B5 vitamins, 10% sucrose, 2% Gelrite ®, pH 5.8. Arsenic-treated plates were supplemented with 100 μM potassium arsenate (Sigma) according to a previously determined sub-lethal growth response curve. Plates were cold stratified at 4°C for 24 hrs and then placed in a growth chamber at 25°C under a 16 hr photoperiod. After 10 d, 2 g of whole plant material (shoots + roots) was harvested from each plate, frozen in liquid nitrogen, and subjected to RNA isolation using Trizol ® reagent (Invitrogen, Carlsbad, CA) according to manufacturer's protocol. A total of three biological replicates were assayed (3 control, 3 treated) where each pooled 2 g sample represented a single biological replicate.

Microarray experiments and aRNA labeling

Total RNA from six biological replicates were purified using RNeasy MiniElute columns (Qiagen, Valencia, CA). A total of 1.25 µg of purified total RNA was subjected to Aminoallyl Message Amp II kit (Ambion, Austin, TX) first strand cDNA synthesis, second strand synthesis, and *in vitro* transcription for amplified RNA (aRNA) synthesis. aRNA was purified according to manufacturers protocol (Ambion, Austin, TX) and quantified using a Nanodrop spectrophotometer. Two 4 µg samples of aRNA were labeled with Cy3 and Cy5 monoreactive dyes (Amersham Pharmacia, Pittsburgh, PA) in order to conduct a dye swap technical replicate for each biological replicate. Each aRNA sample was brought to dryness in a Speedvac and dissolved in 5 µL of 0.2 M $NaHCO_3$ buffer. Five microliters of Cy3 or Cy5 (in DMSO) was added to each sample and incubated for 2 hrs in the dark at room temperature. Labeled aRNA was purified according to kit instructions (Ambion, Austin, TX) and quantified using the Nanodrop spectrophotometer. One-hundred pmol Cy3- and Cy5-labeled aRNA targets were denatured by incubating at 65°C for 5 min and added to a hybridization mix containing 9 µl 20X SSC, 5.4 µl Liquid Block (Amersham Pharmacia, Pittsburgh, PA), and 3.6 µl 2% SDS for a 90 µl total volume.

Hybridization and data analysis

Microarrays comprised of 70-mer oligonucleotides obtained from the University of Arizona were immobilized by rehydrating the slide over a 50ºC waterbath for 10 s and snap drying on a 65ºC heating block for 5 s for a total of four times. Slides were UV-

crosslinked at 180 mJ in a UV cross-linker (Stratagene, La Jolla, CA). The slides were then washed in 1% SDS, dipped in 100% EtOH five times followed by 3 min shaking. Slides were spun dry at 1000 rpm for 2 minutes and immediately placed in a light-proof box. The 90 µl hybridization mix was pipetted onto a microarray slide underneath a lifterslip (Lifterslip, Portsmouth, NH) and placed in a hybridization chamber (Corning, Corning, NY) overnight at 55ºC. After hybridization, slides were washed in 2X SSC, 0.5% SDS for 5 minutes at 55ºC, 0.5X SSC for 5 minutes at room temperature, and 0.05X SSC for 5 minutes at room temperature. Slides were then spun dry at 1000 rpm in a Sorvall centrifuge and scanned with a GenePix 4000B scanner (Axon Instruments, Inc., Union City, CA). The intensity variation was removed by fitting a loess regression using SAS 9.1 (SAS, Cary, NC). Data were log-2 transformed and statistically analyzed using rank product statistics as described by (Breitling *et al.,* 2004) to identify differentially expressed genes. Bioconductor Rank Prod package was used to perform the rank product analysis (Hong *et al.,* 2006; Gentleman *et al*., 2004). Significantly different genes reported in this study exhibited $P<0.001$, as designated by the rank product analysis. The false discovery rate (FDR) value obtained was based on 10,000 random permutations. Since 10,000 random permutations was very computer intensive, 1000 random permutations were performed 10 different times each time starting with a different random seed number and the average FDR value calculated was used for further analysis. The genes that had FDR values less than or equal to 0.01 were considered as differentially expressed.

Microarray Data Quality Control

Global gene expression profiling comparing arsenate-treated *Arabidopsis* plants with control was carried out to better understand the mechanisms of plant response to arsenate stress and to identify genes involved in arsenic metabolism. For microarray data quality control, we examined both dye dependent effects and distribution of the ratio after normalization. Figure 1.5 illustrates the quality of microarray experiments, as well as the overall gene expression pattern. Figure 1.5 shows the normalized M vs. A plot, which was generated as a scatter plot of log intensity ratios $M = log_2 (R/G)$ versus average log intensities $A = log_2 (R*G)/2$, where R and G represent the fluorescence intensities in the Cy3 and Cy5 channels, respectively (Yang and Speed, 2002). As shown by the figure, Loess normalization effectively removed dye dependent effects in the microarray and rendered evenly distributed ratios across all signal intensities. Figure 1.5 also presents a histogram suggesting a normal distribution of the logarithm 2-based transformed ratio. Overall, the microarray experiments generated high quality data without significant dye-dependent effects and skewness of ratio distribution.

Gene ontology analysis

Gene ontology annotations were translated from microarray data using the GO annotations bioinformatics tool available at The Arabidopsis Information Resource Web site (http://www.arabidopsis .org/tools/) where results were based on molecular function.

RT-PCR amplification

Total RNA was extracted from *Arabidopsis thaliana* ecotype Columbia grown for ten days as described for the microarray experiment. Five micrograms of total RNA was reverse-transcribed with oligo$(dT)_{20}$ primers using the Superscript III first-strand cDNA synthesis kit (Invitrogen, Carlsbad, CA). Real-time PCR was performed using the ABI 7000 Sequence Detection System (Applied Biosystems, Foster City, CA). PCR was performed in a 15 µl reaction volume containing QuantiTect SYBR® Green PCR mix (Qiagen, Valencia, CA) and gene-specific primers were designed with PrimerExpress software. Ubiquitin was used as the reference gene, and the primer sequences for *Arabidopsis* ubiquitin gene were CACACTCCACTTGGTCTTGCG (F) and TGGTCTTTCCGGTGAGAGTCTTCA (R). Primers for *Arabidopsis* genes were as follows: At1g08830 -GATGGAACTGCCACCTTCACA (F) and TCATCAGGGTCTGCATGGAC (R), At2g28190 -TCAACAGGACCACATTTCAACC (F) and TCGGCATTGGCATTTATGTTT (R), At1g12520 – ACAGAGCCATTGGGAGACCTG (F) and CCGATAAGGTCTGCAACCTTG (R), and At4g25100 –TCTTGGAACCGAGCTTGAAGG (F) and ACGCCTGAGCAGCGTTGTT (R). After the real-time PCR experiment, Ct number was extracted for both reference gene and target gene with auto baseline and manual threshold.

SOD activity assay

Total protein was extracted from whole *Arabidopsis* plants grown on plates as described above and quantified by the method of Bradford (1976) using BSA as a

standard. Bovine SOD (Sigma) was used in each gel to serve as a positive control for SOD activity. Following electrophoretic separation on a 10% non-denaturing polyacrylamide gel, SOD activity was determined as described by Beauchamp and Fridovich (1971) and modified by Azevedo *et al*. (1998). The gels were rinsed with DDI water and incubated in the dark for 30 min at room temperature in a reaction mixture containing 50 mM potassium phosphate buffer (pH 7.8), 1 mM EDTA, 0.05 mM riboflavin, 0.1 mM nitroblue tetrazolium and 0.3% (v/v) TEMED. Following incubation, gels were rinsed with DDI water and illuminated in water until SOD bands were visible. The gels were then immersed in a 6% (v/v) acetic acid solution to stop the reaction. To confirm specificity of Cu/Zn-SOD activity, H_20_2 and KCN were used as inhibitors as described by Azevedo *et al*. (1998) and modified by Vitoria *et al*. (2001). Mn-SOD is resistant to both inhibitors, Fe-SOD is resistant to KCN and inhibited by H_20_2, and Cu/Zn-SOD is inhibited by both inhibitors, thus allowing classification of SOD activity. Prior to SOD staining, gels containing lanes in triplicate were cut into three parts; one gel was treated as described above, the second and third parts were incubated for 20 min in 100 mM potassium phosphate buffer (pH 7.8) containing either 2 mM KCN or 5 mM H_20_2, respectively. Following incubation, gels were rinsed with DDI water and then stained for SOD activity.

NBT staining for superoxide radical accumulation

Superoxide levels were detected via the reduction of nitroblue tetrazolium (Sigma) according to Song *et al*., (2006). Instead of infiltrating with a syringe, leaves

were vacuum infiltrated with potassium phosphate buffer for 5 min and incubated for 60 min prior to immersion in staining solution. Leaves were boiled in 96% ethanol until clear and stored in 70% ethanol prior to analysis.

References

Alexandersson E, Fraysse L, Sjovall-Larsen S, Gustavsson S, Fellert M, Karlsson M, Johanson U, Kjellbom P (2005) Whole gene family expression and drought stress regulation of aquaporins. Plant Mol Biol 59: 469-484.

Aposhian HV, Zakharyan RA, Avram MD, Kopplin MJ, Wollenberg ML (2003) Oxidation and detoxification of trivalent arsenic species. Toxicol Appl Pharmacol 193: 1-8.

Azevedo RA, Alas RM, Smith RJ, Lea PJ (1998) Response of antioxidant enzymes to transfer from elevated carbon dioxide to air and ozone fumigation, in the leaves and roots of wild-type and a catalase-deficient mutant of barley. Physiol Plant 104: 280–292.

Beauchamp C, Fridovich I (1971) Superoxide dismutase: Improved assays and an assay applicable to acrylamide gels. Anal Chem 44: 276-287.

Benjamini Y, Hochberg Y (1995) Controlling the false discovery rate: A practical and powerful approach to multiple testing. J Royal Stat Soc 57B: 289-300.

Bradford MM (1976) A rapid and sensitive method for the quantitation of microgram quantities of protein utilizing the principle of protein-dye binding. Anal Biochem 72: 248-254.

Breitling R, Armengaud P, Amtmann A, Herzyk P (2004) Rank products: a simple, yet powerful, new method to detect differentially regulated genes in replicated microarray experiments. FEBS Lett 573: 83-92.

Cao X, Ma LQ, Tu C (2004) Antioxidant responses to arsenic in the arsenic-hyperaccumulator Chinese brake fern (*Pteris vittata* L.) Env Poll 128: 317-325.

Catarecha P, Segura MD, Franco-Zorrilla JM, Garcia-Ponce B, Lanza M, Solano R, Paz-Ares J, Leyva A (2007) A Mutant of the arabidopsis phosphate transporter PHT1;1 displays enhanced arsenic accumulation. Plant Cell 19: 1123-1133.

Chakraborti D, Mukherjee SC, Pati S, Sengupta MK, Rahman MM, Chowdhury UK, Lodh D, Chanda CR, Chakraborti AK, Basu GK (2003) Arsenic groundwater contamination in Middle Ganga Plain, Bihar, India: a future danger? Environ Health Perspect 111: 1194-1201.

Devaiah BN, Karthikeyan AS, Raghothama KG (2007) WRKY75 transcription factor is a modulator of phosphate acquisition and root development in Arabidopsis. Plant

Physiol 143: 1789-1801.

Diener AC, Gaxiola RA, Fink GR (2001) Arabidopsis ALF5, a multidrug efflux transporter gene family member, confers resistance to toxins. Plant Cell 13: 1625-1638.

Dong J, Chen C, Chen Z (2003) Expression profiles of the Arabidopsis WRKY gene superfamily during plant defense response. Plant Mol. Biol 51: 21-37.

Eulgem T, Rushton PJ, Robatzek S, Somssich IE (2000) The WRKY superfamily of plant transcription factors. Trends Plant Sci 5: 199-206.

Force A, Lynch M, Pickett FB, Amores A, Yan YL, Postlethwait J (1999) Preservation of duplicate genes by complementary, degenerative mutations. Genetics 151: 1531-1545.

Frova C (2003) The plant glutathione transferase gene family genomic structure, functions, expression, and evolution. Physiol Plantarum 119: 469-479.

Gentleman RC, Carey VJ, Bates DM, Bolstad B, Dettling M, Dudoit S, Ellis B, Gautier L, Ge Y, Gentry J, Hornik K, Hothorn T, Huber W, Iacus S, Irizarry R, Leisch F, Li C, Maechler M, Rossini AJ, Sawitzki G, Smith C, Smyth G, Tierney L, Yang JY, Zhang J (2004) Bioconductor: open software development for computational biology and bioinformatics. Genome Biol 5: R80.

Ghosh M, Shen J, Rosen BP (1999) Pathways of As(III) detoxification in *Saccharomyces cerevisiae*. Proc Natl Acad Sci USA 96: 5001-5006.

Grill E, Loffler S, Winnaker E, Zenk M (1989) Phytochelatins, the heavy-metal-binding peptides of plants, are synthesized from glutathione by a specific γ-glutamylcysteine dipeptidyl transpeptidase (phytochelatin synthase). Proc Natl Acad Sci USA 86: 6838-6842.

Gupta SA, Webb RP, Holaday AS, Allen RD (1993) Overexpression of superoxide dismutase protects plants from oxidative stress. Plant Physiol 103: 1067-1073.

Hartley-Whitaker J, Ainsworth G, Vooijs R, Ten Bookum W, Schat H, Meharg AA (2001) Phytochelatins are involved in differential arsenate tolerance in *Holcus lanatus*. Plant Physiol 126: 299-306.

Hei TK, Liu SX, Waldren C (1998) Mutagenicity of arsenic in mammalian cells: role of reactive oxygen species. Proc Natl Acad Sci USA 95: 8103-8107.

Hong F, Breitling R, McEntee CW, Wittner BS, Nemhauser JL, Chory J (2006) RankProd: a bioconductor package for detecting differentially expressed genes in

meta-analysis. Bioinformatics 22: 2825-2827.

Horling F, Lamkemeyer P, Konig J, Finkemeier I, Kandlbinder A, Baier M, Dietz KJ (2003) Divergent light-, ascorbate-, and oxidative stress-dependent regulation of expression of the peroxiredoxin gene family in Arabidopsis. Plant Physiol 131: 317-325.

International Agency for Research on Cancer (1987) Monograph of the evaluation of carcinogenic risk to humans – Overall evaluation of carcinogenicity: An update of IARC monographs 1 to 42 (Suppl. 47). Lyon: International Agency for Research on Cancer. P. 100.

Kala SV, Neely MW, Kala G, Prater CI, Atwood DW, Rice JS, Lieberman MW (2000) The MRP2/cMOAT transporter and arsenic-glutathione complex formation are required for biliary excretion of arsenic. J. Biol. Chem 275: 33404-33408.

Kertulis-Tartar GM, Ma LQ, Tu C, Chirenje T (2006) Phytoremediation of an arsenic-contaminated site using Pteris vittata L.: a two-year study. Int. J. Phytoremediation 8: 311-322.

Kliebenstein DJ, Monde R, Last RL (1998) Superoxide dismutase in *Arabidopsis*: An eclectic enzyme family with disparate regulation and protein localization. Plant Physiol 118: 637-650.

Lavid N, Schwartz A, Lewinsohn E, Tel-Or E (2001) Phenols and phenol oxidases are involved in cadmium accumulation in the water plants Nymphoides peltata (Menyanthaceae) and Nymphaeae (Nymphaeaceae). Planta 214: 189-195.

Leslie EM, Haimeur A, Waalkes MP (2004) Arsenic transport by the human multidrug resistance protein 1 (MRP1/ABCC1). Evidence that a tri-glutathione conjugate is required. J Biol Chem 279: 32700-32708.

Lippok B, Birkenbihl RP, Rivory G, Brummer J, Schmelzer E, Logemann E, Somssich IE (2007) Expression of AtWRKY33 encoding a pathogen- or PAMP-responsive WRKY transcription factor is regulated by a composite DNA motif containing W box elements. Mol Plant Microbe Interact 20: 420-429.

Liu SX, Athar M, Lippai I, Waldren C, Hei TK (2001) Induction of oxyradicals by arsenic: implication for mechanism of genotoxicity. Proc Natl Acad Sci USA 98: 1643-1648.

Liu Z, Shen J, Carbrey JM, Mukhopadhyay R, Agre P, and Rosen BP (2002) Arsenite transport by mammalian aquaglyceroporins AQP7 and AQP9. *Proc Natl Acad Sci U S A* 99: 6053-6058.

Liu Z, Styblo M, and Rosen BP (2006) Methylarsonous acid transport by aquaglyceroporins. *Environ Health Perspect* 114: 527-531.

Mahalingam R, Shah N, Scrymgeour A, Fedoroff N. (2005) Temporal evolution of the *Arabidopsis* oxidative stress response. Plant Mol Biol 57: 709-730.

Marrs KA, Alfenito MR, Lloyd AM, Walbot V. (1995) A glutathione S-transferase involved in vacuolar transfer encoded by the maize gene Bronze-2. Nature 375: 397-400.

Meharg A, Macnair M (1992) Suppression of the high affinity phosphate uptake system: a mechanism of arsenate tolerance in *Holcus lanatus* L. J Exp Bot 43: 519-524.

Meharg A, Hartley-Whitaker J (2002) Arsenic uptake and metabolism in arsenic-resistant and non-resistant plant species. New Phytologist 154: 29-43.

Meng YL, Liu Z, and Rosen BP (2004) As(III) and Sb(III) uptake by GlpF and efflux by ArsB in Escherichia coli. J Biol Chem 279: 18334-18341.

Misson J, Raghothama KG, Jain A, Jouhet J, Block MA, Bligny R, Ortet P, Creff A, Somerville S, Rolland N, Doumas P, Nacry P, Herrerra-Estrella L, Nussaume, L, Thibaud MC (2005) A genome-wide transcriptional analysis using *Arabidopsis thaliana* Affymetrix gene chips determined plant responses to phosphate deprivation. Proc Natl Acad Sci USA 102: 11934-11939.

Morcuende, R., Bari, R., Gibon, Y., Zheng, W., Pant, B.D., Blasing, O. et al. (2007) Genome-wide reprogramming of metabolism and regulatory networks of Arabidopsis in response to phosphorus. Plant Cell Environ 30: 85-112.

Morgan DO (1997) Cyclin-dependent kinases: engines, clocks, and microprocessors. Annu Rev Cell Dev Biol 13: 261-291.

Mousavi A, Hotta Y (2005) Glycine-rich proteins: a class of novel proteins. Appl Biochem Biotechnol 120: 169-174.

Mukhopadhyay R, Rosen B, Phung L, Silver S (2002). Microbial arsenic: from geocycles to genes and enzymes. FEMS Microbiol Rev 26: 311-325.

Mylona PV, Polidoros AN, Scandalios JG (1998) Modulation of antioxidant responses by arsenic in maize. Free Radic Biol Med 25: 576-585.

National Research Council. Arsenic in drinking water. National Academy Press: Washington, D.C., 1999.

Olsen AN, Ernst HA, Leggio LL, Skriver K (2005) NAC transcription factors:

structurally distinct, functionally diverse. Trends Plant Sci 10: 79-87.

Passardi F, Cosio C, Penel C, Dunand C (2005) Peroxidases have more functions than a Swiss army knife. Plant Cell Rep 24: 255-265.

Petersson UA, Kieselbach T, Garcia-Cerdan JG, Schroder WP (2006) The Prx Q protein of *Arabidopsis thaliana* is a member of the luminal chloroplast proteome. FEBS Lett 580: 6055-6061.

Pickerling I, Prince R, George M, Smith R, George G, Salt D. (2000) Reduction and coordination of arsenic in Indian mustard. Plant Phys 122: 1171-1177.

Qian Y, Castranova V, Shi X (2003) New perspectives in arsenic-induced cell signal transduction. J Inorg Biochem 96: 271-278.

Quaghebeur M, Rengel Z (2003). The distribution of arsenate and arsenite in shoots and roots of *Holcus lanatus* is influenced by arsenic tolerance and arsenate and phosphate supply. Plant Phys 132: 1600-1609.

Ramirez-Solis A, Mukopadhyay R, Rose BP, and Stemmler TL (2004) Experimental and theoretical characterization of arsenite in water: insights into the coordination environment of As-O. *Inorg Chem* 43: 2954-2959.

Rose JK, Braam J, Fry SC, Nishitani K (2002) The XTH family of enzymes involved in xyloglucan endotransglucosylation and endohydrolysis: current perspectives and a new unifying nomenclature. Plant Cell Physiol 43: 1421-1435.

Sappl PG, Onate-Sanchez L, Singh KB, Millar AH (2004) Proteomic analysis of glutathione S -transferases of *Arabidopsis thaliana* reveals differential salicylic acid-induced expression of the plant-specific phi and tau classes. Plant Mol Biol 54: 205-219.

Sanders OI, Rensing C, Kuroda M, Mitra B, and Rosen BP (1997) Antimonite is accumulated by the glycerol facilitator GlpF in Escherichia coli. *J Bacteriol* **179**: 3365-3367.

Schmoger M, Oven M, Grill E (2000) Detoxification of arsenic by phytochelatins in plants. Plant Phys 122: 793-801.

Shimaoka T, Ohnishi M, Sazuka T, Mitsuhashi N, Hara-Nishimura I, Shimazaki K, Maeshima M, Yokota A, Tomizawa K, Mimura T (2004) Isolation of intact vacuoles and proteomic analysis of tonoplast from suspension-cultured cells of *Arabidopsis thaliana*. Plant Cell Physiol 45: 672-683.

Song CJ, Steinebrunner I, Wang X, Stout SC, Roux SJ (2006) Extracellular ATP induces

the accumulation of superoxide via NADPH oxidases in *Arabidopsis*. Plant Physiol 140: 1222-1232.

Srivastava M, Ma LQ, Singh N, Singh S (2005) Antioxidant responses of hyper-accumulator and sensitive fern species to arsenic. J Exp Bot 56: (415) 1335-1342.

Torres Acosta JA, de Almeida Engler J, Raes J, Magyar Z, De Groodt R, Inze D, De Veylder L (2004) Molecular characterization of *Arabidopsis* PHO80-like proteins, a novel class of CDKA;1-interacting cyclins. Cell Mol Life Sci 61: 1485-1497.

Tran LS, Nakashima K, Sakuma Y, Simpson SD, Fujita Y, Maruyama K, Fujita, M, Seki M, Shinozaki K, Yamaguchi-Shinozaki K. (2004) Isolation and functional analysis of *Arabidopsis* stress-inducible NAC transcription factors that bind to a drought-responsive cis-element in the early responsive to dehydration stress 1 promoter. Plant Cell 16: 2481-2498.

Tripathi RD, Srivastava S, Mishra S, Singh N, Tuli R, Gupta DK, Maathuis FJ (2007) Arsenic hazards: strategies for tolerance and remediation by plants. Trends Biotechnol 25: 158-165.

Tu C, Ma LQ, Bondada B (2002) Arsenic accumulation in the hyperaccumulator Chinese brake and its utilization potential for phytoremediation. J. Environ. Qual 31: 1671-1675.

Ulker B, Somssich IE (2004) WRKY transcription factors: from DNA binding towards biological function. Curr Opin Plant Biol 7: 491-498.

Ullrich-Eberius C, Sanz A, Novacky A (1989) Evaluation of arsenate- and vanadate-associated changes of electrical membrane potential and phosphate transport in *Lemna gibba*-G1. J Exp Bot 40: 119-128.

Vitoria AP, Lea PJ, Azevedo RA (2001) Antioxidant enzymes responses to cadmium in radish tissues. Phytochemistry 57: 701-710.

Vranova E, Inze D, Van Breusegem F (2002) Signal transduction during oxidative stress. J Exp Bot 53: 1227-1236.

Wagner U, Edwards R, Dixon DP, Mauch F (2002) Probing the diversity of the *Arabidopsis* glutathione S-transferase gene family. Plant Mol Biol 49: 515-532.

Wan J, Zhang S, Stacey G (2004) Activation of a mitogen-activated protein kinase pathway in Arabidopsis by chitin. Mol Plant Pathol 5: 125-135.

Wei CY, Chen TB (2006) Arsenic accumulation by two brake ferns growing on an arsenic mine and their potential in phytoremediation. Chemosphere 63: 1048-

1053.

Xu X, Chen C, Fan B, Chen Z (2006) Physical and functional interactions between pathogen-induced *Arabidopsis WRKY18*, *WRKY40*, and *WRKY60* transcription factors. Plant Cell 18: 1310-1326.

Yang YH, Speed T (2002) Design issues for cDNA microarray experiments. Nat Rev Genet 3: 579-588.

Zheng Z, Qamar SA, Chen Z, Mengiste T (2006) *Arabidopsis* WRKY33 transcription factor is required for resistance to necrotrophic fungal pathogens. Plant J 48: 592-605.

Zimeri AM, Dhankher OP, McCaig B, Meagher RB (2005) The plant MT1 metallothioneins are stabilized by binding cadmiums and are required for cadmium tolerance and accumulation. Plant Mol Biol 58: 839-855.

Appendix

Table 1.1. Gene ontology based on molecular function for induced genes resulting from rank product analysis of microarray results of arsenic-treated Arabidopsis thaliana "Columbia" plants. Only genes upregulated above 1.5-fold and meeting a significance criteria of $P < 0.001$ and FDR of 1% are shown. Rank products analysis reveals that most significantly induced genes display the lowest RP value.

Molecular function	Gene ID	Locus	FC	RP
Antioxidant activity	Peroxiredoxin Q	at3g26060	1.53	151.4
	peroxidase	at5g64100	2.50	7.3
	peroxidase	at1g05250	1.90	49.0
	peroxidase 57 (PER57) (P57) (PRXR10)	at5g17820	1.68	56.6
	peroxidase	at1g05240	2.05	16.5
	superoxide dismutase [Cu-Zn], chloroplast	at2g28190	4.57	2.3
	superoxide dismutase [Cu-Zn], (SODCC) (CSD1)	at1g08830	2.41	8.6
	superoxide dismutase copper chaperone	at1g12520	3.16	5.2
Metal ion binding	metallothionein-like protein 1A, (MT-1A)	at1g07600	1.67	41.9
	ferredoxin, chloroplast	at1g10960	1.53	95.6
Kinase activity	leucine-rich repeat transmembrane protein kinase	at3g24240	1.59	63.2
	Cyclin-dependent protein kinase	at5g61650	1.64	66.9
Oxygen binding	non-symbiotic hemoglobin 1 (HB1) (GLB1)	at2g16060	1.59	94.2
Hydrolase activity	ATPase, BadF/BadG/BcrA/BcrD-type family	at1g30540	1.62	75.5
	myrosinase-associated protein	at1g54010	1.54	90.5
	myrosinase-associated protein	at1g54000	1.68	47.6
	xyloglucan:xyloglucosyl transferase	at4g37800	1.61	72.0
	glycosyl hydrolase family 1 protein	at3g09260	1.67	50.8
Isomerase activity	peptidyl prolyl cis-trans isomerase	at3g62030	1.64	53.1
Lyase activity	ribulose bisphosphate carboxylase small chain 2B	at5g38420	1.75	36.1
	ribulose bisphosphate carboxylase small chain 3B	at5g38410	1.71	22.4
Alcohol dehydrogenase activity	alcohol dehydrogenase (ADH)	at1g77120	1.74	46.5
Nitrate reductase activity	nitrate reductase 1 (NR1)	at1g77760	1.77	41.8
Sulfate reduction	5'-adenylylsulfate reductase (APR3)	at4g21990	1.53	112.1
Molecular function unknown	Glycine-rich protein	at2g05510	4.31	2.4
	Photoassimilate-responsive protein	at3g54040	1.59	112.1
	Expressed protein	at1g09310	1.67	63.1
	Replication protein	at5g35260	1.62	975.3
	Drought-responsive protein (Di21)	at4g15910	1.67	69.6
	Hypothetical protein related to GB:AAD15331	at2g06480	1.58	81.6
	DREPP plasma membrane polypeptide-related	at5g44610	1.54	106.5
	Pentatricopeptide repeat-containing protein	at1g07590	1.62	74.6
	Meprin and TRAF domain-containing protein	at5g26280	1.60	70.8
	Expressed protein	at4g39675	1.72	86.0
	C2-domain-containing protein	at4g15740	1.76	42.7
	Expressed protein	at1g09340	1.62	78.4
	Late embryogenesis abundant 3 family protein	at4g02380	1.67	52.1
Transporter activity	Plasma membrane intrinsic protein 2B (PIP2B)	at2g37170	1.70	43.3
	Tonoplast intrinsic protein gamma	at2g36830	1.53	104.2
Glutathione transferase activity	Glutathione S-transferase GST20; Tau class	at1g78370	1.68	53.5

Table 1.1, cont.

Molecular function	Gene ID	Locus	FC	RP
RNA binding	Pumilio / Puf RNA-binding domain-containing protein	at1g78160	1.60	67.7
Stress response	Universal stress protein	at3g03270	1.98	19.7
Defense response	Bet v 1 allergen family protein	at1g24020	1.54	98.4
Electron transport	Cytochrome B561 family protein	at5g38360	1.56	97.9
Asparagine biosynthesis	asparagine synthetase 2	at5g65010	1.74	65.1
Carbonic anhydrase activity	Carbonic anhydrase 1, chloroplast	at3g01500	1.67	51.0

Table 1.2. Gene ontology based on molecular function for selected repressed genes resulting from rank product analysis of microarray results of arsenic-treated Arabidopsis thaliana "Columbia" plants. Only genes upregulated above -1.5-fold and meeting a significance criteria of $P < 0.001$ and FDR of 1% are shown. Rank products analysis reveals that most significantly repressed genes display the lowest RP value.

Molecular function	Gene ID	Locus	FC	RP
Catalase activity	catalase 3 (SEN2)	at1g20620	-1.59	191.7
Peroxidase activity	peroxidase	at3g49120	-1.77	165.3
	peroxidase	at5g64120	-1.84	123.2
	cationic peroxidase	at4g25980	-1.52	333.1
Oxidoreductase activity	superoxide dismutase [Fe], chloroplast	at4g25100	-5.17	1.7
	lipoxygenase	at1g72520	-2.41	242.9
	FAD-binding domain-containing protein	at1g26380	-1.50	293.0
	cytochrome p450 83B1	at4g31500	-1.71	142.3
	auxin-responsive family protein	at5g35735	-1.59	156.4
Metal ion binding	germin-like protein	at5g39160	-1.51	319.7
	germin-like protein	at5g39190	-2.13	27.3
	calcium-binding EF hand family protein	at1g76650	-2.00	50.4
	C2-domain containing protein	at4g34150	-1.53	313.4
	touch-responsive protein / calmodulin-related	at2g41100	-1.64	137.9
	ferritin 1 (FER 1)	at5g01600	-1.78	83.0
	ferritin 4	at3g56090	-1.52	201.0
	zinc finger (C2H2 type) protein	at3g46090	-1.51	191.2
	zinc finger (C2H2 type) protein	at3g46080	-1.59	178.8
	zinc finger (C3HC4 type) protein	at5g27420	-1.75	82.2
Hydrolase activity	lipase class 3 family protein	at1g02660	-1.56	218.8
	invertase / pectin methylesterase family protein	at5g62360	-1.75	85.0
	protein phosphatase 2C	at2g30020	-1.52	237.4
	phosphoric monoester hydrolase	at1g73010	-3.01	7.0
	acid phosphatase type 5 (ACP5)	at3g17790	-1.62	290.7
	phosphoric monoester hydrolase	at1g17710	-1.88	118.6
	glycosyl hydrolase family 17 protein	at3g55430	-1.53	201.2
	glycosyl hydrolase family 17 protein	at4g31140	-1.71	248.5
	glycosyl hydrolase family 17 protein	at4g19810	-1.96	99.2
	glycosyl hydrolase family 36 protein	at5g20250	-1.52	201.8
	xyloglucan endotransglucosylase/hydrolase	at4g30280	-1.63	172.2
	xyloglucan endotransglucosylase/hydrolase	at4g14130	-2.00	47.9
	xyloglucan endotransglucosylase/hydrolase	at5g57560	-1.68	97.3
	nudix hydrolase homolog 4	at1g18300	-1.54	215.9
	MERI-5 endo-xyloglucan transferase	at4g30270	-1.96	45.6
Protein binding	calmodulin-binding family protein	at4g33050	-1.78	88.6
	ankyrin repeat family protein	at5g45110	-1.58	252.0
	mitochondrial substrate carrier family protein	at4g24570	-1.50	260.2
	polygalacturonase inhibitory protein	at5g06860	-1.91	65.0
Chitin binding	hevein-like protein (HEL)	at3g04720	-1.53	499.9
Carbohydrate binding legume lectin family protein		at3g16530	-2.03	37.8
Sugar binding	curculin-like lectin family protein	at1g78830	-1.64	138.3
ATP binding	ATP-dependent Clp protease ATP-binding subunit	at5g51070	-1.51	188.7
Jasmonic acid synthesis	allene oxide cyclase	at3g25760	-1.54	279.6
Peptidase activity	vacuolar processing enzyme gamma	at4g32940	-1.65	117.1
	subtilase family protein	at1g32970	-1.91	81.1

Table 1.2, continued

Molecular function	Gene ID	Locus	FC	RP
Ligase activity	v-box domain-containing protein	at2g35930	-1.63	205.5
	asparagine synthetase 1	at3g47340	-1.74	75.5
Transferase activity	glutathione S-transferase (GSTF6); phi class	at1g02930	-2.10	62.9
	glutathione S-transferase (GSTF7); phi class	at1g02920	-2.88	7.6
	branched-chain amino acid amino transferase 2	at1g10070	-1.60	113.8
Nutrient reservoir activity	patatin	at2g26560	-1.81	84.8
Kinase activity	serine / threonine protein kinase 19	at3g08720	-1.55	249.8
Molecular function unknown	hypothetical protein no ATG start	at3g09922	-2.15	33.6
	expressed protein	at2g25510	-1.99	96.9
	expressed protein no ATG start	at5g03545	-2.72	16.8
	expressed protein	at5g42530	-2.01	147.4
	expressed protein	at4g31570	-2.21	45.6
	expressed protein	at1g69890	-1.73	79.9
	expressed protein	at5g20790	-2.33	32.7
	VQ motif-containing protein	at2g22880	-1.83	57.3
	glycine-rich protein	at1g07135	-1.53	167.4
	glycine-rich protein	at3g04640	-1.81	73.9
	glycine-rich protein	at2g05540	-1.85	47.9
	glycine-rich protein	at2g05380	-1.59	146.7
	integral membrane family protein	at4g15610	-1.58	139.7
	gibberellin-responsive protein	at1g22690	-1.88	51.5
	gibberellin-regulated protein (GASA1)	at1g75750	-1.70	93.7
	dehydrin (RAB18)	at5g66400	-1.70	81.1
	unknown protein – similar to glycosyltransferase	at2g41640	-1.54	185.8
	patatin-like protein 8	at4g29800	-1.52	198.7
	phosphate-responsive protein	at5g64260	-1.52	221.0
	phosphate-responsive protein	at1g35140	-1.58	131.5
	similar to LITAF-domain containing protein	at5g13190	-1.54	293.4
Transcription factor activity	DRE-binding protein	at1g12610	-1.74	116.8
	AP2 domain-containing transcription factor	at4g34410	-2.01	50.4
	zinc finger (C2H2 type) protein	at3g46090	-1.51	191.2
	zinc finger (C2H2 type) protein	at3g46080	-1.59	178.8
	WRKY family transcription factor 33	at2g38470	-1.63	157.9
	WRKY family transcription factor 53	at4g23810	-1.55	278.3
	WRKY family transcription factor 40	at1g80840	-1.88	70.9
	NAC domain-containing protein	at5g08790	-1.53	238.7
Senescence-related	senescence-associated family protein	at5g66040	-1.55	164.0
	senescence / dehydration-associated protein	at2g17840	-1.60	256.9
	senescence-associated protein (SEN1)	at4g35770	-1.59	123.9
	SRG3 (senescence-related gene 3)	at3g02040	-2.65	11.0
Transporter activity	MATE efflux family protein	at1g61890	-1.80	108.3
Galactolipid biosynthesis	monogalactosyldiacylglycerol synthase type C	at2g11810	-1.78	130.5
Electron transport	cytochrome p450 family 94 subfamily B	at3g48520	-1.56	249.8
Guanosine tetraphosphate metabolism	RSH 2 (RELA-SPOT HOMOLOG)	at3g14050	-1.52	188.7
N-terminal protein myristoylation	band 7 family protein	at3g01290	-1.54	253.4

Table 1.3. Comparison of microarray expression data with RT-PCR data from arsenate-treated *Arabidopsis thaliana*.

Gene id	gene name	Microarray data		RT-PCR data	
		ratio	*P*-value	ratio	*P*-value
at2g28190	superoxide dismutase [Cu-Zn], chloroplast (CSD2)	4.58	0.0006	3.89	<0.001
at1g12520	superoxide dismutase copper chaperone	3.16	0.0006	6.67	<0.001
at1g08830	superoxide dismutase [Cu-Zn] (SODCC) / (CSD1)	2.38	$8.4\ e^{-5}$	4.72	<0.001
at4g25100	superoxide dismutase [Fe], chloroplast (SODB)	0.23	0.0001	0.27	<0.001

Table 1.4. Comparison of *Arabidopsis thaliana* genes differentially expressed in response to both arsenate and Pi starvation[*].

Locus	Gene ID	As (V) stress response	Pi starvation response [*]
at1g08830	CuZn SOD (CSD1), chloroplast	induced	induced [1]
at5g61650	cyclin-dependent protein kinase	induced	induced [1]
at1g54010	myrosinase-associated protein	induced	induced [1]
at1g54000	myrosinase-associated protein	induced	induced [1]
at2g05510	glycine-rich protein	induced	induced [1]
at4g15740	C2-domain-containing protein	induced	induced [1]
at3g49120	peroxidase	repressed	induced [1]
at5g64120	peroxidase	repressed	repressed [1]
at1g72520	lipoxygenase	repressed	induced [1]
at1g26380	FAD-binding domain protein	repressed	induced [1]
at4g31500	cytochrome p450 83B1	repressed	induced [1]
at5g01600	ferritin 1 (FER 1)	repressed	induced [1]
at5g27420	zinc finger (C3HC4 type) protein	repressed	induced [1]
at1g73010	phosphoric monoester hydrolase	repressed	induced [1, 2]
at3g17790	acid phosphatase type 5 (ACP5)	repressed	induced [1]
at1g17710	phosphoric monoester hydrolase	repressed	induced [1, 2]
at4g19810	glycosyl hydrolase family 17	repressed	induced [1]
at5g20250	glycosyl hydrolase family 36	repressed	repressed [1]
at4g30280	xyloglucan endotransglucosylase	repressed	induced [1]
at5g06860	polygalacturonase inhibitory protein	repressed	induced [1]
at3g04720	hevein-like protein (HEL)	repressed	induced [1]
at1g32970	subtilase family protein	repressed	induced [1]
at2g26560	patatin	repressed	induced [1]
at3g08720	serine / threonine protein kinase 19	repressed	induced [1]
at1g19020	expressed protein	repressed	induced [1]
at2g04460	expressed protein	repressed	induced [1, 2]
at2g15890	expressed protein	repressed	repressed [1]
at5g20790	expressed protein	repressed	induced [1, 2]
at4g23810	WRKY53 transcription factor	repressed	induced [1]
at3g02040	SRG3 (senescence-related gene 3) glycerophosphodiesterase family	repressed	induced [1, 2]
at2g11810	monogalactosyldiacylglycerol synthase type C	repressed	induced [1, 2]

[*] microarray data generated by others that investigated transcriptional responses to Pi starvation
[1] (Mission *et al*., 2005)
[2] (Morcuende *et al*., 2007)

Control As (V)-stressed

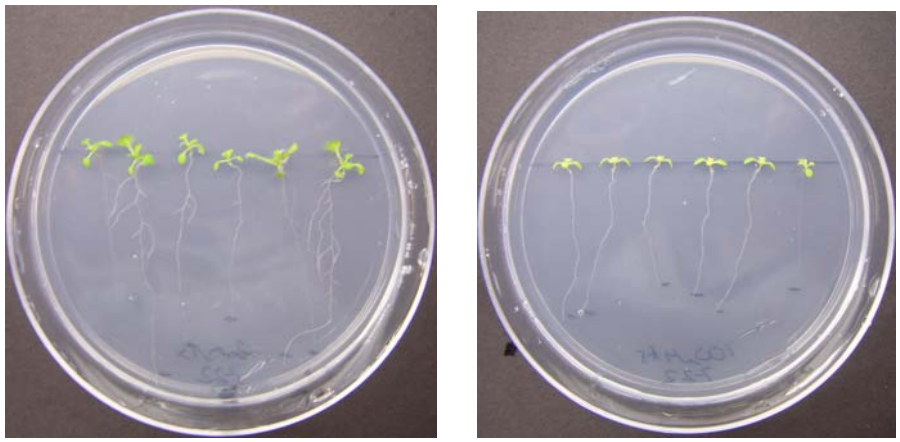

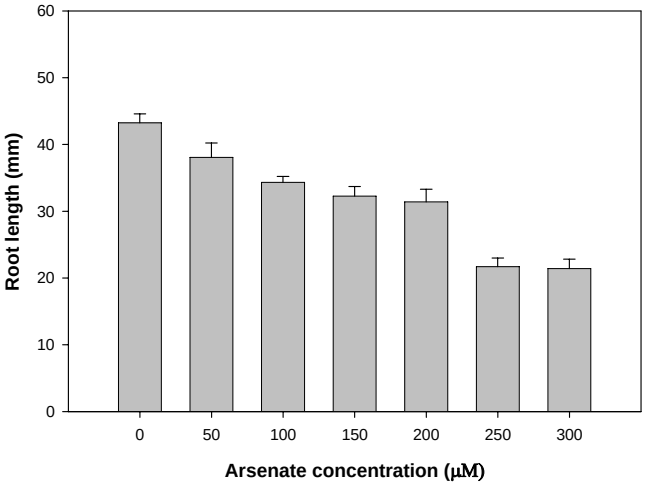

Figure 1.1. Phenotype of arsenate stress in Arabidopsis. *Arabidopsis thaliana* "Columbia" control plants grown for 10 days on MS medium containing either 0 µM As (V) or 100 µM arsenate. Graph depicts *Arabidopsis thaliana* root length at 10 days of growth on medium supplemented with various As (V) concentrations.

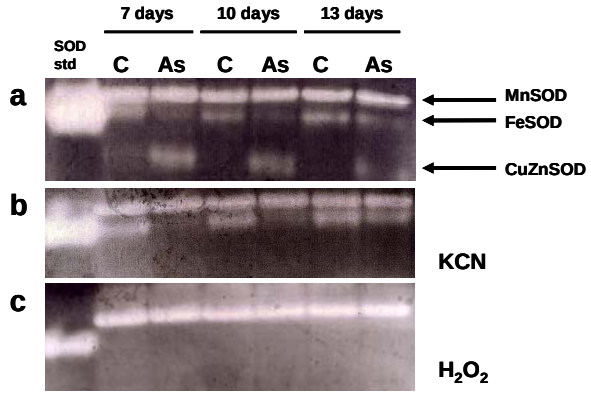

Figure 1.2. SOD activity in Arabidopsis thaliana 'Col' grown on medium containing 100 µM potassium arsenate. A, superoxide dismutase activity without inhibitors, B**,** Gels were preincubated with KCN (which inhibits CuZn SOD), C, H_2O_2 added as an inhibitor (which inhibits both CuZn SOD and Fe SOD). Lane 1, purified bovine SOD positive control. Lane 2, control plants harvested at 7 days, Lane 3, arsenate-treated plants harvested at 7 days. Lane 4, control plants harvested at 10 days, Lane 5, arsenate-treated plants harvested at 10 days. Lane 6, control plants harvested at 13 days, Lane 7, arsenate-treated plants harvested at 13 days.

A

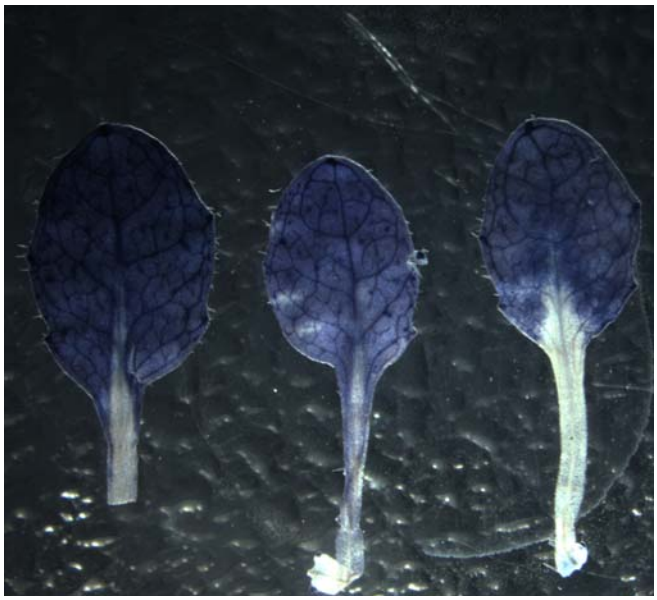

B

Figure 1.3. Nitroblue tetrazolium staining detects lower concentrations of superoxide in leaves of arsenate-treated Arabidopsis plants. A, control leaves at 10 days. B, leaves from plants grown on 100 μM arsenate at 10 days.

A

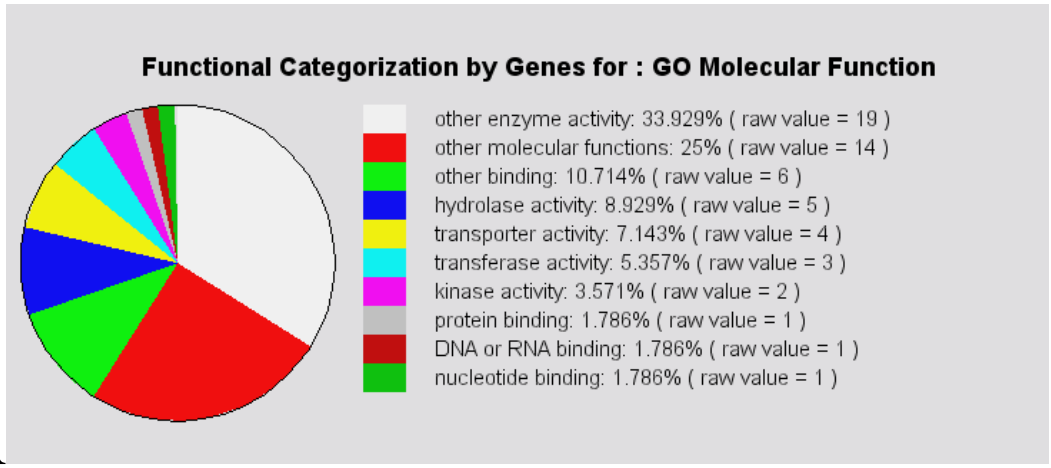

B

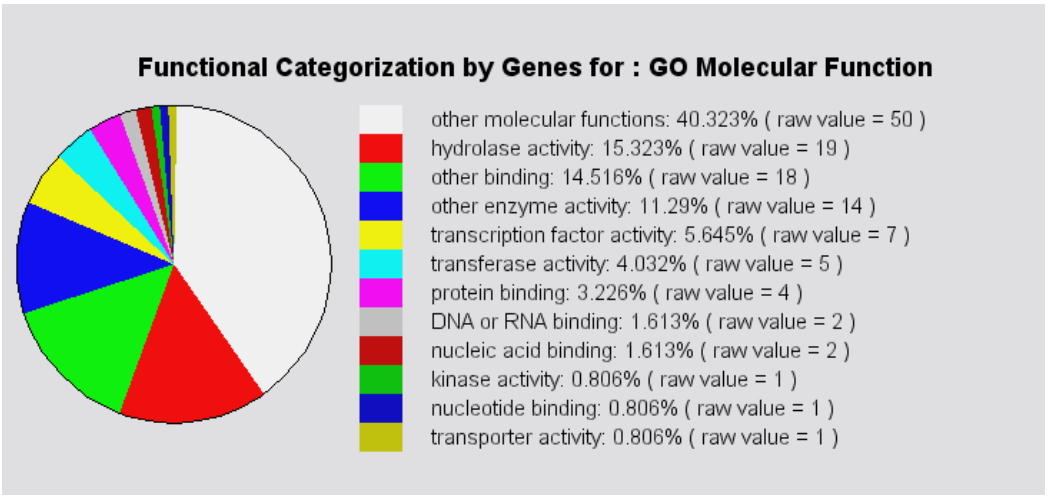

Figure 1.4. Functional characterization of differentially expressed A. thaliana genes in response to arsenate stress. A, gene ontology for genes induced above 1.5-fold. B, gene ontology for genes repressed 1.5-fold. All differentially expressed genes met a significance criteria of $P<0.001$ and had an FDR of < 1%.

Figure 1.5. Microarray quality control for chips used in this study. The top graph shows the M vs. A plot for normalized ratio of all six microarray slides. M vs. A plot is a scatter plot of logarithm transformed ratios $M = log2\ (R/G)$ plotted against average logarithm transformed intensity multiples $A = log2\ (R*G)/2$, where R and G represent the fluorescence intensities in the Cy3 and Cy5 channels, respectively. The bottom graph shows a histogram of distribution of logarithm 2 transformed ratios.

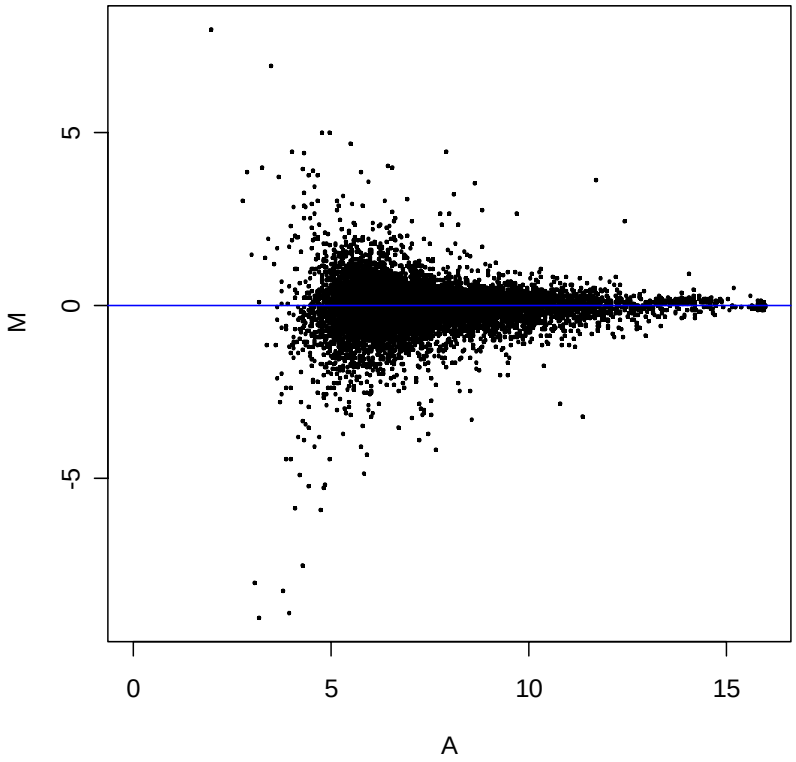
M
5
0
-5
0
5
10
15
A

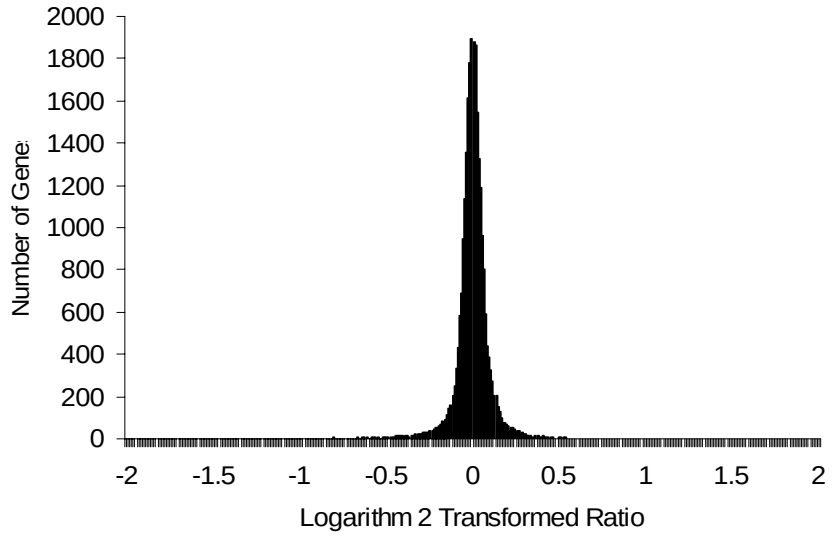
Number of Gene
2000
1800
1600
1400
1200
1000
800
600
400
200
0
-2
-1.5
-1
-0.5
0
0.5
1
1.5
2
Logarithm 2 Transformed Ratio

Towards engineering an As-specific phytosensor utilizing genetic elements of the prokaryotic *ars* operon

Introduction

Prokaryotic genes of the *ars* operon have evolved to confer resistance to arsenic in bacteria. The molecular mechanisms of this genetic system have been well characterized in both Gram-negative and Gram-positive bacteria (Mukhopadhyay et al., 2002; Diorio et al., 1995; Xu et al. 1997; Xu and Rosen, 1997; Cai and DuBow, 1996). Genome sequencing projects have shown that the *ars* operon is not only ubiquitous among prokaryotes, but similar systems have also been discovered in eukaryotes (e.g., *Saccharomyces cerevisiae*) (Rosen, 1999). Present in both chromosomes and plasmids, *ars* operons encode for arsenic-responsive regulatory elements (the ars_p promoter and a trans-acting *arsR* repressor protein), a cytoplasmic reductase (*arsC*) that reduces As (V) to As (III), and a transmembrane efflux pump (*arsAB*) that pumps As (III) out of the cell.

In the absence of As (III) or As (V), the *arsR* repressor protein binds to the *ars* promoter region, blocking transcription of the *ars* operon. When As (III) is present, it binds to cysteine thiolates of *arsR*, which then dissociates from the promoter, permitting transcription. Transcriptional activity of the *ars* operon depends on the concentration of As (III) (Cai and DuBow, 1996). Arsenite-dependent induction of the *ars* operon has been demonstrated in the metal-reducing facultative anaerobe *Shewanella* sp. Strain ANA-3 (Saltikov and Newman, unpublished data). These authors constructed an ars_p-*gfp* transcriptional fusion that showed an increase in fluorescence upon increasing As (III) concentration. Several authors have developed highly sensitive bacterial As-sensing systems utilizing the specificity of the *ars* operon (Cai and DuBow, 1997; Ramanathan et

al., 1998), thus demonstrating the potential for employing such a system for the specific detection of As in contaminated media.

Engineering plants to express prokaryotic sequences requires a promoter that is recognized by the transcriptional machinery of the plant to effectively drive transcription *in vivo*. Dhankher *et al*. (2002) demonstrated that prokaryotic genes of the *ars* operon can be used to engineer plants for increased tolerance and hyperaccumulation of arsenic. The researchers transformed *Arabidopsis* plants with the *Escherichia coli arsC* gene driven by a light-induced soybean rubisco promoter (SRS1p) that showed strong expression in the leaves. While these plants were hypersensitive to arsenate, moderate tolerance was observed in *Arabidopsis* plants expressing the *E. coli* gene encoding gamma-glutamylcysteine synthetase (gamma-ECS) driven by a strong constitutive actin promoter (ACT2p). Surprisingly, plants expressing SRS1p/*arsC* and ACT2p/gamma-ECS together showed increased As-tolerance and accumulated 4- to 17-fold greater fresh shoot weight and 2- to 3-fold more arsenic per gram of tissue than wild type or plants expressing gamma-ECS or *arsC* alone (Dhankher *et al*., 2002).

While most plant genetic engineering efforts focus on identifying novel genes for development of more effective As phytoextraction strategies, similar engineering approaches may enable *phytosensor* technologies, (i.e. transgenic plants that utilize reporter genes (e.g., green fluorescent protein, *gfp*) fused to contaminant-specific inducible promoters to allow for real-time contaminant-specific monitoring). A major advantage of using plants to detect the presence of As in soil at a contaminated site is that only the soluble species As (V) and As (III) are taken up by plant roots, therefore plant-based detection would represent a reflection of the bioavailable levels of As present. The

results from employing *gfp* in plant genetic transformation studies that GFP is a reliable indicator of recombinant protein synthesis in transgenic plants, thus allowing it to become a standard tool in biological and biotechnological research (Stewart, 2001). Unlike other reporter genes (i.e., firefly luciferase and *gus*), *gfp* requires no cofactors or substrates, can report in real-time, and may potentially be remotely sensed (Kooshki et al., 2003; Stewart et al. 2005).

In this study, we aim to engineer a phytosensor for rapid, cost-effective *in situ* monitoring and detection of bioavailable arsenic in As-contaminated sites. Our initial strategy was to clone DNA elements from the well characterized *Escherichia coli ars* operon. Recalling that in the presence of arsenic, the *arsR* repressor protein dissociates from the ars_p promoter, transgenic plants constitutively expressing the *arsR* repressor gene and containing the ars_p promoter driving expression of the *gfp* gene may enable the As-dependent expression of the fluorescent reporter. The following research describes our attempts at engineering such a system, first by cloning the ars_p promoter from *E. coli* in a transcriptional fusion to the *gfp* gene and characterizing the *gfp* expression from those plants in order to select the highest expressors.

Due to the low levels of GFP protein expression, an alternative strategy was implemented that involved the site-directed mutagenesis of the *CaMV* 35S promoter to contain the DNA-binding domain of the *E. coli* arsR repressor protein. Our goal here was to enable constitutive *gfp* expression in plants with potential for *arsR* binding to repress *gfp* expression completely in the absence of As, thereby allowing As-specific *gfp* fluorescence. Simultaneously, we cloned the *arsR* repressor from *E.coli* that binds to the ars_p promoter into tobacco. Once these plants were characterized, crosses were made to

introduce the mutated *CaMV* 35S promoter-driven *gfp* gene into a constitutively expressed *arsR* genetic background in order to determine if the presence of the repressor protein would diminish *gfp* expression. A separate *arsR* gene was synthesized and introduced into tobacco for optimized plant codon usage. Our transient expression experiments suggest that the binding of the *arsR* may occur to some degree, however not to the extent at which the gfp signal is completely repressed. We discuss the implications of these data, suggest further characterization to obtain more quantitative assessments, and highlight some As-induced physiological processes that may disrupt the efficacy of this approach.

Results

Transforming of the ars_p promoter into tobacco

Various cloning strategies were employed to generate transgenic tobacco plants with the ars_p promoter from *E. coli* driving expression of the *gfp* gene (Figure 2.1), however *gfp* expression was only detectable when the construct included a transcriptional enhancer from the Cauliflower Mosaic Virus 35S sequence. GFP levels were quantified by ELISA and found to be quite low compared to a high-expressing *gfp* line pBIN19-m*gfp*5er (Table 2.1). Because of the low levels of *gfp* expression observed in these transgenic plants, a new strategy was implemented that involved engineering of the *arsR* DNA binding domain into the *CaMV* 35S promoter.

Site-directed mutagenesis of the CaMV 35S promoter does not affect gfp expression

Transient expression assays demonstrated that introducing the three-nucleotide mutation near the TATA box of the *CaMV* 35S promoter (Table 2.2) does not affect *gfp* expression (Figure 2.2) and in fact, demonstrated that the resulting GFP fluorescence was quite similar between the two constructs. This observation allowed us to conclude that pMDC110c would serve as an effective control, thereby enabling comparisons of GFP fluorescence between mutated and non-mutated constructs.

Transgenic tobacco crosses (pMDC32-arsR x pMDC11035smut) generate progeny with pMDC32-arsR and pMDC110 transgenes

Three transgenic tobacco lines expressing pMDC32-*arsR*, three transgenic tobacco lines expressing pMDC11035Scontrol and three transgenic lines expressing pMDC11035Smutated were selected at random and grown in the greenhouse. GFP expression level was determined by sampling young leaves at the four leaf stage and observing green fluorescence under blue light at 200x magnification. Each image shown was taken at 4.5s exposure time except the positive pBIN19-mGFP5-ER positive control, which was taken at 1.9s exposure time (Figure 2.3). Paternal crosses from high expressing GFP lines (pMDC11035Sc-6; pMDC11035Smut-15) were made to two different maternal lines representing the highest expressors, as indicated by northern blot (Figure 2.4) for a total of four crosses. The resultant progeny were screened under the epifluorescence microscope to assure successful genomic insertion of the *gfp* transgene. Interestingly, more variation in GFP fluorescence was observed among progeny of the mutated *35S-gfp* parents, indicating that some of the progeny may have lower *gfp*

expression as a result of *arsR* binding to the mutated 35S promoter. Eight individuals from the progeny of each respective cross will be self-pollinated and subject to further characterization (i.e., GFP ELISA, Southern analysis).

Synthesis of a novel arsR gene for optimal plant expression and nuclear targeting

In order for this phytosensor strategy to be functional, the *arsR* protein must be translated into a functional protein and this protein must localize to the nucleus to effectively bind to the appropriate motif for repression of *gfp* transcription. Therefore, we generated a synthetic *arsR* (Blue Heron Biotechnology, Bothell, WA) that was codon-optimized for expression in plants and attached a 15-amino acid nuclear localization signal (C2NLS; Grebenok et al., 1997) to ensure nuclear targeting of the *arsR* to the respective DNA binding domain.

Transient expression of arsR from E. coli and codon optimized arsR in tobacco reveals localization

To test the effectiveness of the nuclear localization tag (Grebenok et al., 1997) engineered to promote binding of *arsR* to the DNA binding domain, we produced *arsR*-*gfp* fusions to assess if there was indeed nuclear targeting for both native and synthetic *arsR* proteins (Figure 2.5). The results suggest that there is faint nuclear targeting of the *arsR* repressor protein from *E. coli* in the GFP fusion, however nuclear targeting does not seem to occur in the codon-optimized construct. Instead, the fusion protein seems to be cytoplasmic and targeted to the endoplasmic reticulum. This indicates a potential problem

to solve before optimizing a construct to utilize for fern transformation. However, there seemed to be more GFP attenuation in the *arsR*-codon optimized co-infiltrations than was observed for co-infiltrations containing the native arsR protein (Figure 2.6).

Repression is suggested by lower transient expression of pMDC11035Smut in transgenic tobacco expressing arsR

Agrobacterium infiltrations of pMDC11035Smut versus pMDC11035Scontrol were performed to determine if transient expression of *gfp* would be lower in the presence of the *arsR* repressor protein, thereby suggesting the binding of the arsR protein to the DNA binding motif within the 35S promoter. *Nicotiana tabacum* allows for effective comparisons of the two constructs, as the infiltrations become compartmentalized in sectors between leaf veins (Figure 2.7). Therefore, this experimental setup was used for T_2 homozygous lines expressing the native *arsR* gene (Figure 2.8), as well as the T_1 trangenic lines expressing the *arsR* gene codon-optimized for plant expression (Figure 2.9). Figure 2.8 and Figure 2.9 show three separate replications of infiltration comparisons between the mutated and the control 35S constructs. Both experiments reflect similar results, in that the level of gfp fluorescence appears lower in sectors of leaf representing the pMDC35Smut infiltration compared to the non-mutated control infiltrations. However, these observations were less obvious under blue light illumination using the lower magnification of the dissecting scope. Nevertheless, *gfp* expression still occurs to a great extent in these infiltrations, suggesting that our OD_{600} was too high for detecting the effect, if any, of the *arsR* repressor on the expression of *gfp* in the mutated constructs. Therefore, repeat experiments using lower OD_{600} is warranted.

Discussion

The concept of harnessing the specificity of the *ars* operon for the purposes of developing an As-specific biosensor (but not phytosensor) has been previously reported (Ramanathan et al., 1998; Cai and DuBow, 1997). Ramanathan et al. (1997) engineered a chemiluminescent bacterial system of As detection using β-galactosidase that utilized the As-specific dissociation and repression of the *E. coli arsR* regulatory protein. These authors measured β-galactosidase activity by chemiluminescence and demonstrated detection of antimonite/arsenite at sub-picomolar concentrations. A similar strategy by Cai and DuBow (1997) utilized a luciferase transcriptional gene fusion (*arsB::luxAB*) that demonstrated As (V)-specific luminescence in a dose-dependent manner. It was shown that this system had detection limits near 10 ppb and that cells exhibited higher induction when starved for phosphate, an ion of which arsenate is a competitive analog. Despite these exciting findings, these approaches are limited by the presence of a chemical substrate and the limitations inherent in a bacterial system; more susceptibility to contamination by other organisms and the dependence of labor intensive, laboratory-based culture maintenance. Employing a sentinel plant to detect As would not only report the presence of As in real time in contaminated media, but would require little maintenance and no chemical substrates due to the nature of the fluorescent GFP. Additionally, incorporating such a system into a perennial As-hyperaccumulator (i.e. *Pteris vittata*) would enable As detection in combination with As phytoextraction. The perennial nature of the plant would allow As removal with each harvest until the GFP signal was no longer detected, thus indicating when levels of bioavailable As were below the levels of detection.

The most promising candidates for As-phytosensor proof-of-concept will certainly be individuals that are homozygous for both *arsR* and the mutated 35S-*gfp,* but that also exhibit an As-inducible GFP fluorescence. It is clear from the results of this study that transient expression assays will not be effective determinants of whether *arsR* protein produced by plants bind to an engineered DNA binding domain, or for that matter, whether the *arsR* protein is even synthesized and/or functional in plants. At least these experiments should be repeated using lower OD_{600} values in attempts to capture a threshold vector concentration where *arsR* may effectively bind to the mutated constructs. Nevertheless, the obvious hurdles to overcome in this project will be to 1) obtain purified plant-synthesized *arsR* protein , 2) demonstrate binding of plant-produced *arsR* to the engineered *CaMV* 35S promoter, and 3) if ideal double-transgenic individuals are eventually identified that demonstrate As-induced *gfp* fluorescence, then experimentation will be needed to show this response is specific for arsenite.

The increased variation in GFP fluorescence observed among progeny of the mutated *35S-gfp* parents may be indicative of lower *gfp* expression as a result of *arsR* binding to the mutated 35S promoter in these progeny. Of course, the other possibility is that the *gfp* gene was not incorporated into the genome, therefore we have selected a subset of progeny from these crosses to capture the observed variation in *gfp* expression by testing for the presence of the *gfp* gene. GFP quantification (i.e. ELISA) in combination with Southern analysis of homozygous individuals (via self-pollination) from the progeny of each respective cross should allow us to determine the underlying causes of the observed variation in GFP fluorescence.

Attempting to engineer a sensor for arsenic in plants is not without inherent difficulties and challenges due to the evolved mechanisms that plants employ for arsenic tolerance, transport, and detoxification. For example, it is known that As (V) is taken up through the high-affinity phosphate transporters, reduced by either arsenate reductase or reduced glutathione to As (III), and subsequently bound by phytochelatins and compartmentalized in the vacuole (Meharg and McNair, 2002). Therefore, it would be unlikely that arsenite would localize to the nucleus unless either the phytochelatin and/or glutathione concentration was compromised or the arsenite concentration in the cell was sufficiently high. From an engineering standpoint, perhaps an RNAi approach to silence phytochelatin synthase would enable higher concentrations in the cell. This approach was recently demonstrated by Dhanker et al. (2006) to be effective in inducing As hyperaccumulation in *A. thaliana*. These authors identified an arsenate reductase in *A. thaliana* (*ACR2*) that had moderate sequence homology to the yeast arsenate reductase and silenced its expression using RNAi. The resulting knockdown lines accumulated 60 to 20-fold more As in the shoot compared to wild-type plants. These transgenic lines were sensitive to high concentrations of arsenate, but not arsenite. It was clearly demonstrated that the *ACR2* gene was involved in blocking the long-distance transport of As from root to shoot. If we can show that *arsR* binding to the mutated 35S promoter occurs in our transgenic tobacco plants, then combining the RNAi approach to induce As hyperaccumulation in those lines would likely improve the sensitivity of the system or at least increase the above-ground cellular concentration of As, thereby increasing the likelihood of As-induced dissociation of the *arsR* repressor from the DNA binding motif.

Materials and methods

Plants and growth conditions

Nicotiana tabacum cv. Xanthi and *Nicotiana benthamiana* were used for *Agrobacterium*-mediated transformation. To generate stable transformants, seeds were surface sterilized, grown under aseptic conditions in a growth chamber at 25ºC and a 16 h photoperiod, and 4-week old leaf tissue was transformed using the *Agrobacterium tumefaciens* leaf disc transformation method (Horsch et al., 1985). Transgenic shoots and callus were cultured on a modified MS medium (Murashige and Skoog, 1962) under hygromycin selection. Hygromycin-resistant transgenic plants were transplanted to soil, allowed to self-pollinate in the greenhouse, and brought to the T_2 generation to ensure homozygosity. All self- and cross pollinations were performed in the greenhouse. After crossing, plants were allowed to set seed in the greenhouse.

DNA and RNA analyses

Genomic DNA was isolated from transgenic tobacco plants using a CTAB method (Stewart and Via, 1993). Total RNA was isolated from plants using Trizol ® reagent (Invitrogen, Carlsbad, CA) according to manufacturer's protocol. Ten micrograms of total RNA was separated on a 1.2% formaldehyde agarose gel.

Cloning of the ars_p promoter and the arsR gene

Gateway®-compatible cloning vectors produced by Curtis and Grossniklaus (2003) pMDC110, pMDC32, and pMDC201 were provided by Mark Curtis (Institute of Plant Biology, Zurich, Switzerland) and used for cloning of the ars_p promoter and the *arsR* gene. The ars_p promoter was amplified from *E.coli* K-12 (NCBI accession NC 000913) genomic DNA with forward primer containing the sequence 5'-GGGGACAAGTTTGTACAAAAAAGCAGGCTACACATTCGTTAAGTCAT-3' and the reverse primer contained the sequence 5'-GGGGACCACTTTGTACAAGAAAGCTGGGTATTGCGCTCCTGATTGTT-3'. The region between -209 and -46 of the 35S promoter has been used as an enhancer, regardless of its position and orientation, to activate the transcription of promoters in both monocots (Omirulleh et al., 1993) and dicots (Fang et al., 1989). This particular sequence was used as an enhancer to activate transcription of the ars_p promoter in our engineered plants. The *arsR* gene was also amplified from *E. coli* K-12 genomic DNA using forward primer containing the sequence 5'-GGGGACAAGTTTGTACAAAAAAGCAGGCTAAGCTTATGTCATTTCTGTTACC C-3' and the reverse primer contained the sequence 5'-GGGGACCACTTTGTACAAGAAAGCTGGGTATTAACTGCAAATGTTCTTACT-3'. To amplify the arsR gene minus the stop codon for gfp fusion construct the reverse primer contained the sequence 5'-GGGGACCACTTTGTACAAGAAAGCTGGGTAACTGCAAATGTTCTTACT-3'. The products of BP clonase and LR clonase reactions were used to transform competent *E.*

coli strain DH5α using heat shock. DNA was isolated from single colonies, confirmed via sequencing, and introduced into *Agrobacterium tumefaciens* strain GV3850 for leaf disc transformation.

CaMV 35S promoter mutation

To engineer the ars*R* DNA binding domain into the CaMV 35S promoter, three mismatched nucleotides were incorporated into the reverse primer. Forward primer (CaMV35Sup) contained the sequence 5'-AGATTAGCCTTTTCAATTTCAG-3' and the non-mutated reverse primer (CaMV35Sdwn) contained the sequence 5'-CGTGTTCTCTCCAAATGAAA-3'. The reverse primer designed to include the mismatch for mutation (CaMV35SmutDWN) was 5'-CGTCAAATCTCCAAATGAAATGAACTT-3' (mismatched nucleotides underlined). Both mutated and non-mutated PCR products were cloned into pcr8/GW/TOPO using the TA cloning kit (Invitrogen, Carlsbad, CA) and resulting vectors were used to transform SE DH5α competent *E. coli* cells (Invitrogen, Carlsbad, CA). Sequence-confirmed plasmid DNA was cloned into pMDC110 using Gateway LR clonase (Invitrogen, Carlsbad, CA) and subsequently used to transform *Agrobacterium tumefaciens* strain GV3850 for tobacco leaf disc transformation.

Transient expression assays

Transient expression assays were performed in *N. tabacum* and *N. benthamiana* via infiltration with a needleless syringe according to Sparkes et al (2006). Each

infiltration consisted of 200 µL of *Agrobacterium* (strain EHA101) transformed with 1 µg of DNA. Transient expression of *gfp* was observed first under a dissecting microscope and subsequently under an epifluorescence microscope using blue light excitation with a FITC filter. Images were recorded using Q capture imaging software (Quantitative Imaging Corporation, British Columbia, Canada).

References

Cai, J., and DuBow, M.S. (1996) Expression of the *Escherichia coli* chromosomal ars operon. *Can J Microbiol* **42**: 662-671.

Cai, J., and DuBow, M.S. (1997) Use of a luminescent bacterial biosensor for biomonitoring and characterization of arsenic toxicity of chromated copper arsenate (CCA). *Biodegradation* **8**: 105-111.

Curtis M, and Grossnilaus U. (2003). A Gateway cloning vector set for high-throughput Functional analysis of genes in planta. *Plant Phys*. 133: 462-469.

Dhankher O, Rosen B, Shi J, Salt D, Senecoff J, Sashti N, and Meagher R. (2002) Engineering tolerance and hyperaccumulation of arsenic in plants by combining arsenate reductase and γ-glutamylcysteine synthetase expression. *Nat. Biotech*. 20:1140-1145.

Dhankher OP, Rosen BP, McKinney EC and Meagher RB (2006) Hyperaccumulation of arsenic in the shoots of Arabidopsis silenced for arsenate reductase (ACR2). *Proc Natl Acad Sci U S A* 103: 5413-5418.

Diorio C, Cai J, Marmor J, Shinder R, and DuBow M. (1995) An *Escherichia coli* chromosomal *ars* operon homolog is functional in arsenic detoxification and is conserved in gram-negative bacteria. *J. Bacteriol.* 177: 2050-2056.

Fang R, Nagy F, Sivasubramaniam S, and Chua N. (1989) Multiple *cis* regulatory elements for maximal expression of the cauliflower mosaic virus 35S promoter In transgenic plants. *Plant Cell*. 1: 141-150.

Grebenok R, Pierson E, Lambert G, Gong F, Afonso C, Halderman-Cahill R, Carrington J, and Galbraith D. (1997) Green-fluorescent protein fusions for efficient characterization of nuclear targeting. *The Plant Journal*. 11 (3): 573-586.

Horsch R, Fry N, Hoffman D, Eichholtz S, Rogers R, and Fraley A. (1985) A simple and general method for transferring genes into plants. *Science*. 227: 1229-1231.

Kooshki M, Ayalew M, and Stewart CN. (2003) Pathogen inducible reporting in transgenic tobacco using a GFP construct. *Plant Sci*. 165:213-219.

Ma L, Komar K, Tu C, Zhang W, Cai Y, and Kennelley E. (2001) A fern that hyperaccumulates arsenic. *Nature* 409:579.

Meharg A and Macnair M. (1992) Suppression of the high affinity phosphate uptake system: a mechanism of arsenate tolerance in *Holcus lanatus* L. *J. Exp. Bot*. 43:519-524.

Mukhopadhyay R, Rosen B, Phung L, and Silver S. (2002) Microbial arsenic: from geocycles to genes and enzymes. *FEMS Microbiol. Rev*. 26:311-325.

Murashige T. and Skoog F. (1962) A revised medium for rapid growth and bioassays with tobacco tissue cultures. *Physiol. Plant* 15: 473-497.

National Research Council. (1999) *Arsenic in drinking water*. National Academy Press: Washington, D.C., 1999.

Omirulleh S, Abraham M, Golovkin I, Stefanov M, Karabaev L, and Mustardy L. (1993) Activity of a chimeric promoter with the doubled *CaMV* 35S enhancer element in protoplast-derived cells and transgenic plants in maize. *Plant Mol. Biol*. 21: 415-428.

Pickerling I, Prince R, George M, Smith R, George G, and Salt D. (2000) Reduction and coordination of arsenic in Indian mustard. *Plant Phys*. 122:1171-1177.

Pilon-Smits E and Pilon M. (2002) Phytoremediation of metals using transgenic plants. *Critical Rev. Plant Sci.* 21:439-456.

Quaghebeur M and Rengel Z. (2003) The distribution of arsenate and arsenite in shoots and roots of *Holcus lanatus* is influenced by arsenic tolerance and arsenate and phosphate supply. *Plant Phys*. 132:1600-1609.

Quiros C, Grellet F, Sadowski J, Suzuki T, Li G, and Wroblewski T. (2001) *Arabidopsis* and *Brassica* comparative genomics: Sequence, structure, and gene content in the ABI1-Rps2-Ck1 chromosomal segment and related regions. *Genetics* 157:1321-1330.

Rosen B. (1999). Families of arsenic transporters. *Trends Microbiol*. 7:207-212.

Salt D, Smith R, and Raskin I. (1998) Phytoremediation. *Annu. Rev. Plant Physiol. Plant Mol. Biol.* 49:643-668.

Schmoger M, Oven M, and Grill E. (2000) Detoxification of arsenic by phytochelatins in plants. *Plant Phys*. 122:793-801.

Sparkes IA, Runions J, Kearns A and Hawes C. (2006) Rapid, transient expression of fluorescent fusion proteins in tobacco plants and generation of stably transformed plants. *Nat Protoc* 1: 2019-2025.

Stewart CN and Via L. (1993) A rapid CTAB DNA isolation technique useful for RAPD fingerprinting and other PCR applications. *Biotechniques*. 14: 748-751.

Stewart CN Jr. (2001) The utility of green fluorescent protein in transgenic plants. *Plant Cell Rep.* 20:376-382.

Stewart CN, Jr., Millwood RJ, Halfhill MD, Ayalew M, Cardoza V, Kooshki M et al. (2005) Laser-induced fluorescence imaging and spectroscopy of GFP transgenic plants. *J Fluoresc* 15: 697-705.

Xu C, Shi W, and Rosen B. (1997) The chromosomal *arsR* gene of *Escherichia coli* encodes a *trans*-acting metalloregulatory protein. *J. Biol. Chem*. 271:2427-2432.

Xu C, and Rosen B. (1997) Dimerization is essential for DNA binding and repression by the *arsR* metalloregulatory protein of *Escherichia coli. J. Biol. Chem.* 272:15734-15738.

Appendix

Table 2.1. Green fluorescent protein (GFP) expression in transgenic tobacco lines as determined by ELISA assay.

Transgenic Line	Event No.	Concentration ng/µL	Total Soluble Protein %
35Se ars$_p$min	10	0.0034	0.0052
35Se ars$_p$min	11	0.0036	0.0061
35Se ars$_p$min	12	0.0004	0.0007
35Se ars$_p$min	13	0.0056	0.0096
pBIN19 (mGFP5er)	NA	0.27	0.28
Xanthi control	NA	0	0

Table 2.2. Site-directed mutagenesis of three nucleotides introduced the arsR DNA binding motif within the CaMV 35S promoter region. The TATA box is underlined and the arsR binding motif is highlighted and underlined in red.

Native *CaMV*35S promoter sequence

tatataaggaagttcatt**tcatttggagagaac**acgaagggc

Mutated *CaMV*35S promoter sequence

tatataaggaagttcatt**tcatttggagatttg**acgaagggc

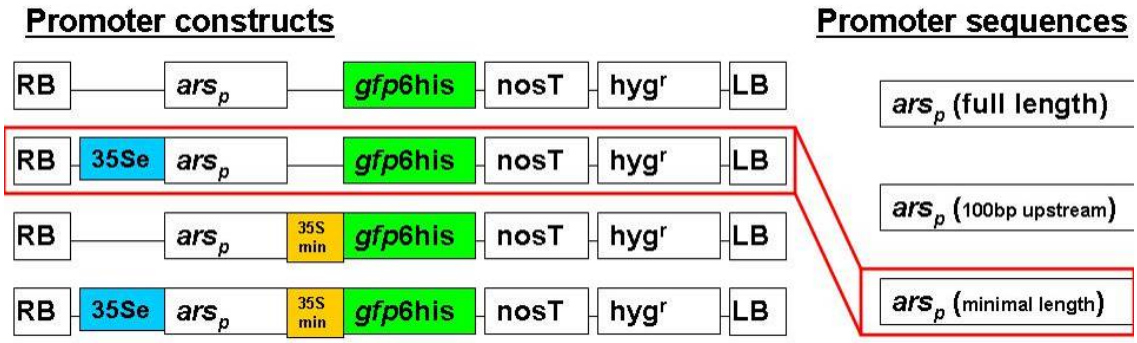

Figure 2.1. Constructs generated to enable gfp expression driven by the prokaryotic arsp promoter in *N. tabacum*. Various combinations of constructs shown were cloned with three different lengths of the arsp promoter. The combination highlighted in red indicates the construct with the highest level of *gfp* expression.

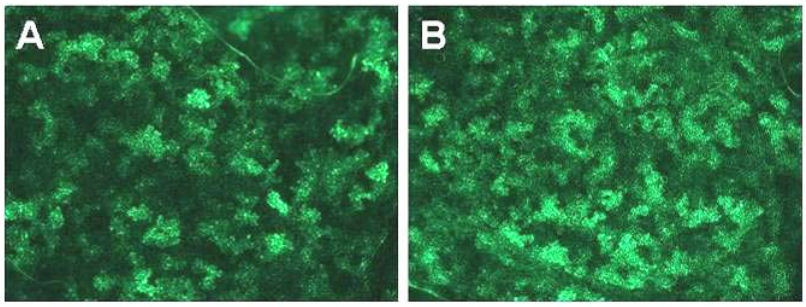

Figure 2.2. Site-directed mutagenesis of *CaMV* 35S promoter does not affect GFP expression in pMDC110. A, transient expression after *Agrobacterium* infiltration of pMDC11035Scontrol in *N. benthamiana*. B, transient expression after *Agrobacterium* infiltration of pMDC11035Smutated in *N. benthamiana*. Images were taken at the same exposure length and infiltrations were performed at the same OD_{600} (0.3).

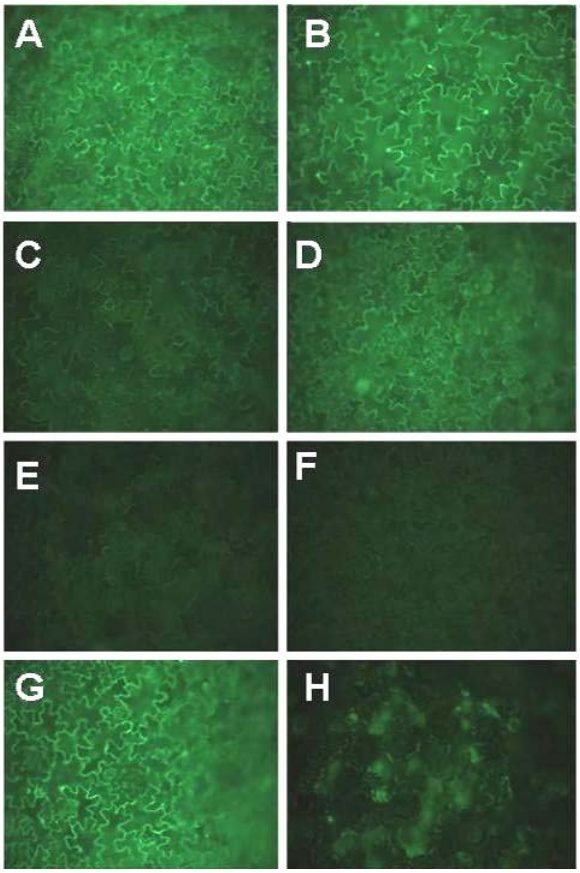

Figure 2.3. Selection of high-expressing GFP tobacco lines for introduction of 35S-mutated-gfp construct into a high-expressing arsR tobacco line. A (pMDC11035Sc) and B (pMDC11035Smut), are images taken from leaves of the highest expressors of *gfp* that were selected as paternal parents to cross with homozygous *arsR*-native tobacco lines. C-F show that significant variation in *gfp* expression exists among transgenic events (i.e. pMDC110control and pMDC110mut) G, represents a positive control (pBIN19-mGFP5-ER) with an unaltered 35S promoter controlling the mGFP5-ER gene and H, shows an image of a non-transgenic control plant. The similar expression levels observed in the highest expressing events of mutated and control promoters indicates that the mutation does not affect expression in the absence of the repressor protein.

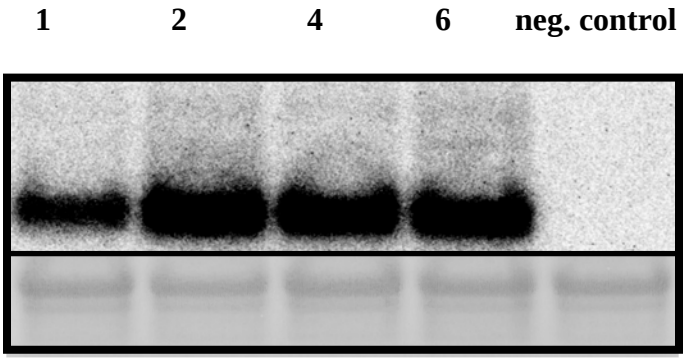

Figure 2.4. Northern blot of T_2 transgenic tobacco lines showing high transcript abundance for the *arsR* gene from *E. coli*.

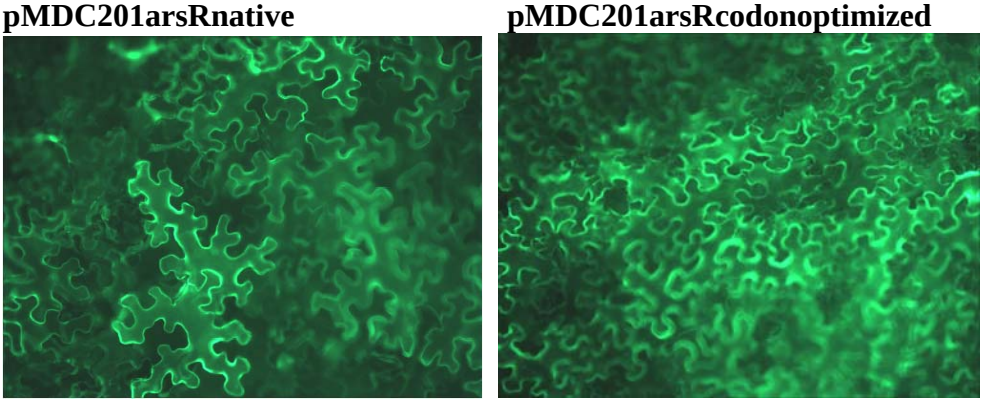

Figure 2.5. Transient expression of *arsR-gfp* fusion constructs in tobacco. Both constructs clearly indicate that each repressor is cytoplasmic and located in the endoplasmic reticulum, however only faint nuclear localization is observed for the native arsR fusion, whereas the codon-optimized arsR does not seem to be nuclear localized. These results are contrary to our expectations, as the codon-optimized arsR contains a nuclear localization tag.

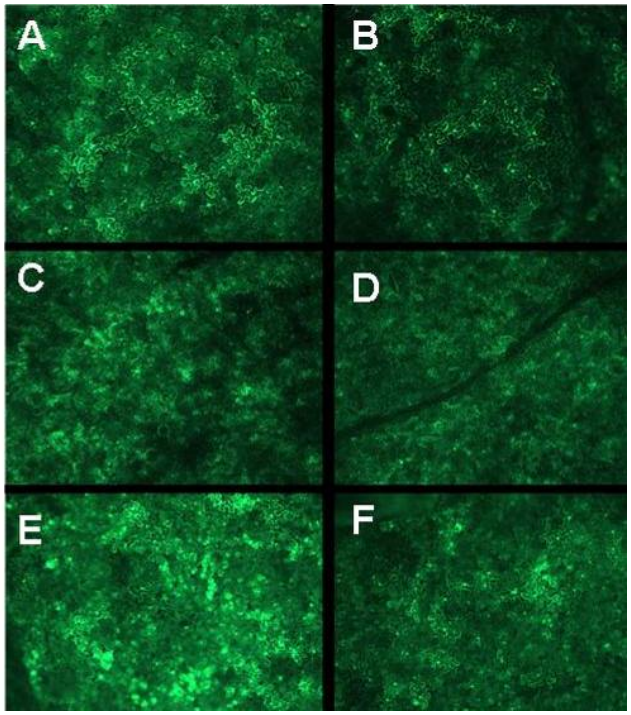

Figure 2.6. Co-infiltrations of pMDC110 35S and pMDC32-arsR constructs. These comparative groups of images were taken at the same exposure length and magnification 48 hrs post infiltration. A/B, taken at 286 ms exposure and 100X magnification, C/D, taken at 1.9 s exposure and 40X magnification, and E/F were taken at 351 ms exposure and 100X magnification. These coupled comparisons represent 200 μL infiltrations. Each construct has a finalOD_{600} of 0.3. In these cases, non-transgenic tobacco plants were infiltrated with the mutated 35S or control 35S GFP promoter construct in combination with an *arsR* construct.

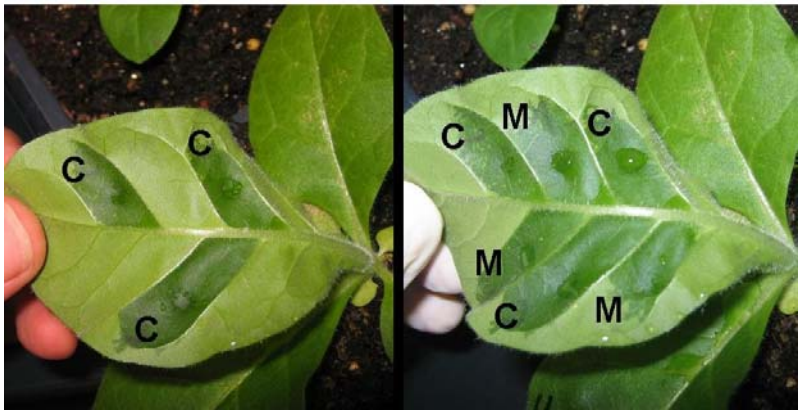

Figure 2.7. Experimental design for comparisons of transient expression in transgenic tobacco line constitutively expressing the arsR gene. *Agrobacterium* infiltrations of M, pMDC110-mutated 35S and C, pMDC110-control native 35S enabled high statistical power and adjacent contrasts to determine if the plant synthesized *arsR* protein repressed *gfp* expression.

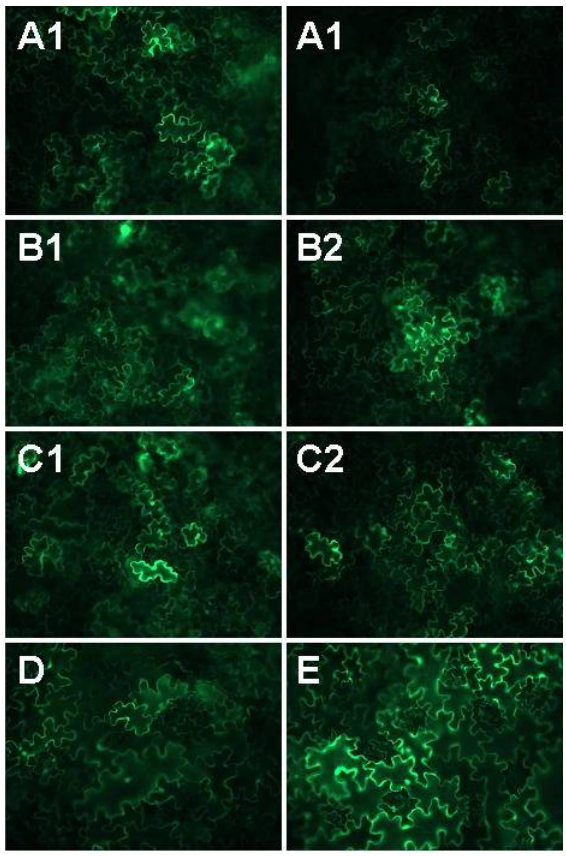

Figure 2.8. Transient expression of *gfp* as a result of *Agrobacterium* infiltrations of transgenic tobacco expressing the *arsR*-native construct. A1-C1 represent biological replicates of pMDC11035Scontrol infiltrations, whereas A2-C2 are respective infiltrations of the pMDC11035Smutated construct on the same tobacco leaf. D and E show transient *gfp* expression in a non-transgenic tobacco leaf from infiltrations of pMDC11035Scontrol and pMDC11035Smutated, respectively.

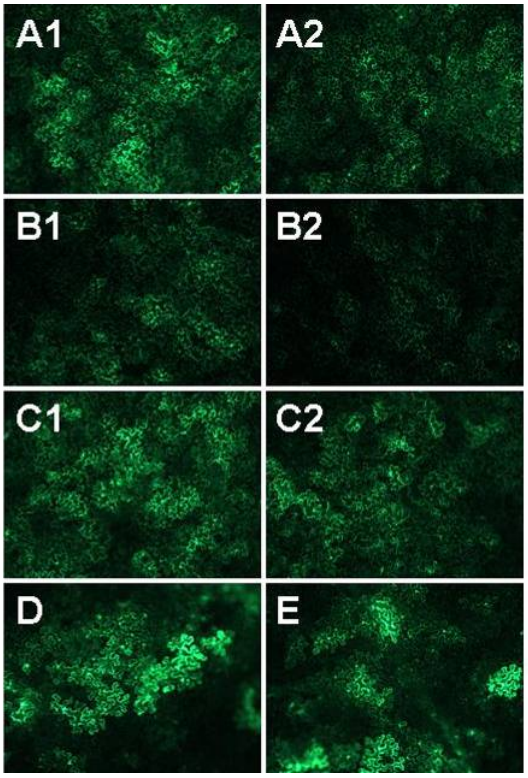

Figure 2.9. Transient expression of gfp as a result of Agrobacterium infiltrations of transgenic tobacco expressing the arsR-codon optimized construct. A1-C1 represent biological replicates of pMDC11035Scontrol infiltrations, whereas A2-C2 are respective infiltrations of the pMDC11035Smutated construct on the same tobacco leaf. D and E show transient *gfp* expression in a non-transgenic tobacco leaf from infiltrations of pMDC11035Scontrol and pMDC11035Smutated, respectively.

Towards genetic transformation of *Pteris vittata* and *Pteris cretica*: Transient expression of green fluorescent protein and *β*-glucuronidase in *Pteris cretica* and PCR amplification of *Pteris vittata rbcS* promoter sequence from *Pteris cretica*

Abstract

Currently, little is known about the potential for genetic transformation in ferns. The recent discovery of arsenic hyperaccumulation in members of the *Pteris* genus has prompted investigations to elucidate the underlying mechanisms of this interesting trait. An efficient genetic transformation protocol would facilitate these endeavors. In efforts to develop a transformation method for *Pteris vittata* and *Pteris cretica*, two known As-hyperaccumulators, experiments were conducted to optimize callus induction and regeneration of transformants. The efficacy of various transformation methodologies (i.e. biolistic bombardment, *Agrobacterium*-mediated transformation) were evaluated and low levels of transient expression were observed using constructs containing either GFP or GUS driven by *CaMV* 35S and maize ubiquitin promoters, respectively. This prompted us to pursue cloning of a partial RUBISCO promoter sequence (*rbcS*) from *Pteris vittata* and attempts to sequence the entire *Pteris vittata rbcS* promoter using an inverse PCR approach. Poor genomic DNA yields forced us to focus on PCR products amplified from *Pteris cretica* genomic DNA. Our efforts have identified a putative PCR product that may represent an *rbcS* promoter sequence from *Pteris cretica* and enabled new approaches toward the first genetic transformation method for a fern species.

Introduction

Arsenic hyperaccumulation has recently been discovered in the fern species *Pteris vittata* (Ma et al., 2001), and as a result, has generated intense research efforts towards elucidating the mechanisms by which this process occurs. While several groups have demonstrated the efficacy of this high biomass crop for field-scale remediation of As-contaminated sites (Wei et al., 2006; Wei et al., 2007; Wang et al., 2006; Wang et al., 2007), others have studied the molecular mechanisms involved in As hyperaccumulation (Wang et al., 2002; Dong 2005; Gumaelius et al., 2004; Caille et al., 2005; Pickering et al., 2006; Ellis et al., 2006).

Previous studies have reported on tissue culture systems for *Pteris vittata* and *Pteris cretica*. Kwa et al. (1991) successfully induced callus formation in *Pteris vittata* pinnae strips using modified MS medium (Murashige and Skoog, 1962) containing the synthetic auxin 2,4-D. Furelli and Garcia (1987) developed a protocol for callus induction and explant regeneration in *Pteris cretica*.

Reverse genetic studies are enabled through DNA sequence availability and facilitated through tissue culture and efficient genetic transformation methods. To date, there is minmal sequence available for members of the *Pteris* genus. Eilenberg et al. (1998) provided the RUBISCO gene sequence from *Pteris vittata* that included a characterized, but incomplete promoter sequence. Therefore, the objectives of this study were to 1) develop an efficient tissue culture system for *Pteris vittata* and *Pteris cretica,* 2) to test the effectiveness of biolistic bombardment and *Agrobacterium*-mediated transformation methods on these ferns employing a 35S-*gfp* construct and a maize

ubiquitin-GUS construct, and 3) to capture the complete sequence of the *Pteris vittata rbcS* promoter using an inverse PCR approach using sequence specific primers for the known region (Eilenberg 1998). In this paper, we also discuss new strategies for the genetic transformation of ferns (i.e. protoplast transformation).

Results

Optimization of Pteris tissue culture

We demonstrated successful regeneration of mature sporophytic *Pteris cretica* and *Pteris vittata* plants (Figure 3.1) from the induction of undifferentiated callus, generation of embryogenic tissue via cytokinin treatment, and subsequent recovery of mature plants following growth on medium supplemented with indole acetic acid (IAA) through a modified protocol similar to that of Furelli and Garcia (1987). Although these plants are not transgenic, a working protocol for the induction of callus and regeneration of mature plants has been established.

Antibiotic dose response studies have been performed and glufosinate ammonia has emerged as the most likely candidate for use in *Pteris* transformation. *Pteris* calli were hypersensitive to hygromycin, whereas kanamycin showed little toxic response in developing calli (Table 3.1). Therefore, bombardments with a vector containing a maize ubiquitin promoter driving expression of GUS and a glufosinate selectable marker have been employed in bombardment experiments.

Transient expression of GFP and GUS via biolistic bombardment

Results from bombarding *Pteris cretica* callus have demonstrated very low levels of transient expression (Figure 3.2). Previous bombardments have been performed on calli consisting of undifferentiated cells induced by 2,4-D. However, in order for embryogenic tissue to arise from these cells, it is believed that treatment of calli with cytokinins is required (Furelli and Garcia 1986). Bombardments performed on calli following treatment for one month with cytokinins were thought to improve efficiency of transient expression, but our experiments have not demonstrated this (data not shown).

Agrobacterium infiltration of Pteris cretica

Observed transient expression in *Agrobacterium* infiltration of *Pteris cretica* was low and difficult to interpret, as negative controls produced similar types of fluorescence observed in infiltrations of GFP-containing constructs (Figure 3.3). Therefore, the observed fluorescence may potentially be a result of autofluorescence of damaged tissue.

PCR amplification of the Pteris vitatta rbcS promoter (partial sequence)

Seven PCR products were amplified from *Pteris cretica* genomic DNA using sequence specific primers from the *Pteris vittata rbcS* promoter. High-yielding, good quality genomic DNA has been difficult to obtain from *Pteris vittata*, therefore we tried amplification of *Pteris cretica* genomic DNA because we could obtain high yields of intact genomic DNA from this closely related species. We were relying on the highly conserved nature of the rubisco sequence to enable amplification of the *rbcS* promoter. A

gradient PCR revealed that 45ºC was the optimal annealing temperature for amplification. A range of genomic DNA concentrations were used as template and all yielded 7 to 8 separate PCR products ranging in size from 500bp to 1500bp (Figure 3.4). These PCR reactions were excised and gel purified for cloning into vector pCR8/GW/TOPO. According to *Pteris vittata* sequence, we expected to see a 518bp product, therefore we sequenced clones containing a ~500bp product and a ~750bp product. BLAST (NCBI) searches revealed no significant homology, therefore we plan to sequence the remaining 5 clones.

Inverse PCR strategy to capture the complete Pteris vittata rbcS promoter

The *Pteris vittata rbcS* promoter (Figure 3.5) was selected for cloning and expression of transgenes in our experiments with *Pteris cretica* because of its constitutive expression and characterized promoter elements (i.e. TATA box, CAAT box, LRE, etc) (Eilenberg 1998). Due to its incomplete sequence, an inverse PCR strategy was designed to capture the remaining unknown upstream sequence of the *rbcS* promoter using long and accurate PCR. These efforts are ongoing due to an unsuccessful cloning of the candidate PCR product (Figure 3.6). Additionally, poor quality genomic DNA extractions have prevented us from obtaining *rbcS* PCR products.

Discussion

The development of an efficient transformation the As hyperaccumulators *Pteris cretica* and *Pteris vittata* would present an excellent opportunity to study the mechanisms involved in As hyperaccumulation. As a result of the low level of transient expression observed in *Pteris* leaves and callus (Figure 3.2), we conclude that maize ubiquitin and *CaMV* 35S promoters do not effectively drive transcription of transgenes in *Pteris cretica* or *Pteris vittata*. Therefore, we have selected the *rbcS* as a putative candidate for driving expression of transgenes in bombarded fern calli. Attempts are ongoing to obtain quality genomic DNA from *Pteris vittata*, as current efforts have been unsuccessful, perhaps due to a lack of PVP in the CTAB buffer. Once quality genomic DNA is obtained from *Pteris vittata*, our inverse PCR strategy will allow the sequencing of the complete rbcS promoter.

For the predominant duration of our efforts towards developing an efficient tissue culture protocol for callus induction and plantlet regeneration, we have used a modified version of the Furelli and Garcia (1987) method of *Pteris cretica* tissue culture. The biggest problem we have experienced with this system is that the integrity of the calli seems to be short-lived and produces a darker green, "mushy" phenotype, one not optimal for perpetuating in culture or using for biolistic bombardments. We are continuing to optimize a callus induction method that may produce more rigid callus that is lighter in color. The clarity seen in the callus in Figure 1A is a rare event. We cultivated such pieces that stand out in culture as lighter in color. Recently, a new paper has emerged that describes a tissue culture protocol specific to *Pteris vittata* (Yang et al.

2007) where the authors also demonstrate As hyperaccumulation by callus. These authors present a new method of callus induction that varies from the method of Furelli and Garcia (1987), therefore we have begun to experiment with this protocol as well. Using both liquid and solid cultures as described by Yang et al. (2007), We have had difficultly in replicating their results. Interestingly, these authors report for the first time that *Pteris vittata* callus was also found to hyperaccumulate As.

Another strategy that we have recently begun to employ is the regeneration of gametophytes from isolated protoplasts. Due to the difficulty of genetic transformation that seems inherent in this genus, we are attempting to test whether protoplast transformation is a feasible alternative. My objective here would be to transform isolated protoplasts and assess their capacity for gametophyte and sporophyte regeneration and evaluate their subsequent survival as stable transgenics. Binding et al. (1992) demonstrated that mature plants could be recovered from isolated protoplasts from members of Bryophyta, Pteridophyta, and Spermatophyta. Several members of our lab have recently isolated protoplasts from *Pteris vittata* and *Pteris cretica*, therefore opening the door to begin testing the efficacy of protoplast transformation in these species.

Materials and methods

Plant material

Spores of *Pteris cretica* cv. 'Mayii' and *Pteris vittata* provided by Edenspace corporation (Dulles, VA) were sterilized in 20% Clorox bleach for two minutes, followed by a 70% ethanol wash for two minutes, then washed three times with sterile water.

Spores were sown on plates containing solid MS basal medium (Murashige and Skoog, 1962) and grown at 25ºC and under a 16 h photoperiod until gametophytes developed (~ 2 months).

Initiation and maintenance of callus

Gametophytes were transferred in replicates of four to solid MS medium supplemented with 5 μ*M* 2,4-Dichlorophenoxyacetic acid (2,4-D) (Sigma) and incubated in the dark at room temperature for three weeks. Upon development of opaque to light green calli approximately 0.25 cm in diameter, opaque sectors of callus were subcultured on fresh medium containing 2,4-D every two weeks until bombardment. To evaluate the effect of osmotic treatment on transient expression, calli were either placed on callus induction medium or callus induction medium containing 0.25, 0.5, 0.75, or 1.0 *M* mannitol 4 hr prior to bombardment until 16 hr after bombardment.

Biolistic transformation experiments

Calli or 8-week old and 12-week old leaves were placed in replicates of six on either callus induction medium or osmotic medium in a PDS 1000/He device (Bio-Rad, Richmond, CA). The plasmid pAHC25 (Christensen and Quail, 1996) containing the *bar* gene and the *gusA* reporter driven by the maize ubiquitin promoter and containing a *nos* terminator (GUS) was used for bombardment. We also used another plasmid pSKA35Se-*gfp* that contained a *CaMV* 35S enhancer element with a 35S minimal promoter driving the expression of the *gfp* gene in a pBluescript® SK+ backbone.

Besides osmotic treatment, rupture disk pressure (450, 650, and 900 psi) was evaluated as a parameter in order to optimize the bombardment protocol. 2 μg of plasmid DNA was precipitated onto 3 mg of 1.0 μm gold (Bio-Rad, Richmond, CA) particles according to Klein et al. (1987). Five microliter samples were spread evenly onto macrocarriers (Bio-Rad, Richmond, CA). Tissue was bombarded at a distance of 7 cm from the stopping screen at a vacuum pressure of 22 in. Hg. To visualize transient expression, three individual calli or leaves were randomly chosen for GUS activity staining with 2-bromo-3-chloro-4-indolyl- β-glucuronic acid (X-Gluc) (Jefferson et al. 1987) 48 hr post bombardment. The remaining three calli were used for selection of stable trangenics.

Selection and regeneration of transgenic plants

Dose response curves for glufosinate ammonium (Sigma), Kanamycin (Sigma), and Hygromycin (Sigma) were generated by evaluating *Pteris cretica* callus growth in a range between 1-50 μ*M* glufosinate ammonium, 10-200 mg/L Hygromycin, and 10-300 mg/L Kanamycin. These concentrations were selected based on the range of commonly used concentrations observed in the tissue culture literature. Calli health was evaluated daily for 14 days (Table 3.1).

Inverse PCR strategy to capture the complete Pteris vittata rbcS promoter

An inverse PCR strategy was developed in order to obtain a complete sequence of the *Pteris vittata rbcS* promoter based on the published complete coding sequence and incomplete promoter sequence (Eilenberg et al. 1998). Primers were designed according

to known restriction sites (XbaI and EcoRV) within the *rbcS* sequence (Table 3.2) in an orientation that would amplify through the unknown sequence between known promoter and the upstream ORF. Five micrograms of genomic DNA was digested with either XbaI or EcoRV in a 200µL volume overnight at 37ºC. Enzymes were heat inactivated (EcoRV for 20 min at 80 ºC and XbaI for 20 min at 65 ºC) and 1 microgram of digested DNA (40 µL from the 5 µg digestion) was subjected to ligation with 5 µL of T4 ligase in a 1000 µL reaction volume. Ligated products were purified with QIAquick PCR purification kit (QIAGEN, Valencia, CA) and subjected to LA PCR (Takara Bio Inc., Madison, WI).

Amplification of Pteris vittata rbcS promoter sequence

Primers for the amplification of the *Pteris vittata rbcS* promoter sequence were designed for cloning into TOPO cloning vector pCR8/GW/TOPO (Invitrogen, Carlsbad, CA). Forward primer sequence was 5'-GGCTAAACCATCAACAAT-3' and reverse primer sequence was 5'-TGCTACTGATACGCTAGAG-3'. A gradient PCR was performed from 40-60ºC to determine optimal annealing temperature

References

Binding H, Gorschen E, Hassanein A, Qing, LH, Mordhorst G, Puck G, Rudnick J, Rong WG, and Truberg B (1992). Plant development from protoplasts of members of Bryophyta, Pteridophyta, and Spermatophyta under identical conditions. *Physiol Plant* 85: 295-300.

Caille N, Zhao FJ and McGrath SP (2005) Comparison of root absorption, translocation and tolerance of arsenic in the hyperaccumulator *Pteris vittata* and the nonhyperaccumulator *Pteris tremula*. *New Phytol* 165: 755-761.

Christensen AH and Quail PH (1996) Ubiquitin promoter-based vectorsfor high level expression of selectable and/or screenable marker genes in monocotyledonous plants. *Transgen Res* 5:213–218.

Dong R. (2005) Molecular cloning and characterization of a phytochelatin synthase gene, PvPCS1, from *Pteris vittata* L. *J Ind Microbiol Biotechnol* 32: 527-533.

Ellis DR, Gumaelius L, Indriolo E, Pickering IJ, Banks JA, and Salt DE. (2006) A novel arsenate reductase from the arsenic hyperaccumulating fern *Pteris vittata*. *Plant Physiol* 141: 1544-1554.

Furelli I and Garcia EC (1987) Regeneration of plants from foliar explants of the fern *Pteris cretica* 'Winsettii " Tropical agronomy. 37 (1-3): 19-30

Gumaelius L, Lahner B, Salt DE and Banks JA (2004) Arsenic hyperaccumulation in gametophytes of *Pteris vittata*. A new model system for analysis of arsenic hyperaccumulation. *Plant Physiol* 136: 3198-3208.

Klein TM, Wolf R, and Sanford JC (1987) High velocity microprojectiles for delivering nucleic acids into living cells. Nature. 327: 70-73.

Kwa SH, Wee YC and Loh CS (1991) Production of aposporous gametophytes and calli from *Pteris vittata* L. pinnae strips cultured in vitro. Plant Cell Reports 10(8): 392-393.

Jefferson RA, Kavanagh TA, and Bevan MW (1987) GUS-fusions: *β*-Glucuronidase as a sensitive and versatile gene fusion marker in higher plants. EMBO J 6: 3901-3907.

Pickering IJ, Gumaelius L, Harris HH, Prince RC, Hirsch G, Banks JA, Salt DE and George GN (2006) Localizing the biochemical transformations of arsenate in a hyperaccumulating fern. *Environ Sci Technol* 40: 5010-5014.

Wang J, Zhao FJ, Meharg AA, Raab A, Feldmann J and McGrath SP (2002) Mechanisms of arsenic hyperaccumulation in *Pteris vittata*. Uptake kinetics, interactions with phosphate, and arsenic speciation. *Plant Physiol* 130: 1552-1561.

Wang HB, Ye ZH, Shu WS, Li WC, Wong MH and Lan CY (2006) Arsenic uptake and accumulation in fern species growing at arsenic-contaminated sites of southern China: field surveys. International Journal of Phytoremediation 8, 1-11.

Wang HB, Wong MH, Lan CY, Baker AJ, Qin YR, Shu WS et al. (2007) Uptake and accumulation of arsenic by 11 Pteris taxa from southern China. *Environ Pollut* 145: 225-233.

Wei CY, Sun X, Wang C, and Wang WY (2006) Factors influencing arsenic accumulation by *Pteris vittata*: a comparative field study at two sites. *Environ Pollut* 141: 488-493.

Wei CY, Wang C, Sun X and Wang WY (2007) Arsenic accumulation by ferns: a field survey in southern China. *Environ Geochem Health* 29: 169-177.

Yang X, Chen H, Xu W, He Z and Ma M (2007) Hyperaccumulation of arsenic by callus, sporophytes and gametophytes of *Pteris vittata* cultured in vitro. *Plant Cell Rep* 26: 1889-1897.

Table 3.1. Dose-dependent effects of Kanamycin (Kan), Hygromycin (Hyg), and Glufosinate ammonium (Gluf) on *Pteris cretica* calli after two weeks of treatment. "survived" indicates treatments where all calli were healthy in appearance at 14 days.

Antibiotic	Concentration (mg/L)	Days until 100% mortality
Kan	10	survived
Kan	25	survived
Kan	50	survived
Kan	100	survived
Kan	200	survived
Kan	300	survived
Hyg	10	2
Hyg	25	1
Hyg	50	1
Hyg	100	1
Hyg	200	1
Gluf	2.5	survived
Gluf	5.0	6
Gluf	7.5	5
Gluf	10.0	5
None	0.0	survived

Table 3.2. Primers designed for inverse PCR amplification of the *Pteris vittata* rbcS promoter.

Primer	Sequence	id	location
RbcSEcoRVfwd	5'-taacgtgtgagaaggggctaaaggg-3'	a	293-317
RbcSXbaIfwd	5'-ccccaagtgcgccaacccccctcgcc-3'	b	609-633
RbcSrev	5'-ttggccaaccttatccgtcttgcct-3'	c	21-45
RbcSrev2	5'-tcttgccttcattgttgatggttta-3'	d	4-28
RbcSEcoRVfwd2	5'-acttagaagtggtggataatttaca-3'	e	353-377
RbcSXbaIfwd2	5'- tgtctccgcaatgcttgtgcgtaca-3'	f	651-675

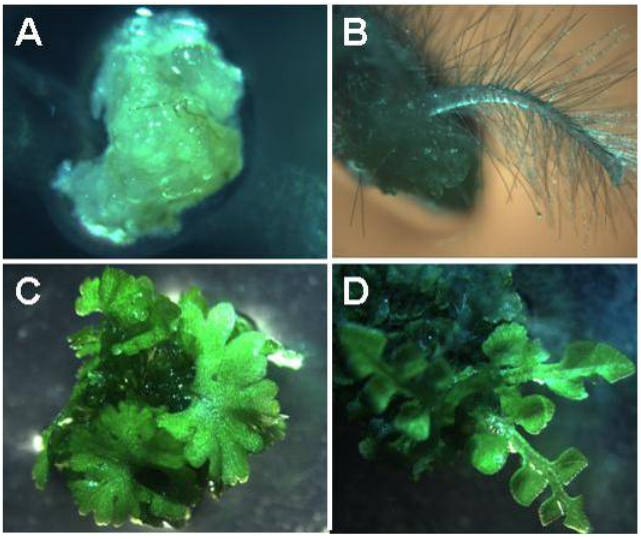

Figure 3.1. Mature *Pteris vittata* and *Pteris cretica* plants (non-transgenic) recovery from tissue culture. Successful callus induction of gametophytic tissue, development of embryo-like structures via cytokinin treatment, and subsequent development of plantlets following treatment with IAA is shown. A, callus; B, root emerging from callus incubated in dark; C, *Pteris cretica* plantlets generated from embryogenic callus; D, *Pteris vittata* plantlets generated from embryogenic callus.

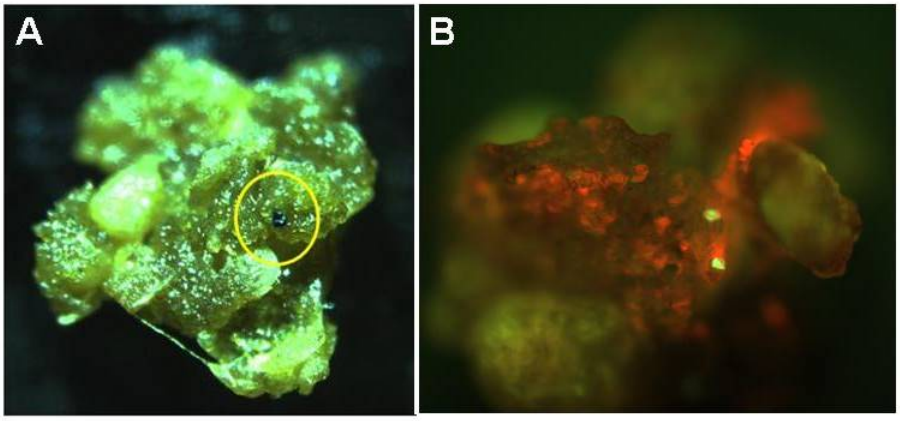

Figure 3.2. *Pteris cretica* callus tissue displaying transient expression of GUS and gfp trangenes. A, yellow circle indicates cells that are expressing GUS reporter gene (driven by maize ubiquitin promoter). B, cells displaying transient expression of a 35S-GFP after bombardment.

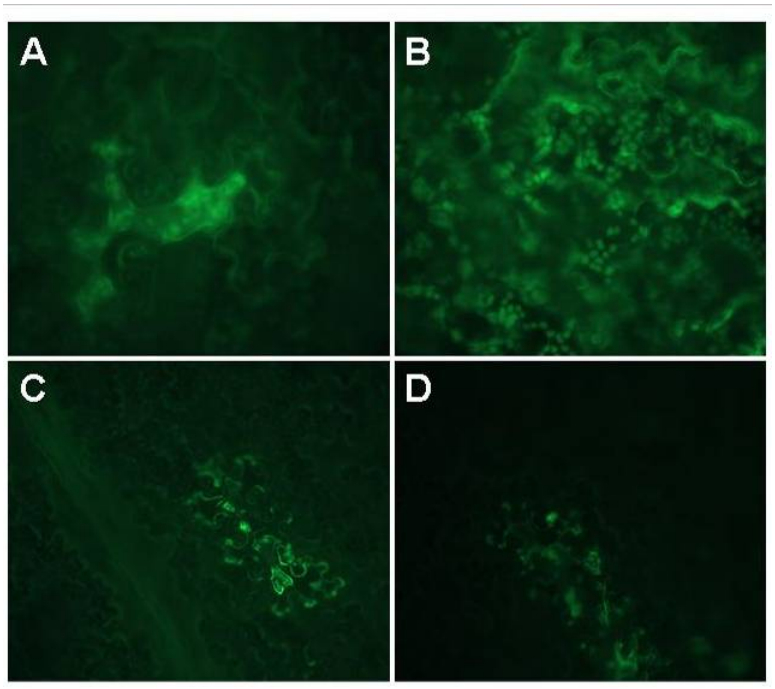

Figure 3.3. Agrobacterium infiltrations of pMDC11035Smut and pBINmGFP5er in *Pteris cretica*. A, pMDC11035Smut at 3.24s exposure 200X mag. B, pBIN19mGFP5er at 2.4s exposure 200X mag. C, pBIN19mGFP5er at 6s exposure 200X mag. D, no plasmid control at 6s exposure 200X mag.

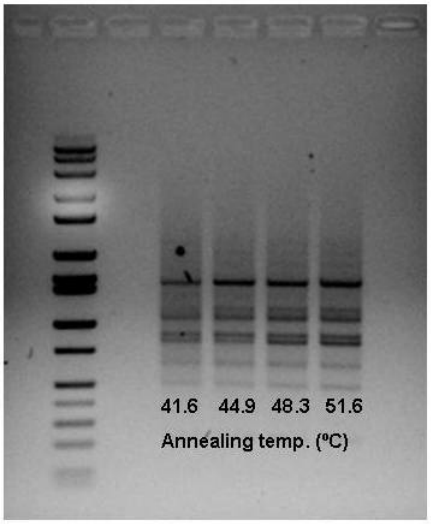

Figure 3.4. Agarose gel showing a gradient PCR (40-60ºC annealing temp.) of *Pteris vittata rbcS* gene amplification in *Pteris cretica*. This PCR resulted in the amplification of 7 recoverable products from *Pteris cretica* genomic DNA that ranged from 500bp-1500bp.

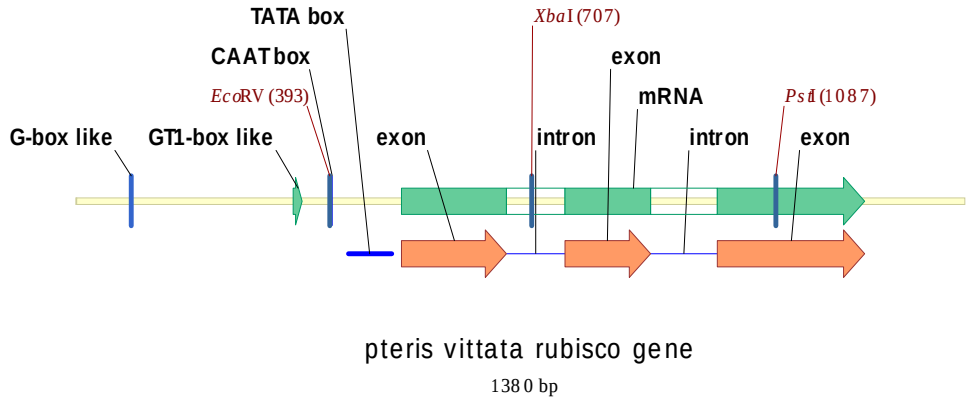

Figure 3.5. Identification of restriction sites (XbaI and EcoRV) within the *Pteris vittata* RUBISCO gene to enable an inverse PCR approach to obtain the complete promoter sequence.

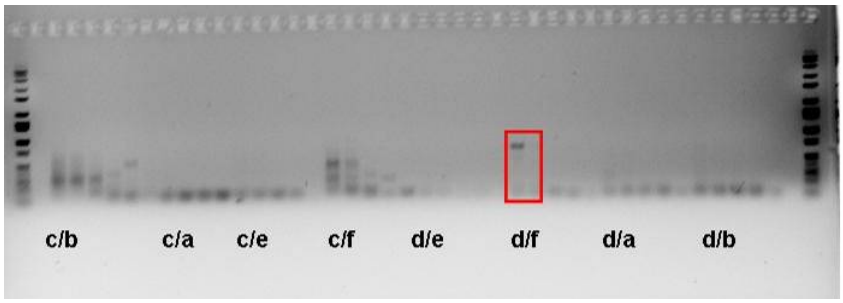

Figure 3.6. Gradient PCR amplification of *Pteris vittata rbcS* promoter sequence. Red box indicates a PCR product of ~1 kb that was selected for cloning. Each group of five lanes correspond to a gradient from 45ºC to 65ºC, ascending in temperature equally from left to right. Letter combinations reflect various primers used (Table 2).

Aluminum accumulation in *Pteris cretica* and metal uptake in vegetation growing on an abandoned aluminum smelter site in Knoxville, TN USA.[2]

[2] The following manuscript has been submitted to Environmental Pollution and is under review.

Authors:

Jason M. Abercrombie[a], Melanie Stewart[b], Murali R. Rao[a], Michael E. Essington[b], and C. Neal Stewart, Jr.[a]

[a] Department of Plant Sciences, University of Tennessee, 2431 Joe Johnson Blvd., Knoxville, TN 37996-4561, USA

[b] Department of Biosystems Engineering and Soil Science, University of Tennessee, 2506 E.J. Chapman Dr., Knoxville, TN 37996-4531, USA

Abstract

Smokey Mountain Smelters in South Knoxville, Tennessee is an abandoned secondary aluminum smelter where smelter waste (slag) was dumped on site, potentially posing a threat to nearby human and ecosystem health. Nitric acid-extractable metal concentrations in the slag (Al, As, Cd, Co, Cr, Cu, Ni, Pb, Se, Zn) were quantified by inductively-coupled plasma spectrophotometry (ICP) and the solids were characterized by x-ray diffraction (XRD). The highest metal concentrations observed were 223 g kg^{-1} Al, 281 mg kg^{-1} As, 132 mg kg^{-1} Se, and 2910 mg kg^{-1} Cu. Metal uptake was quantified in leaves from plants growing naturally on slag, as well as *Pteris cretica* plants employed to extract As from slag. Our data suggests that *P. cretica* accumulates Al in high concentrations, but not As, when grown in slag. Metal concentrations in vegetation growing on slag were lower than controls grown in uncontaminated soil, suggesting low metal availability in slag or exclusion mechanisms in roots.

Introduction

The smelting of metal ores has resulted in extensive emissions of toxic metals into surrounding environmental media (Nriagu and Pacyna 1988). The waste generated during the smelting process is sometimes within close proximity to developed areas, thus posing a significant threat to human health. Smokey Mountain Smelters (SMS) is an abandoned secondary aluminum smelter in South Knoxville, TN that was declared a Superfund site in 2001 due to massive piles of smelter slag and other unknown wastes over most of the 29 acre property. The site is located within a mile radius of numerous residential and commercial properties, wells, schools, and churches. The site is also directly adjacent to a large public housing complex (Figure 4.1). Because the slag material is exposed and uncovered, the surrounding community has no protection from potential pollution derived from groundwater leaching, stormwater runoff, and wind dispersal of the slag-borne metals.

Phytoremediation, or the use of plants to remediate contaminated sites, may serve as a complementary technology in the remediation of grossly polluted soils, such as the SMS site. Plants that can tolerate and thrive on metal-contaminated soils can prevent dispersal by creating a barrier to wind, but may also facilitate safer removal of contaminants via harvesting the above-ground shoot tissue, where metals may accumulate (Salt 1998). Surveys of native plants able to grow on metal-polluted land (e.g. slag spoils) provide more useful candidates for creating a site-specific, vegetative cap because the plants are well-suited to local conditions (Remon et al. 2005). Vegetative caps may serve to prevent erosion of the barren and exposed areas, while at

the same time, initiate the processes of soil formation and vegetative succession (Munshower 1993). Plants that have evolved mechanisms of metal tolerance generally employ one of two main strategies; (1) uptake and accumulation in the vacuole or cell wall or (2) exclusion via organic acid exudates and suppression of root transporters (Baker 1987).

Mounting evidence has demonstrated the utility of *Pteris vittata* for the phytoextraction of arsenic from contaminated soils (Ma et al. 2001; Wei et al 2006a; Wei et al. 2006b; Wei et al. 2007; Wang et al. 2006; Wang et al. 2007). This species is desirable for field-scale phytoextraction of arsenic due to its high biomass and accumulation of > 2% of its dry mass as arsenic (Wang et al. 2002). Fayiga et al. (2004) investigated the effects of metals on the growth and arsenic accumulation in *Pteris vittata* in a greenhouse study. They found that the fern was able to hyperaccumulate arsenic despite the presence of Cd, Ni, Pb, and Zn. Less is known about the performance of *Pteris cretica*, an arsenic-hyperaccumulating relative of *Pteris vittata*, thus prompting its use in this investigation. Because preliminary data indicated high nitric-acid extractable levels of As and the observation that wild vegetation could thrive on the slag piles warranted a test of the hypothesis that *Pteris cretica* could grow in the slag and extract As from the media. A preliminary greenhouse study using slag from the smelter site demonstrated that *Pteris cretica* grew at a reduced rate compared to controls, but showed no other signs of phytotoxicity (Figure 4.2), thus providing the impetus for a field-scale trial of its performance at the SMS site.

The SMS site offers a unique opportunity for scientific investigation due to the various plant species that grow without symptoms of toxicity and predominate on the

otherwise barren landscape of the metal-laden property. Therefore, the objectives of this study were to (1) characterize and quantify the trace metals found in the slag piles, (2) evaluate the shoot tissue for metal accumulation in plants that were found thriving on the piles, and (3) evaluate the capacity of arsenic phytoextraction in *Pteris cretica* when challenged with the mixed slag waste.

Results

Soil pH and metal content of smelter slag and adjacent control soils

Table 4.1 summarizes the metal content (Al, As, Cu, Cr, Cd, Co, Se, Ni, Pb, Zn) and pH of each designated plot (1-6) located within the smelter slag waste area, as well as the nearby uncontaminated soils (A-D), the locations of which are indicated in Figure 4.1. Pb was not detected in any of the slag samples, but was present at low concentrations (<7 mg kg^{-1}) in control soils A-C (data not shown). XRD analysis of the slag material revealed the presence of the $Al(OH)_3$ polymorphs bayerite and gibbsite, spinel ($MgAl_2O_4$), calcite ($CaCO_3$), and calcium aluminum oxide ($Ca_3Al_2O_6$) (Figure 4.3). Statistical comparisons of the mean metal content in slag and control soils reveal significant differences between slag material and control soils (Table 4.1). No significant differences in metal content were found to exist between the two depths assayed. Slag pH values ranged from 7.33 to 8.27, whereas raw pH values for the control soils ranged from 3.86 to 7.66 (Table 4.1). Metal content and pH for uncontaminated control soil employed in the *Pteris cretica* experiment is represented by control soil D (Table 4.1). Although relatively high in Al, As was not detected in nitric acid-extractable samples in

this soil. Additionally, Zn, Ni, Cu, Cr, and Co, were all relatively low in the fern control soil, thereby presenting concerns for interpretation of *Pteris cretica* metal uptake data that are discussed later.

Metal uptake in slag-grown Pteris cretica

Figure 4.4 illustrates the metal content in fronds of field-grown *P. cretica* plants harvested two months after planting. Despite the absence of As in the control soils used for this experiment, As uptake was observed to be restricted in the slag-grown ferns (Figure 4.4). However, Al was accumulated in high concentrations in the slag-grown ferns, ranging from 569 mg kg^{-1} to 4 380 mg kg^{-1}, and averaging 1 821 mg kg^{-1}. Slag-grown ferns also accumulated significantly higher amounts of Cu, Mo, Se, Zn, and Ni than were observed for control ferns.

Metal uptake in slag-grown vegetation and bioaccumulation factors

A comparison of the metal content in leaves of wild vegetation found growing on the slag heaps versus nearby uncontaminated control soils is illustrated in Figure 4.5. Surprisingly, restricted uptake of several species analyzed was indicated by significantly higher metal uptake in plants harvested offsite on uncontaminated soil compared to the slag-grown plants (Figure 4.5.), especially evident for the uptake of As, Se, Cu, and Co. One exception to this trend was demonstrated by the pioneering species *Verbascum thapsus*, accumulating the highest levels of aluminum uptake among slag-grown plants, as well as among controls (323 mg kg^{-1} and 137 mg kg^{-1}, respectively). Slag-grown *V.*

thapsus also exhibited the highest Ni and As uptake, however all control plants exhibited significantly higher As uptake compared to the slag-grown plants. *Carduus nutans* growing offsite accumulated the highest levels of As, Cr, Co, and Cd. *Phytolacca americana* contained the highest concentrations of Zn in leaf tissues harvested from plants growing in uncontaminated soil.

Bioconcentration factors (BCFs) (i.e. the ratio of metal concentrations in the shoot to those in the soil) indicate the efficiency at which plants extract metals from the soil. Slag-grown *P. cretica* exhibited the highest BCF values with respect to Al and Se (Figure 4.6). All plant species analyzed from uncontaminated soil had significantly higher BCFs for Al, As, Cu, Cr, Se, Ni, and Cd, with the exception of slag-grown *P. cretica* which exhibited much higher BCFs for Al, As, and Se. BCF for Zn in *P. cretica* grown in uncontaminated soil exceeded 50, significantly higher than any other species. *Carduus nutans* grown in uncontaminated soil had the highest BCFs for As, Ni, and Cd.

Discussion

Metal uptake and bioaccumulation factors in wild vegetation

Numerous investigators have surveyed wild plant populations growing on or nearby metal-contaminated sites, generally with intentions of discovering species with novel remediation traits, such as metal tolerance and accumulation. Del Rio et al. (2002) studied trace metal uptake in 99 wild plant species growing in an area contaminated from a spill of toxic pyretic sludge. These authors identified 11 plant species that

demonstrated promising utility in the phytoremediation of Pb, Zn, Cu, Cd, and As due to their observed metal tolerance, accumulation, and high biomass. If phytoextraction is not a feasible means of remediation, then natural revegetation of a contaminated site can serve to stabilize the contamination by minimizing stormwater runoff and wind dispersal (Vangronsveld et al. 1995). In the current study, most plants exhibited significantly lower concentrations of trace elements in their leaves compared to control plants (Figure 4.5), thereby suggesting that these plants were able to survive in the metalliferous medium via exclusion mechanisms. Alternatively, due to the neutral pH range of the slag and the abundance of aluminum (hydro)oxides, trace metal adsorption resulted in very low metal availability. Similar reports by Gonzalez and Gonzalez-Chavez (2006) suggest that most plants growing near mining wastes were employing exclusion mechanisms because metals did not accumulate in shoot tissues despite the high concentrations found in the soil. Despite the exclusion behavior found in those plants, two species, *Polygonum aviculare* and *Jatropha dioica* were reported to accumulate Zn at concentrations near the criteria for hyperaccumulation. Similarly, we report that slag-grown *Verbascum thapsus* was not only tolerant to the slag metal concentrations, but exhibited significantly higher accumulation of Ni and Al than those growing in uncontaminated soil (Figure 4.5). Regardless, the highest metal content observed in *V. thapsus* (462 mg kg^{-1}) was lower than sufficient for hyperaccumulator status. In a recent study of metal (Cu, Fe, Mn, Ni, Pb, Zn) content in a close relative, *Verbascum olympicum*, Guleryuz et al. (2006) reported that metal contents in different organs were highly correlated to metal content found in the soil.

The BCF values for these species demonstrate that most of the wild species have no reasonable utility for employment in phytoextraction at the SMS site. McGrath and Zhao (2003) demonstrate that the two key components necessary for a plant to be of feasible utility in the phytoextraction of metals are high biomass and high BCF (i.e. the metal concentrations in the above-ground biomass should exceed those found in the soil). Some of the species that grew on the slag exhibited substantial biomass. One obvious explanation for the low BCF values observed for slag-grown plants is the elevated metal concentrations found in the slag (Table 4.1). Even in the control plants that exhibited significantly higher BCFs than slag-grown plants, no wild species had a BCF close to 1. McGrath and Zhao (2003) present a useful model for selecting feasible candidates for phytoextraction. According to these authors, in order to reduce the metal concentration in the top 20 cm of topsoil by half, with a BCF of 1, even high biomass crops (20 t ha^{-1}) would require approximately 100 crop harvests.

Trace element uptake in Pteris cretica

Arsenic hyperaccumulation in members of the *Pteris* genus is well documented and the list of field-capable As-hyperaccumlating *Pteris* species and cultivars continues to grow as surveys of *Pteris* taxa found at As-contaminated sites are being conducted (Wei et al 2006; Wei et al. 2007; Wang et al. 2006; Wang et al. 2007). We selected *P. cretica* cv. Mayii because of its proven field-scale and hydroponic performance in As hyperaccumulation (Wei et al. 2006; Poynton et al. 2004; Fayiga et al. 2005). We were primarily interested in whether the fern was capable of extracting the high concentrations

of As found in the slag material. Interestingly, the fern accumulated high amounts of Al during the 8 weeks of growth in the slag waste.

The most common criteria for a plant to be considered a hyperaccumulator is that the shoot metal concentration must exceed 1.0% for Zn and Mn, 0.1% for Al, As, Se, Ni, Co, Cr, Cu, and Pb and 0.01% for Cd (Branquinho et al. 2007). In this study, *P. cretica* clearly met these criteria for Al, however the extremely high concentrations of Al found in the growth medium (slag) contributed to a low BCF value, thus negating a characterization of *P. cretica* as a hyperaccumulator of aluminum at this time. However, the interesting observation that *P. cretica* exhibited a BCF of over 50 for Zn uptake (Figure 4.6) warrants further investigation into the uptake dynamics of *P. cretica* under Zn-deficient conditions, as was observed in control soils used in the *P. cretica* experiment. These results are similar to those found by An et al. (2006) who reported Zn tolerance and accumulation in *Pteris vittata*. These authors demonstrated that *P. vittata* accumulated up to 737 mg kg^{-1} Zn in fronds in the field, but could also accumulate As under high Zn concentrations, suggesting that *P. vittata* could be useful in sites co-contaminated with Zn and As. We did not detect the presence of As in the uncontaminated soil used for the *P. cretica* control plants in this study, thus explaining the very low amount of As observed in these plants.

Although aluminum (hydro)oxides were the predominant minerals found in the SMS slag, these minerals are also ubiquitous in soils and affect the fate and transport of ionic pollutants (Cox and Ghosh, 1994). Cox and Ghosh (1994) demonstrated that the adsorption of As(V), $CH_3AsO(OH)_2$, and $(CH_3)_2AsOOH$ to amorphous $Al(OH)_3$, gibbsite, α-Al_2O_3, and γ-Al_2O_3 increased up to pH 7, but decreased sharply at higher pH

values. Extractions to determine the bioavailability of As in the slag material were not performed. However, based upon the uptake measurements observed in slag-grown *P. cretica*, we believe that the arsenic is likely adsorbed to the aluminum oxides/hydroxides found to predominate in the slag, thereby making As unavailable for uptake. This phenomenon has recently been reported in a study that characterized arsenate adsorption on aluminum oxide and phyllosilicate mineral surfaces in smelter-impacted soils (Beaulieu et al. 2005). These authors suggested that As originally released from the smelter was oxidized, dissolved, and adsorbed onto soil minerals and that the mildly acidic pH conditions found in the soil allowed for stable sorption complexes, thus preventing significant As mobilization. It is known that As mobility in soils is affected by pH (Adriano 1986). A recent study of As mobility in sites impacted by As mining and smelting suggested that As is mobile at extreme pH values (<2 or >8), such as those observed in mine tailings and tailings-impacted alluvial soils, however all other soils exhibited very low As mobility (Krysiak and Karczewska, 2007). Our data only reflects the pH values found in the top 20 cm of the slag piles, however since some of the plots exhibited pH values near 8 and greater (Table 4.1; plot 4 and 5), pH and resulting absorptive capacities in deeper zones may differ from those at the slag surface, thereby potentially mobilizing Al-bound As species into the groundwater.

Aluminum tolerance and accumulation

Aluminum toxicity in acid soils is a global agricultural dilemna, therefore much attention has been given towards understanding Al tolerance in plants. Attempts to

identify genes involved in Al tolerance have been made in studies of Arabidopsis, wheat, barley, and, rye (reviewed by Magalhaes 2006). A major mechanism of Al tolerance that has been elucidated in these species is associated with the chelation of Al via exudation of the organic acid malate from the root apex, thereby preventing Al uptake via exclusion (Magalhaes 2006).

Conversely, Al accumulation has been reported for 127 species within the Melastomataceae family in the Order Myrtales, however the mechanisms through which this occurs are unknown (Jansen et al. 2002). Al accumulators have also been reported for members of the Rubiaceae and it is believed that these plants may utilize Si for Al detoxification, as relatively high Si levels were also observed in these plants (Jansen et al. 2003). However, this finding has not been confirmed because the Si : Al mole ratio widely varied among species (Jansen et al. 2003). The Al uptake in *Pteris cretica* observed in this study certainly warrants follow-up investigation. Because of the high number of environmental variables found in a field-scale study such as this, more controlled experiments are needed, paying particular attention to effects of pH and nutrient availability on Al content in various tissues. However, high Al accumulation was observed for all six plots, spanning a wide spatial range at the study site, thereby suggesting that the ferns are able to employ some mechanisms of accumulation.

Our data suggests that for wild vegetation growing on slag, Al is excluded, possibly via exudation of organic acids (i.e. malate, citrate) similar to well-characterized Al tolerance mechanisms. It is known that the solubility of Al is significantly reduced at pH 5.0 and above (Reid et al. 1971). Additionally, elevated concentrations of cations (i.e.

Ca^{2+}, Mg^{2+}) in the rhizosphere are known to ameliorate Al toxicity (Brady et al 1993; Kinraide et al 1992). XRD analyses have revealed the presence of spinel ($MgAl_2O_4$), calcite or $CaCO_3$, and calcium aluminum oxide ($Ca_3Al_2O_6$), indicating the presence of these cations, thereby leading us to speculate that despite the abundantly high concentrations of Al found in the slag, the effects of pH and abundance of Ca^{2+} and Mg^{2+} ions likely decrease the concentration of Al^{3+} ions and ameliorate the phytotoxicity of the slag Al.

Conclusions

Our discovery that aluminum accumulation occurs in *Pteris cretica* when challenged with slag containing high concentrations of other toxic metals and metalloids has prompted us to investigate this phenomenon under controlled experimental conditions. We are particularly interested in the dynamics of As and Al uptake in *P. cretica* in the context of their bioavailability. Also as a result of this study, we intend to characterize the capacity for *P. cretica* to accumulate Cu and Zn.

It would be unreasonable to employ phytoremediation to cleanup a site as grossly contaminated as the SMS site, however this study has provided new insights that extend beyond phytoextraction. The windborne dispersal of metals at the SMS site may be lowered by continued succession of the known tolerant ecotypes found growing directly on the slag material. Therefore, phytostabilization of the slag may serve as an interim measure in prevention of contaminant spread that precedes appropriate remediation of this potential danger to the local community.

Additionally, we have identified several plant species as candidates for further study that may contribute to our understanding of aluminum tolerance. Because Al toxicity is such a significant global agricultural problem, exploring the molecular mechanisms that play a role in the exclusion of Al in the species evaluated in this study is warranted.

Materials and Methods

Study site: site history, hydrogeologic setting, and EPA site inspection summary

The Smoky Mountain Smelter site is located in Knoxville, TN (83°55'36.77" West longitude and 35°55'06.68" North latitude). The 29-acre property is partially wooded, but significantly barren and covered with large piles of unknown wastes thought to derive primarily from the secondary aluminum processing facility that operated onsite from 1979 until the close of operations sometime after May 1994. Prior to Smokey Mountain Smelters and the existence of environmental regulations, the site was home to Knoxville Fertilizer Company from at least 1922 until 1948, and subsequently associated with several agricultural chemical manufacturing companies until 1965 (Maupin 2005). The agricultural facility could have discharged wastes into settling ponds (TDHE 1983). No information is known concerning the regulatory status of the site prior to 1980.

During the years of SMS operation, owners Daniel E. Johnson and David A. Witherspoon, Jr. received numerous citations from the local division of air pollution

control due to numerous complaints from local residents (KCDAPC 1985; KCDAPC 1989). The site historically had a strong ammonia odor and the waste was often burning (KCDAPC 1983). In addition to air pollution violations, the TN Division of Solid Waste Management issued a citation for operating a landfill without a permit and a geologic inspection of the site characterized the site as unsuitable for use as an industrial landfill (TDHE/DSWM 1983a; TDHE/DSWM 1983b). Materials that were incinerated in the smelters included by-products of primary aluminum production (i.e. aluminum dross, pot pads, pot bottoms, bath pads, and crushed material containing "non-processible" carbon, iron, cryolite (Na_3AlF_6), dust, etc. (Maupin 2005). Pot pads, pot bottoms, and bath pads are all generated inside of and in contact with spent potliners, which are listed Hazardous Wastes, designated as hazardous waste number K088 under the EPA Resource Conservation and Recovery Act (RCRA) (Maupin 2005). Maupin (2005) reported that between 1985 and 1992 SMS received large quantities of materials (oily scraper chips, furnace bottoms, magnetic separator accumulations, tabular balls, selee filters, south ingot furnace bottoms, mold line floor sweepings, can rec skim, and other miscellaneous materials derived from primary aluminum production) from a nearby primary aluminum production facility in the city of Alcoa, TN. Large quantities of hazardous substances derived from the materials sent by the primary processing facility are known to still be present at the site (Maupin 2005).

The East Tennessee valley, in which the SMS site is situated, is oriented in a northeast-southwest direction as a result of folding and fracturing (TDC/DG 1956). The underlying geology of the SMS site is Middle Ordovician shale and characterized by extensive Karst development (TDC/DG 1956). Groundwater movement in such areas is

restricted to largely interconnected fractures, thus potentially targeting approximately 2524 people that use groundwater in the 4 mi radius surrounding the SMS site (Maupin 2005). Previous analytical results of groundwater samples from the site indicated the presence of antimony, arsenic, pentachlorophenol, dieldrin, and various toxic metals (except Cd), all exceeding the primary drinking water maximum contaminant levels as declared by the US EPA (Maupin 2005). This report also concluded that the onsite, unlined waste lagoon posed a serious threat to groundwater quality, considering the permeable subsurface. Similar conclusions were also reported for the vulnerability of local wetlands and downstream fisheries.

As a result of the aforementioned evidence, the TN Division of Remediation site inspection report suggested that the SMS site has potential to be placed on the National Priorities List for cleanup and recommended immediate remedial action. It is clear that trespassing occurs on the site by local children; the adjacent housing project, Montgomery Village, currently houses hundreds of individuals and an elementary school is located approximately one mile away. For example, large gaps in the chain-link fencing on the side facing the adjacent public housing complex, well worn footpaths leading between the complex, and the predominance of graffiti within the dilapidated warehouse surrounding the rotary furnaces of the smelter raise obvious concerns for the health of local children.

Soil and plant sampling

During the month of May 2006, leaves were sampled from plants growing on smelter waste piles, but displaying no apparent symptoms of toxicity. Species selected for analysis were those found in multiple locations among the slag heaps, initially leading us to speculate that these species were employing some mechanisms of tolerance to potentially high concentrations of several metals. These species were: *Verbascum thapsus, Lirodendron tulipifera, Carduus nutans, Solidago □mericana□, Ailanthus altissima*, *Parthenocissus quinquefolia, Platanus occidentalis,* and *Phytolacca □mericana.* Representative control samples for each species collected at the site were taken from an uncontaminated area adjacent to the site. Leaf samples were only collected for each species that appeared to best represent a mirror image of plant age, which was performed by on-site comparisons of leaf size and plant height. Each treatment (species) sampled consisted of ≥4 biological replicates.

Slag and soil samples were taken with an auger to represent a depth ranging from 0-20 cm. All soil samples were air dried and sieved to < 2 mm prior to analysis. Each soil sampling was performed in triplicate at each plot from the *Pteris cretica* experiment, as well as the uncontaminated control plots. Due to the high clay content of the soil found in the nearby representative control soil samples (A, B, C; Figure 4.1), less compact soil with a higher organic content was selected for the *Pteris cretica* planting controls.

Pteris cretica experiment

Six 1 m^2 plots of waste soil were chosen to span the spatial range of the site for uptake experiments using *Pteris cretica* cv. Mayii. Within each plot, fifteen 5-month-old ferns were transplanted, spaced 20 cm apart, fertilized with 20-20-20 N:P:K Osmocote® fertilizer, and treated with a 3 kg application of lime. Shade cloth structures were employed randomly to three of the six plots, as well as one of the two control plots which were located adjacent to the contaminated area on uncontaminated soil. All plots were watered as needed with water from the on-site waste lagoon. After two months of growth in the field (June 1 – July 30th, 2006), above-ground biomass for each sample was harvested for metal analysis.

Sample preparation and chemical analysis

Soil, smelter slag, and plant tissue nitic acid-extractable metals (Al, As, Cd, Co, Cr, Cu, Mo, Ni, Pb, Se, Zn) were determined. Three and a half grams were subjected to a 4 M nitric acid overnight reflux at 70 ºC according to Chang et al. (1984). One gram of leaf tissue from each plant analyzed was oven-dried at 60 ºC for 72 hrs and ashed in a muffle furnace at 450 ºC overnight. Ashed samples were digested with 10 ml of 1 M HNO_3, heated to dryness, then warmed to near boiling in 10 ml of HCl. Samples were brought to 50 ml volume with deionized H_20 and filtered using Whatman no. 42 paper prior to ICP analysis by a SPECTRO CIROS CCD EOP inductively coupled plasma spectrophotometer (ICP) with an AS400 autosampler (SPECTRO Analytical Instruments, Kleve, Germany). To characterize the mineralogy of the smelter slag, samples were

subjected to x-ray diffraction (XRD) analysis using a D8 Advance with a K760 generator (Bruker AXS, Inc., Madison, WI). A simple fizz test was performed by adding a few drops of 10% HCl to confirm the presence of calcium carbonate in the slag material. Soil and slag pH was determined after a 1 hr shaking incubation of a 1:1 mixture of soil: 0.1 M $CaCl_2$.

Statistical analysis

Because all field data did not meet the assumptions for normality, a one-way Mann-Whitney *U* test was employed to evaluate the differences in mean metal uptake between slag-grown and control wild vegetation, as well as in comparisons of mean slag and control soil metal concentrations using JMP statistical software (SAS Inc., Cary, NC).

References

Adriano DC (1986) Trace elements in the terrestrial environment. Sringer-Verlag, New York.

An ZZ, Huang ZC, Lei M, Liao XY, Zheng YM, and Chen TB (2006) Zinc tolerance and accumulation in *Pteris vittata* L. and its potential for phytoremediation of Zn- and As-contaminated soil. Chemosphere 62: 796-802.

Baker A, McGrath S, Reeves R, and Smith J (2000) Metal hyperaccumulator plants: a review of the ecology and physiology of a biochemical resource for phytoremediation of metal-polluted soils. In : Terry, N., Banuelos, G. (Eds.), Phytoremediation of contaminated soils and waters. Lewis Publishers, Boca Raton, FL, 85-107.

Beaulieu BT and Savage KS (2005) Arsenate adsorption structures on aluminum oxide and phyllosilicate mineral surfaces in smelter-impacted soils. Environmental Science and Technology 39: 3571-3579.

Brady DJ, Edwards DG, Asher CJ, and Blamey FCP (1993) Calcium amelioration of aluminum toxicity effects on root hair development in soybean (*Glycine max* L.) Merr. New Phytologist 123(3): 531-538.

Branquinho C, Serrano HC, Pinto MJ and Martins-Loucao MA (2007) Revisiting the plant hyperaccumulation criteria to rare plants and earth abundant elements. Environmental Pollution 146: 437-443.

Cox DD and Ghosh MM (1994) Surface complexation of methylated arsenates by hydrous oxides. Water Research 28 (5): 1181-1188.

Del Rio M, Font R, Almela C, Velez D, Montoro R and De Haro Bailon A (2002) Heavy metals and arsenic uptake by wild vegetation in the Guadiamar river area after the toxic spill of the Aznalcollar mine. Journal of Biotechnology 98: 125-137.

Fayiga AO, Ma LQ, Cao X and Rathinasabapathi B (2004) Effects of heavy metals on growth and arsenic accumulation in the arsenic hyperaccumulator *Pteris vittata* L. Environmental Pollution 132: 289-296.

Fayiga AO, Ma LQ, Santos J, Rathinasabapathi B, Stamps B and Littell RC Effects of arsenic species and concentrations on arsenic accumulation by different fern species in a hydroponic system. International Journal of Phytoremediation 7: 231-240.

Gonzalez RC and Gonzalez-Chavez MC (2006) Metal accumulation in wild plants surrounding mining wastes. Environmental Pollution 144: 84-92.

Guleryuz G, Arslan H, Izgi B and Gucer S (2006) Element content (Cu, Fe, Mn, Ni, Pb, and Zn) of the ruderal plant *Verbascum olympicum* Boiss. From East Mediterranean. Zeitschrift fur Naturforschung 61: 357-362.

Jansen S, Watanabe T and Smets E (2002) Aluminium accumulation in leaves of 127 species in Melastomataceae, with comments on the order Myrtales. Annals of Botany (Lond) 90: 53-64.

Jansen S, Watanabe T, Dessein S, Smets E and Robbrecht E (2003) A comparative study of metal levels in leaves of some Al-accumulating Rubiaceae. Annals of Botany (Lond) 91: 657-663.

Kinraide TB, Ryan PR and Kochian LV (1992) Interactive effects of Al, H, and other cations on root elongation considered in terms of cell-surface electrical potential. Plant Physiology 99: 1461-1468.

KCDAPC (1983) Facility inspection report, David Witherspoon, Inc. – Witherspoon and Johnson Dump. Inspected by the Knox County Department of Air Pollution Control, December 5.

KCDAPC (1985) David Witherspoon – Historical record, Knox County Department of Air Pollution Control.

KCDAPC (1989) List of complaints, inspections, and departmental action: Knox County Department of Air Pollution Control, August 10.

Krysiak A and Karczewska A (2007) Arsenic extractability in soils in the areas of former arsenic mining and smelting, SW Poland. Science of the Total Environment 379: 190-200.

Magalhaes JV (2006) Aluminum tolerance genes are conserved between monocots and dicots. Proceedings of the National Academeies of Science U S A 103, 9749-9750.

Maupin BH (2005) Expanded site inspection report: Smokey Mountain Smelters, Knox County, TN 37920, TN Division of Remediation site # 47-559, U.S. EPA ID # TN0002318277 Vol. 1.

McGrath SP and Zhao FJ (2003) Phytoextraction of metals and metalloids from contaminated soils. Current Opinion in Biotechnology 14: 277-282.

Munshower FF (1993) Practical handbook of disturbed land revegetation. Lewis

Publishers, Boca Ratton, FL.

Nriagu JO and Pacyna JM (1988) Quantitative assessment of worldwide contamination of air, water and soils by trace metals. Nature 333: 134-139.

Poynton CY, Huang JW, Blaylock MJ, Kochian LV and Elless MP (2004) Mechanisms of arsenic hyperaccumulation in Pteris species: root As influx and translocation. Planta 219: 1080-1088.

Reid DA, Fleming AI and Foy CD (1971) A method for determining aluminum response of barley in nutrient solution in comparison to response in Al-toxic soil. Agronomy Journal 63: 600-603.

Remon E, Bouchardon JL, Cornier B, Guy B, Leclerc JC and Faure O (2005) Soil characteristics, heavy metal availability and vegetation recovery at a former metallurgical landfill: Implications in risk assessment and site restoration. Environmental Pollution 137: 316-323.

Salt DE, Smith RD and Raskin I (1998) Phytoremediation. Annual Review of Plant Physiology and Plant Molecular Biology 49: 643-668.

TDC/Division of Geology (DG) (1956) Groundwater Resources of East Tennessee., State of Tennessee, Department of Conservation, Division of Geology. Bulletin 58, Part 1., 6-9, 12, 43-4, 245-68.

TDHE/DSWM (1983a) Letter to D. Johnson (Smokey Mountain Smelters), RE: Geologic evaluation of proposed industrial storage yard and landfill, November 18.

TDHE/DSWM (1983b) Report of geologic investigation, by G. Pruitt (DSWM), November 4.

Vangronsveld J, Van Assche F and Clijsters H (1995) Reclamation of a bare industrial area contaminated by non-ferrous metals: in situ metal immobilization and revegetation. Environmental Pollution 87: 51-59.

Wang J, Zhao FJ, Meharg AA, Raab A, Feldmann J, and McGrath SP (2002) Mechanisms of arsenic hyperaccumulation in *Pteris vittata*. Uptake kinetics, interactions with phosphate, and arsenic speciation. Plant Physiology 130: 1552-1561.

Wang HB, Ye ZH, Shu WS, L, WC, Wong MH and Lan CY (2006) Arsenic uptake and accumulation in fern species growing at arsenic-contaminated sites of southern China: field surveys. International Journal of Phytoremediation 8: 1-11.

Wang HB, Wong MH, Lan CY, Baker AJ, Qin YR, Shu WS (2007) Uptake and accumulation of arsenic by 11 Pteris taxa from southern China. Environmental Pollution 145: 225-233.

Wei CY and Chen TB (2006a) Arsenic accumulation by two brake ferns growing on an arsenic mine and their potential in phytoremediation. Chemosphere 63: 1048-1053.

Wei CY, Sun X, Wang C and Wang WY (2006b) Factors influencing arsenic accumulation by *Pteris vittata*: a comparative field study at two sites. Environmental Pollution 141: 488-493.

Wei CY, Wang C, Sun X and Wang WY (2007) Arsenic accumulation by ferns: a field survey in southern China. Environmental Geochemistry and Health 29: 169-177.

Appendix

Table 4.1

HNO_3-extractable metal concentrations (mg kg^{-1}; Al given in g kg^{-1}) in smelter slag (plots 1-6) and uncontaminated control soil (A-C) expressed as mean ± sd. *P* values represent one-way Mann-Whitney *U* test comparisons of slag and control means.

Plot	depth (cm)	pH	Al	As	Zn	Se	Ni	Cu	Cr	Co	Cd
1	1-10	7.65	178 ± 13	196.1 ± 14.0	318.4 ± 128.8	19.7 ± 1.2	333.3 ± 105.5	924.8 ± 378.4	47.8 ± 4.4	6.6 ± 0.8	15.2 ± 1.0
	10-20	7.60	170 ± 19	182.3 ± 20.0	457.2 ± 196.8	21.8 ± 4.2	239.0 ± 118.5	790.8 ± 398.4	49.2 ± 11.8	5.8 ± 0.3	14.2 ± 1.4
2	1-10	7.64	203 ± 6	219.6 ± 5.7	610.8 ± 298.2	25.2 ± 6.8	1 196.5 ± 648.7	999.0 ± 775.0	67.6 ± 23.0	7.9 ± 2.9	17.0 ± 0.7
	10-20	7.58	189 ± 29	204.0 ± 27.3	233.4 ± 118.0	17.9 ± 9.2	1 750.4 ± 223.7	2 082.5 ± 208.4	42.0 ± 25.8	7.7 ± 1.5	16.0 ± 2.3
3	1-10	7.42	181 ± 13	202.6 ± 12.4	879.2 ± 85.0	53.4 ± 2.9	318.0 ± 22.2	1 479.3 ± 53.3	111.4 ± 8.6	9.0 ± 0.5	17.1 ± 0.5
	10-20	7.62	168 ± 14	185.7 ± 13.7	767.0 ± 159.2	49.1 ± 3.5	309.1 ± 30.0	1 873.5 ± 469.7	103.3 ± 8.5	8.1 ± 1.1	15.8 ± 0.8
4	1-10	7.78	201 ± 23	212.2 ± 23.2	160.0 ± 25.0	111.1 ± 16.6	82.9 ± 24.1	685.1 ± 169.9	309.1 ± 57.0	4.0 ± 0.7	15.9 ± 2.5
	10-20	8.13	185 ± 14	189.7 ± 15.8	105.3 ± 12.9	116.3 ± 15.6	61.2 ± 15.6	500.4 ± 32.8	345.9 ± 41.1	4.2 ± 0.8	16.5 ± 1.4
5	1-10	7.55	209 ± 17	209.1 ± 6.2	255.6 ± 80.2	19.4 ± 3.4	531.8 ± 18.4	827.5 ± 124.4	44.1 ± 4.9	6.9 ± 0.3	18.3 ± 0.5
	10-20	7.99	198 ± 6	207.5 ± 9.1	436.1 ± 237.6	36.0 ± 15.9	324.8 ± 121.6	871.8 ± 195.5	81.9 ± 36.8	6.6 ± 0.8	18.2 ± 0.8
6	1-10	7.60	210 ± 9	221.1 ± 11.8	676.9 ± 156.4	34.4 ± 7.7	882.6 ± 473.3	1 639.5 ± 319.3	82.8 ± 22.7	9.2 ± 0.9	19.8 ± 1.0
	10-20	7.78	223 ± 17	230.3 ± 26.2	719.2 ± 255.0	27.0 ± 8.6	691.5 ± 672.5	1 440.8 ± 628.7	65.2 ± 22.3	8.3 ± 2.8	20.5 ± 2.3
A	1-10	6.46	20 ± 0.1	41.4 ± 2.0	4 645.4 ± 219.2	nd	24.6 ± 0.9	990.8 ± 43.8	20.9 ± 0.9	30.1 ± 1.3	13.0 ± 0.6
	10-20	7.43	24 ± 2	43.0 ± 4.9	3 284.5 ± 509.2	2.5 ± 0.7	28.3 ± 3.2	742.6 ± 116.7	23.5 ± 3.1	25.9 ± 2.4	11.3 ± 1.1
B	1-10	6.73	40 ± 0.7	53.2 ± 1.2	289.6 ± 64.3	16.4 ± 2.1	44.0 ± 0.6	187.5 ± 16.4	32.5 ± 0.4	18.5 ± 1.4	8.6 ± 0.4
	10-20	6.44	14 ± 23	58.7 ± 5.6	267.5 ± 44.3	19.8 ± 0.6	53.7 ± 6.5	215.0 ± 37.4	35.3 ± 2.6	22.4 ± 0.9	9.4 ± 0.8
C	1-10	6.36	0.4 ± 0.01	36.1 ± 0.7	147.5 ± 35.2	79.1 ± 2.7	39.8 ± 3.0	57.3 ± 20.7	29.6 ± 0.8	34.0 ± 1.8	0.8 ± 0.0
	10-20	6.26	0.4 ± 0.05	nd	120.3 ± 12.0	77.3 ± 1.6	38.5 ± 1.0	42.9 ± 5.7	29.6 ± 1.1	32.3 ± 0.8	0.8 ± 0.0
D	1-10	5.65	42 ± 0.2	nd	0.7 ± 0.0	nd	5.5 ± 0.1	2.7 ± 0.1	0.5 ± 0.0	0.6 ± 0.1	0.8 ± 0.0
	10-20	5.80	29 ± 3	nd	0.7 ± 0.1	nd	5.9 ± 0.6	2.8 ± 0.4	0.5 ± 0.1	0.5 ± 0.0	0.9 ± 0.1
P			***	***	***	***	***	***	***	***	***

P<0.01,P<0.001,*** P<0.0001*

Figure 4.1. Satellite image of the abandoned Smokey Mountain Smelter site in South Knoxville, TN, USA (Image from Google™ Earth). The large building on the property houses two rotary furnaces and an incinerator. Slag from the smelting process now exists in piles over much of the property. Numbers 1-6 and respective black spots designate plots of *Pteris cretica* plantings and slag sampling. The white line outlines the waste lagoon. Letters A-D indicate approximate locations of uncontaminated soil sampling. The right side of the image shows the adjacent public housing project.

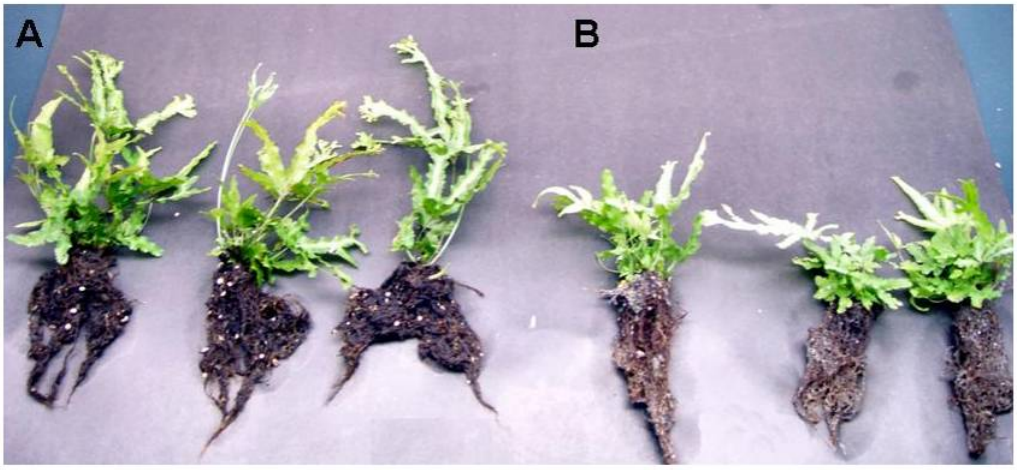

Figure 4.2 Phenotype of *Pteris cretica* grown for two months in the greenhouse on SMS slag material. A, *Pteris cretica* grown in uncontaminates soil. B, *Pteris cretica* grown for two months in smelter slag.

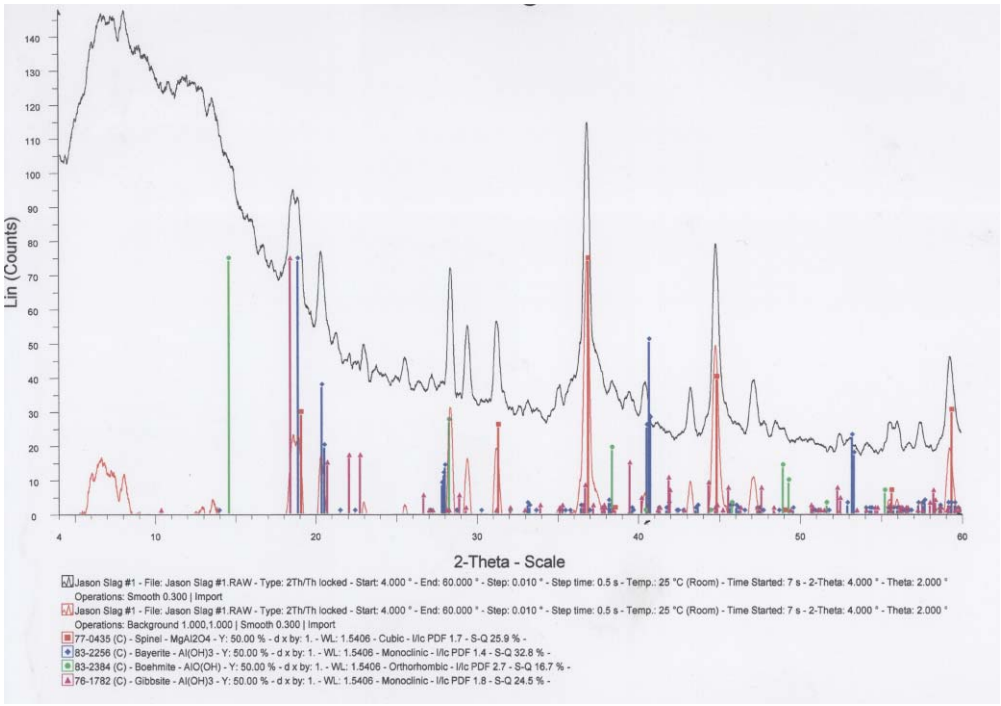

Figure 4.3 XRD analysis of slag from the Smokey Mountain Smelter site.

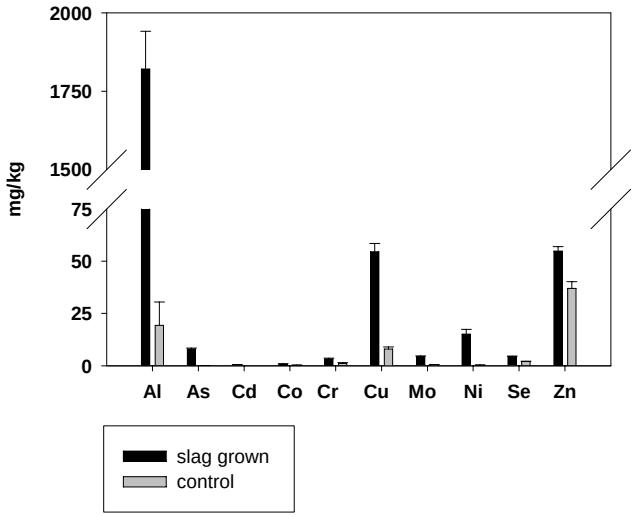

Figure 4.4. Trace element accumulation (mg kg^{-1}) in *Pteris cretica* grown on slag piles at the SMS site for 8 weeks. Black bars indicate plants grown on slag piles and grey bars refer to plants grown in uncontaminated control soil D (Table 1).

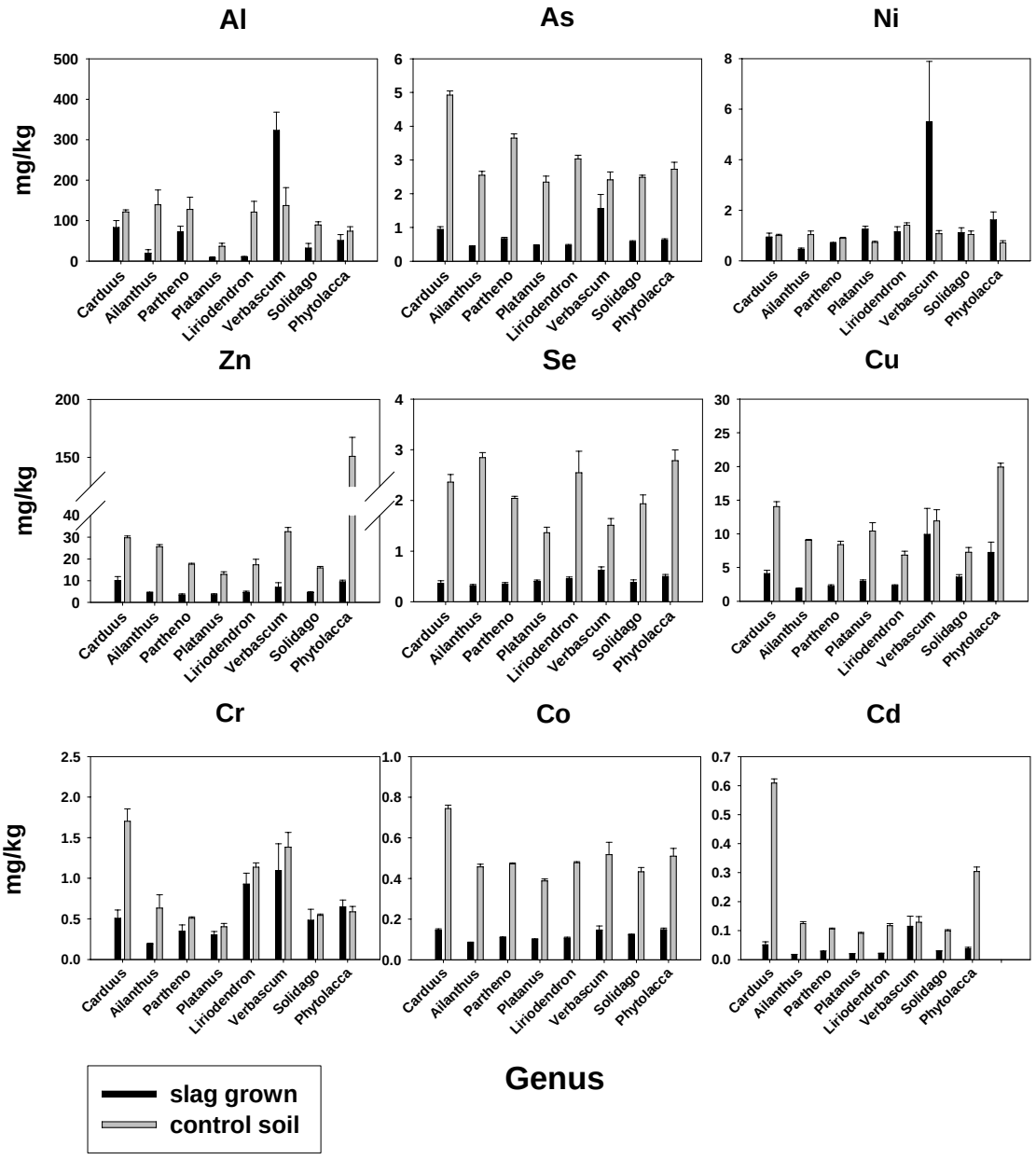

Figure 4.5. Trace element accumulation (mg kg^{-1}) in wild vegetation found growing on slag piles at the SMS site. Species represented are *Verbascum thapsus, Lirodendron tulipifera, Carduus nutans, Solidago □mericana□, Ailanthus altissima*, *Parthenocissus quinquefolia, Platanus occidentalis,* and *Phytolacca □mericana.* Black bars indicate plants grown on slag piles and grey bars refer to plants grown in uncontaminated control soils represented by controls A, B, and C (Table 1).

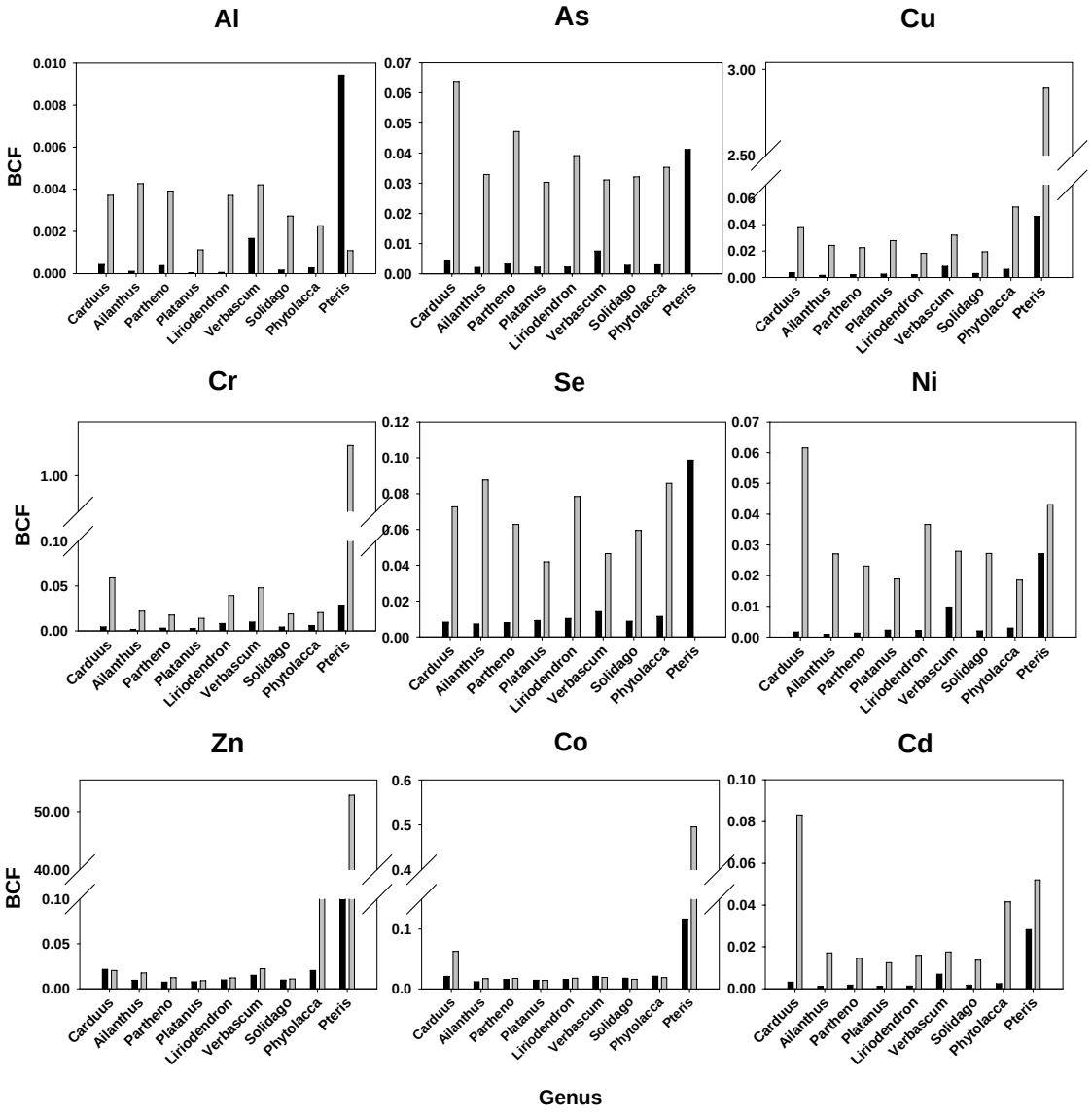

Figure 4.6. Bioconcentration factors (BCF) of trace elements in slag-grown wild vegetation and *Pteris cretica*. Species represented are *Verbascum thapsus, Lirodendron tulipifera, Carduus nutans, Solidago □mericana□, Ailanthus altissima*, *Parthenocissus quinquefolia, Platanus occidentalis, Phytolacca □mericana* and *Pteris cretica.* Black bars indicate plants grown on slag piles and grey bars refer to plants grown in uncontaminated control soils. Control BCFs for wild vegetation were calculated from control soils A, B, and C, whereas BCFs for *Pteris cretica* controls were derived from control soil D.

Vita

Jason Miles Abercrombie was born in Orangeburg, South Carolina on February 10th, 1978 and spent most of his childhood in Lexington, SC, but lived for several years in Ft. Lauderdale, Florida. He graduated from Lexington High School in 1996 and started his undergraduate education that same year at the College of Charleston in Charleston, SC, where he received a B.S. in Biology. He also received a Master of Science in Environmental Science at the College of Charleston. In 2003, he started his doctorate work at the University of Tennessee, Knoxville.